

Cosmological Aspects of String Compactifications

L. P. McAllister

Stanford Linear Accelerator Center
Stanford University
Stanford, CA 94309

SLAC-Report-750

Prepared for the Department of Energy
under contract number DE-AC02-76SF00515

Printed in the United States of America. Available from the National Technical Information Service, U.S. Department of Commerce, 5285 Port Royal Road, Springfield, VA 22161.

This document, and the material and data contained therein, was developed under sponsorship of the United States Government. Neither the United States nor the Department of Energy, nor the Leland Stanford Junior University, nor their employees, nor their respective contractors, subcontractors, or their employees, makes an warranty, express or implied, or assumes any liability of responsibility for accuracy, completeness or usefulness of any information, apparatus, product or process disclosed, or represents that its use will not infringe privately owned rights. Mention of any product, its manufacturer, or suppliers shall not, nor is it intended to, imply approval, disapproval, or fitness of any particular use. A royalty-free, nonexclusive right to use and disseminate same of whatsoever, is expressly reserved to the United States and the University.

COSMOLOGICAL ASPECTS
OF
STRING COMPACTIFICATIONS

A DISSERTATION
SUBMITTED TO THE DEPARTMENT OF PHYSICS
AND THE COMMITTEE ON GRADUATE STUDIES
OF STANFORD UNIVERSITY
IN PARTIAL FULFILLMENT OF THE REQUIREMENTS
FOR THE DEGREE OF
DOCTOR OF PHILOSOPHY

Liam Patrick McAllister
March 2005

Copyright © 2005 by Liam P. McAllister
All rights reserved.

Acknowledgements

It is a great pleasure to acknowledge the many people who have contributed to this dissertation, and, more broadly, to my education in theoretical physics.

First of all, I am deeply indebted to my advisor, Shamit Kachru, for his truly outstanding guidance. He has been exceptionally generous with his time and his knowledge, and his foresight in suggesting research directions has been invaluable. Shamit's tireless work and high scientific standards continue to be an inspiration for me. I feel extremely fortunate to have worked with him.

I am likewise most grateful to Eva Silverstein, who has at many points acted as a co-advisor. By her unique example she has convinced me that choosing topics that inspire laughter and joy is the best guide to superior research. Her insistence on working out details on the blackboard has substantially improved my own style of work.

Furthermore, I am happy to thank Stephen Shenker for his help and guidance. Before I had a formal adviser, Steve was kind enough to integrate me into the theory group, and I felt fortunate to work under his watchful eye.

I am also grateful to Savas Dimopoulos, Renata Kallosh, Andrei Linde, Michael Peskin, Leonard Susskind, Scott Thomas, and Sandip Trivedi for sharing their insights and accumulated wisdom with me.

Most of my education at Stanford has been due to the efforts of my colleagues, who have shaped and refined my understanding of physics with their countless answers and questions. Among these friends, I owe the most to Michal Fabinger and Xiao Liu, for innumerable insights. I am likewise grateful to Lukasz Fidkowski, Ben Freivogel, Jon Hsu, Ben Lillie, Sergey Prokushkin, Darius Sadri and Alex Saltman. I had fewer years to learn from Chad Davis, Alexander Giryavets, Peter Graham, and Marc Schreiber, but I have been improved nonetheless. I would also like to thank those more senior colleagues who took the time to explain many things to me: Allan Adams, Stephon Alexander, Marcus Berg, Keshav Dasgupta, Michael

Haack, Amir Kashani-Poor, Alex Maloney, John McGreevy, Aaron Pierce, Michael Schulz, and Jay Wacker.

The results presented in this dissertation are the work of many hands. Great thanks are due to my collaborators: Sergei Gukov, Shamit Kachru, Renata Kallosh, Lev Kofman, Andrei Linde, Juan Maldacena, Alex Maloney, Indrajit Mitra, Eva Silverstein, and Sandip Trivedi.

The formatting of this work was substantially simplified by a TeX package prepared by Michael Schulz, whose efforts I appreciate.

I carried out this research with essential support from an NSF Graduate Research Fellowship, and with partial support from the DOE under contract DE-AC03-76SF00515. I am sincerely grateful to the U.S. government for its willingness to invest in theoretical physics.

My time in the theory group at Stanford and at SLAC would not have been the same without the generous and efficient assistance of Sharon Jensen, Mariel Haag, and Karin Slinger. Karin, in particular, went to extraordinary lengths to take care of all her children, from students to faculty, and I am in her debt.

I am grateful to all my friends for their companionship, and most specially to Henry Fu, Kaiwen Kam, and Albert Pan.

None of this could have been without the constant love and support of my parents, Timothy and Noreen, and my sister, Tara, who have sustained me through this, as through all other labors.

Most of all, I am deeply grateful to my wife, Josephine, for her love.

Stanford University
March 2005

Liam McAllister

Contents

Acknowledgements	v
1. Introduction	1
1.1. The Status of Cosmology	1
1.1.1. Dark Energy	1
1.1.2. Inflation	3
1.2. Prospects for String Cosmology	5
1.2.1. The Moduli Problem in String Cosmology	5
1.2.2. Techniques of Moduli Stabilization	6
1.2.3. Inflationary Models in String Theory	8
1.3. Organization of this Thesis	9
2. Bouncing Brane Cosmologies	13
2.1. Introduction	13
2.2. Brane Cosmology in a Warped Calabi-Yau Compactification	15
2.2.1. The Compactifications	15
2.2.2. The Klebanov-Strassler Geometry	17
2.2.3. Trajectory of a Falling Brane	19
2.2.4. The Induced Cosmology	20
2.2.5. Issues of Backreaction	24
2.3. Four-dimensional Lagrangian Description	26
2.3.1. Effective Lagrangian	26
2.3.2. Relation to Warped Backgrounds	30
2.4. Discussion	30
3. Moduli Trapping at Enhanced Symmetry Points	33
3.1. Introduction	34
3.1.1. Moduli Trapping Near Enhanced Symmetry Points	34
3.1.2. Relation to Other Works	37
3.2. Moduli Trapping: Basic Mechanism	38
3.2.1. Quantum Production of χ Particles	39
3.2.2. Backreaction on the Motion of ϕ	41
3.2.3. The Example of Moving D-branes	43

3.3. Moduli Trapping: Detailed Analysis	45
3.3.1. Formal Description of Particle Production Near an ESP	45
3.3.2. Moduli Trapping: Numerical Results	49
3.3.3. The Special Case of One-Dimensional Motion	50
3.4. Trapped Moduli in an Expanding Universe	54
3.4.1. Rapid Trapping	54
3.4.2. Scanning Range in an Expanding Universe	55
3.4.3. Trapping in an Expanding Universe	57
3.4.4. Efficiency of Trapping	58
3.5. String Theory Effects	59
3.5.1. Large χ Mass	59
3.5.2. Large v and the Hagedorn Density of States	60
3.5.3. Light Field-Theoretic Strings	61
3.6. The Vacuum Selection Problem	61
3.6.1. Vacuum Selection in Quantum Field Theory	62
3.6.2. Vacuum Selection in Supergravity and Superstring Cosmology	62
3.6.3. Properties of the Resulting Vacua	64
3.7. The Moduli Problem	65
3.8. Trapped Inflation and Acceleration of the Universe	66
3.9. Conclusion	70
3.A. Particle Production Due to Motion on Moduli Space	70
3.B. Annihilation of the χ Particles	73
3.C. Classical Trapping Versus Quantum Trapping	75
 4. Relativistic D-brane Scattering	 79
4.1. Introduction	79
4.2. Overview of the Trapping of Nonrelativistic Branes	83
4.3. The Interaction Amplitude for Moving D-branes	86
4.3.1. Interaction Potential from the Annulus Diagram	86
4.3.2. Imaginary Part and Pair-Production Rate	88
4.4. Backreaction from Energetics	90
4.4.1. Open String Energy	90
4.4.2. Estimate of the Stopping Length	93
4.4.3. Corrections from Deceleration	97
4.5. Further Considerations	100
4.5.1. Production of Closed Strings	100
4.5.2. Summary of the Argument	104
4.5.3. Regime of Validity and Control	105
4.6. Discussion	107
4.A. Masses of Strings Between Moving Branes	109
4.B. Theta Function Identities	110

5. Heterotic Moduli Stabilization	113
5.1. Introduction	113
5.2. Gaugino Condensation in the Heterotic String	116
5.2.1. Effective Lagrangian for the Heterotic Theory	116
5.2.2. Superpotential from Flux and a Gaugino Condensate	120
5.2.3. Conditions for a Stabilized Dilaton	121
5.3. Fractional Flux Induced by Gauge Fields	123
5.3.1. Quantization Conditions for Three-Form Flux	123
5.3.2. Three-cycles with Fractional Flux	124
5.3.3. Formulas for the Chern-Simons Invariant	127
5.3.4. A Global Worldsheet Anomaly from Fractional Chern-Simons Invariants	128
5.4. Dilaton Stabilization	131
5.5. Dilaton <i>and</i> Volume Stabilization in Calabi-Yau Models	133
5.5.1. One-loop Correction	133
5.5.2. Stabilization of Multiple Kähler Moduli	135
5.5.3. A Strong Coupling Problem	136
5.5.4. Fractional Invariants and Weak Coupling	140
5.5.5. Summary of Requirements	142
5.6. Duality to Type IIA and M-theory	143
5.6.1. Heterotic/Type IIA Duality	143
5.6.2. Lift to M-theory	146
5.7. Domain Walls	147
5.8. Discussion	151
 6. Towards Inflation in String Theory	 155
6.1. Introduction	155
6.2. Brief Review of $D3/\overline{D3}$ Inflation	159
6.3. Inflation in a Warped Background: Essential Features	160
6.3.1. Gravity in an AdS Background	161
6.3.2. Brane Dynamics	163
6.4. A Concrete Example in String Theory	166
6.4.1. The Compactification	166
6.4.2. The Klebanov-Strassler Geometry	167
6.4.3. Inflation from Motion in the KS Region	168
6.5. Volume Stabilization: New Difficulties for D-brane Inflation	170
6.5.1. Scenario I: Superpotential Stabilization	172
6.5.2. Scenario II: Kähler Stabilization	177
6.6. Conclusion	177
6.A. General Discussion of Brane-Antibrane Potentials	179
6.B. The $D3/\overline{D3}$ Potential in Warped Geometries	182
6.C. Warped Inflation	184

6.D. Eternal Inflation	187
6.E. Exit from Inflation	188
6.F. Fine-tuning of the Superpotential	189
7. An Inflaton Mass Problem from Threshold Corrections	195
7.1. Introduction	195
7.2. The Eta Problem in Supergravity	198
7.2.1. F-term Inflation and the Eta Problem	199
7.2.2. D-term Inflation	199
7.3. Nonperturbative Superpotentials and Volume Stabilization	200
7.3.1. The Necessity of Volume Stabilization	200
7.3.2. Nonperturbative Superpotentials and Volume Stabilization	201
7.3.3. Threshold Corrections to Nonperturbative Superpotentials	202
7.4. The Eta Problem in String Compactifications	203
7.4.1. Inflaton-Volume Mixing and the Eta Problem	204
7.4.2. Solving the Eta Problem with Geometric Shift Symmetries	205
7.5. Threshold Corrections Change the Inflaton Mass	206
7.5.1. General Results	207
7.5.2. The Example of the D3-D7 Model	208
7.5.3. Discussion	210
7.6. Conclusion	211
7.A. A Field-Theory Model of the Brane Interaction	214
References	217

1. Introduction

1.1 The Status of Cosmology

1.1.1 Dark Energy

Spectacular advances in observational cosmology have revolutionized our view of the universe. We now understand that ordinary matter in all its forms makes up a negligible fraction of the mass of the cosmos: the visible stars and galaxies are an insignificant foam drifting on a vast ocean of dark energy. This mysterious substance pervades the vacuum and forces the expansion of the universe to accelerate. No one knows what it is.

The first sign of dark energy came from measurements of type Ia supernovae, which are explosions of a white dwarf following accretion of matter from a companion star. We have a rudimentary understanding of the intrinsic luminosity of these events, so the discovery that very distant supernovae were unexpectedly dim [1,2] presented a problem. After eliminating alternative explanations, the authors of [1] proposed that the most distant supernovae, and the galaxies that contain them, must be accelerating away from us. This amounts to a modification of the famous Hubble Law, which states that the recession velocity of a galaxy is proportional to its distance from us. The supernova observations showed that the expansion rate of the cosmos must have been different, and indeed smaller, in the past.

This accelerating expansion was a profound shock to most theorists. A universe full of any sort of known matter and radiation cannot accelerate, any more than a stone tossed into the air can accelerate upward in flight. A cosmos exploding outward from the violence of the Big Bang may expand indefinitely, but the universal attraction of gravity will inevitably slow the expansion. The only way to accomodate

the observed acceleration was to invoke the infamous cosmological constant, the ‘energy of the vacuum’.

The cosmological constant problem has mythic status among the deep problems of fundamental physics. Einstein first invoked a constant term in his field equations to create eternal, stationary cosmological solutions, which he found philosophically appealing. The added term was necessary to keep the universe from contracting and collapsing under its own gravitation. Later, faced with Hubble’s observation that our own universe is expanding, Einstein recanted and called the addition of a cosmological constant the biggest blunder of his life.

The crisis, however, is not simply that the Einstein equations contain an unknown constant. The problem is that quantum field theory makes a prediction about the vacuum energy, and it is nearly impossible to square this prediction with cosmology. This is very important, because we understand quantum field theory extremely well in the range of energies accessible to particle accelerators.

Precise predictions are difficult or impossible, but essentially any scheme for computing the vacuum energy in quantum field theory will give an energy density $\rho_{QFT}^{1/4} \gtrsim 10^3$ GeV. Typical schemes suggest that in fact $\rho_{QFT}^{1/4} \sim 10^{19}$ GeV. However, although the vacuum energy measured in our universe does dwarf the energy density of matter, it still amounts to only $\rho_{\Lambda}^{1/4} \sim 10^{-3}$ eV. The theoretical prediction exceeds the measured value by more than 120 orders of magnitude!

The cosmological constant problem is thus a deep conflict between the macroscopic and the microscopic, and between the two great structures of twentieth-century physics: general relativity and quantum field theory. We believe we understand each theory separately, but our inability to understand the vacuum energy proves that we do not understand how to combine them. After decades of effort, the cosmological constant problem still overshadows every scenario in which gravity couples to vacuum energy to source accelerating expansion. Even worse, the new cosmological paradigm requires a gradual transition between stages of acceleration at utterly different scales, from the cataclysmic stretching of inflation to the gentle tug of dark energy today, so the problem is more complex and more acute than ever.

String theory is a theory of quantum gravity: among many other virtues, it provides a complete and consistent description of the quantization of the gravitational field. Should we not expect string theory to resolve the cosmological constant problem and predict, or at least accommodate, the observed value?

Unfortunately, string theory has *not* provided any means of predicting the observed vacuum energy, at least not in any conventional sense of prediction. However, advances in moduli stabilization with fluxes [3,4,5] have provided a method of accommodating the smallness of the vacuum energy within string theory, i.e. of constructing string vacua that contain a minuscule amount of dark energy. This is dramatic progress from the point of view of string theory, but it has not yet shed any light on the observed universe.

In this work we will not provide a solution to any aspect of the cosmological constant problem. The issue, however, is powerful and pervasive, and it underlies all our discussions of moduli stabilization, in Chapter 5, and of string cosmology, in Chapters 6 and 7. Our only concrete step toward accommodating the cosmological constant in string theory is our construction, in Chapter 5, of the first stable solutions of the weakly-coupled heterotic string with non-vanishing vacuum energy. The positive sign and small value of this energy remain out of our reach.

1.1.2 Inflation

A second great advance in our knowledge of the large-scale universe comes from studies of the cosmic microwave background (CMB) radiation. This is the afterglow of the Big Bang, but it has been redshifted by the subsequent expansion down to a mere 2.7 K. The CMB is the first ‘light’ available to us: most of its microwave photons last scattered off matter when the universe first became transparent, when it was roughly 300,000 years old, so there is no direct way to see farther back using the electromagnetic spectrum. The CMB photons are pervasive and surprisingly numerous: at 411 per cubic centimeter, they far outnumber baryons. The discovery of the CMB by Penzias and Wilson was dramatic evidence for the Big Bang theory, and the detailed properties of the CMB are now providing essential clues about the very early universe.

The most surprising thing about the CMB is its uniformity: the fractional temperature difference between various points on the sky is no more than one part in 10^5 . Even before this result was known precisely, the near-uniformity presented a striking problem for the Big Bang model. Each patch of sky of size roughly one degree is a region that was in causal contact at the moment that the universe became transparent: physical signals would have been able to cross this region in the available time, so causal processes could establish thermal equilibrium. Thus,

it would not be at all surprising to find that the temperature does not vary within a patch of size one degree or smaller. Amazingly, it is the entire sky that has a very nearly uniform temperature! The challenge was to explain why the temperature of the sky is uniform, and, in a related vein, why the distribution of matter is so nearly homogeneous and isotropic. Without a causal mechanism to smooth the cosmos, how could all these regions have contrived to look so similar? Moreover, what could explain the immense entropy, age, and size of the universe?

The theory of inflation [6] provides a superb answer to all of these questions. An initial epoch of tremendously violent, accelerated expansion could stretch causal signals across a gigantic space, smoothing inhomogeneities and establishing causal relations between widely-separated points. When the positive energy driving this inflation decayed to more ordinary quanta, the resulting temperature was very nearly uniform, with a predictable spectrum of minute temperature anisotropies.

Since its creation, the inflationary scenario has had outstanding explanatory power. However, the source of much recent excitement is the prospect of testing the predictions of inflation, particularly the spectrum of temperature anisotropies, through precision measurements of the CMB [7]. Certain models have already been ruled out, and there is a limited possibility of confirming the whole scenario by finding traces of gravitational waves in the CMB. This is an irreplaceable opportunity for contact between inflation and reality: no terrestrial experiment is likely to probe the energy scales relevant for inflation, so cosmological data is the only means of testing the theory.

As a theoretical structure, inflation is appealing but incomplete. For example, many well-studied models require field expectation values larger than the Planck mass; although this is arguably acceptable even without an ultraviolet completion for the theory, it would be most reassuring to check this assertion in a full theory of quantum gravity. Furthermore, inflationary potentials need to be exceptionally flat, but this is hard to achieve in most settings: various corrections, particularly terms suppressed by the Planck mass, tend to curve the potential. Thus, a complete computation of an inflating potential in a theory of quantum gravity, such as string theory, would be invaluable.

1.2 Prospects for String Cosmology

String theory and cosmology have much to gain from each other. In the preceding section I have reviewed two of the deep questions of theoretical cosmology, the nature of the dark energy and the fundamental physics underlying inflation. As a mathematically consistent theory of quantum gravity, string theory ought perhaps to have something to offer towards solutions of these puzzles, but no clear answer has yet emerged.

However, in recent years there has been very significant progress toward theoretically satisfying, and experimentally testable, string cosmology. For many years the most significant barrier to meaningful contact between string theory and cosmology has been the moduli problem. Correspondingly, most of the progress in recent years is due to advances in moduli stabilization, culminating in the first stable string vacua with positive cosmological constant [5]. We will therefore turn our attention now to the problems posed by compactification moduli, and then, in §1.2.2, to the solution to these problems: moduli stabilization with fluxes and nonperturbative effects.

1.2.1 The Moduli Problem in String Cosmology

A modulus is a massless scalar field, often one which parameterizes the couplings of a field theory or the deformations of a geometry. Geometric moduli are endemic in string compactifications: the preferred compactification manifolds, most notably Calabi-Yau spaces, have complicated topology, and admit correspondingly numerous deformations of the complex structure and of the Kähler parameters. Before accounting for the superpotentials arising from fluxes and from nonperturbative effects, each of these scalars appears with vanishing potential in the four-dimensional theory. Their couplings are of gravitational strength.

Moduli present several problems for cosmological models. First of all, gravitational experiments place strong constraints on the existence of light scalars with gravitational interactions. In addition, some moduli, especially the string dilaton and the compactification volume, affect the couplings of Standard Model fields. Variations in the Newton constant [8] or in the electromagnetic fine-structure constant [9] are strongly bounded, so once again we find that typical moduli are incompatible with the results of experiment. Taken together, these constraints suggest that moduli must somehow be removed from any workable model.

Finally, among the great successes of the Big Bang model, and of early universe cosmology, are the predictions of Big Bang nucleosynthesis. In the first few minutes of expansion, protons and neutrons combined to form light nuclei, primarily helium, but with predictable relative abundances of deuterium and lithium. This provides a powerful tool for excluding new particles that could disrupt this relatively delicate process of synthesis. Moduli are problematic because they almost inevitably store energy during inflation, by being displaced from their zero-temperature minima. Unless the moduli acquire rather large masses, this energy causes one of two problems. If the moduli mass m_χ is smaller than around 100 MeV, the moduli will not have decayed by the present day, and the energy they stored during inflation will overclose the universe. If $100\text{MeV} \lesssim m_\chi \lesssim 30\text{TeV}$ then the moduli will have decayed, but in the process will have released enough entropy to dilute the products of nucleosynthesis [10]. Only if all the moduli have masses above 30 TeV can we maintain the success of nucleosynthesis. Thus, we conclude that in the absence of a mechanism for generating such masses, models based on string compactifications are incompatible with cosmological observations.

Of great importance for us will be one particularly dangerous modulus, the overall compactification volume. In the presence of a positive energy density, this field develops an instability: it becomes energetically favorable for the internal space to expand. This lifts the volume modulus, but the result is not a stable model: instead we find a runaway decompactification.

This observation is significant for cosmological models because both inflation and the present-day acceleration require positive energy density. These two features, arguably the most important of the new cosmological paradigm, simply cannot be achieved in string compactifications without moduli stabilization.

1.2.2 Techniques of Moduli Stabilization

Moduli stabilization is a procedure that generates a potential for the moduli. This potential is usually required to have a minimum in a reasonable range of field values. For example, the introduction of a spacetime-filling positive-energy source creates a potential for the volume modulus whose minimum is at infinite volume. This actually destabilizes the volume modulus, decompactifying the internal space, and certainly does not qualify as volume stabilization!

In order to understand what effects are needed to lift the moduli, it will be helpful to have a partial classification of the moduli of a string compactification on a Calabi-Yau threefold. The geometric moduli are the complex structure moduli, which parameterize the space of choices of complex structure on the manifold, and the Kähler moduli, which govern the sizes of even-dimensional cycles. In heterotic string compactifications and type I or type II compactifications with D-branes, there will also in general be bundle moduli, which control the deformations of the corresponding vector bundles. Finally, there can be open string moduli associated with the locations of D-branes.

In the best-understood setting of type IIB orientifolds, the most numerous and important moduli are the complex structure and Kähler moduli. Intuitively, complex structure moduli control the shapes of cycles, so what is needed is a physical ingredient that associates an energy cost to changes of shape. Three-form fluxes, the field strengths of the two-form Neveu-Schwarz and Ramond-Ramond potentials B_{ij} and C_{ij} , provide just such an effect [4]. This flux is integrally quantized, so inclusion of a real three-form flux amounts to a choice of one integer for each three-cycle in the internal space. There are actually two real three-form fluxes in the type IIB theory, $H_3 = dB_2$ and $F_3 = dC_2$, and it is useful to form the complex combination $G_3 = F_3 - \tau H_3$, where τ is the axio-dilaton. Turning on generic G-flux usually fixes all the complex structure moduli and the dilaton. (In certain special cases such as tori this may not be true.)

Kähler moduli, in contrast, are not lifted by the inclusion of flux. In fact, they cannot appear in the perturbative superpotential: the combination of holomorphy of the superpotential and the shift symmetry [11] of the axion paired with each volume modulus implies that the superpotential can acquire volume-dependence only nonperturbatively. We must therefore seek nonperturbative effects that are sensitive to the volume moduli. Two effects are suitable for this purpose [5]: gaugino condensation on a stack of D7-branes wrapping a divisor, and Euclidean D3-branes wrapping a divisor [12]. The former requires a suitably small matter content in the D7-brane gauge theory, and the latter is possible (in the absence of flux) only if the divisor satisfies a certain topological condition [12].

We conclude that to achieve complete stabilization of the geometric moduli [5], one must introduce generic three-form fluxes and verify that every independent divisor admits either gaugino condensation or Euclidean D3-branes.

1.2.3 Inflationary Models in String Theory

Given a reliable technique for constructing stable string vacua with positive energy, it is quite easy to imagine concrete inflationary models. Slow-roll inflation does not require much more than the relaxation of an overdamped scalar field in a potential with a large positive energy. One therefore needs to search for a relatively flat potential that interpolates between a high-energy configuration and one of approximately zero energy. Ideally, quantum corrections to this potential would be computable and under control. The scale and slope of this potential rather directly determine the magnitude and the spectral index of the density perturbations that we see as CMB temperature anisotropies. One might also hope to explain the very small amplitude of these perturbations, i.e. the near-isotropy of the CMB.

As we will see in Chapter 6, the separation of a D3-brane and an anti-D3-brane in a warped deformed conifold [13] can provide an interaction potential with appropriate properties. This is merely a concrete example, a toy model for string inflation; it seems quite clear that much more generic models remain to be discovered.

One striking consequence of brane inflation models is the possibility of forming networks of stable cosmic superstrings [14,15]. The literature on cosmic strings had largely discounted the possibility of a connection to string theory, in part because the tensions of ordinary F-strings and D-strings in superstring theory are much too large to be compatible with observations. However, progress in brane inflation, particularly in warped models, led to the realization that the strings of string theory could potentially be cosmic in scale.

Cosmic strings stretch for light-years and are so massive that they bend starlight, creating distinctive lensing signals. Moreover, they emit a powerful flux of gravitational radiation, with occasional high-intensity bursts. These metric fluctuations affect the travel time of pulsar signals, so pulsar timing experiments can be used to put bounds on the cosmic string tension. Lensing surveys and direct observation of gravitational waves are other promising routes to discovering or ruling out cosmic strings. In the event of a discovery, it is just possible that we could distinguish a network of F-strings and D-strings from the more conventional cosmic string scenarios that are unrelated to string theory. This thrilling prospect of direct contact between string theory and experiment is another important opportunity for string cosmology.

1.3 Organization of this Thesis

The organization of this work is as follows. In Chapters 2,3, and 4 we discuss the dynamics of unfixed moduli in quantum field theory and in string theory, with emphasis on applications to cosmological model-building. Moduli-stabilizing effects are not included, because our goal is to understand the evolution of moduli whose potentials remain approximately flat. In Chapter 5 we develop a technique for stabilizing moduli in the heterotic string, and we construct the first stabilized, weakly-coupled heterotic vacua. In Chapter 6 we utilize advances in the stabilization of type IIB compactifications to build the first models of inflation in stabilized string vacua. Finally, in Chapter 7 we examine the effects of volume-stabilization on the inflaton mass in closely-related scenarios of string inflation.

Chapter 2 presents a bouncing cosmology seen by an observer on a moving D3-brane: this is a universe whose scale factor decreases to a minimum value and then smoothly re-expands [16]. Singularity theorems usually forbid solutions of this form [17], so we explain the rather surprising way in which our system circumvents these theorems. The relevant modulus in this model is the position of the D3-brane along the radial direction of a warped deformed conifold [13]. This particular modulus will be lifted in the presence of nonperturbative stabilization of the compactification volume, a result that will have great importance in Chapters 6 and 7.

In Chapter 3 we consider quantum corrections to the dynamics of a system of coupled moduli in quantum field theory. Certain particles are light at special points in moduli space, which often exhibit enhanced symmetry. (For example, the light fields could be gauge bosons whose mass is large away from the special points, and in this case the enhanced symmetry would be gauged.) We discover that quantum production of these light particles traps moving moduli at these points of enhanced symmetry [18]. This effect, which we call moduli trapping, has a variety of implications for cosmology. Moduli trapping may ameliorate the cosmological moduli problem by situating moduli at extrema of their effective potential during inflation. It can lead to a short period of accelerating expansion, which we call trapped inflation. The most interesting result is that moving moduli are most powerfully attracted to the points with the highest degree of symmetry. Given suitable initial conditions, this could help to explain why our universe exhibits a relatively large degree of (spontaneously broken) symmetry. Some of the surprising symmetries of our world might have an explanation in the dynamics of moduli.

In Chapter 4 we study an interesting special case [19] of the moduli trapping scenario. When the moduli in motion correspond to the relative positions of D-branes, the quantum effect relevant for moduli trapping is pair-production of stretched open strings. For slow-moving D-branes this is captured by the analysis of Chapter 2. However, relativistic D-branes exhibit a tremendously strong trapping effect. We show that the brane trajectory receives strong corrections from copious production of highly-excited open strings, whose typical oscillator level is proportional to the square of the rapidity. This purely stringy effect makes relativistic brane collisions exceptionally inelastic. We trace this surprising effect to velocity-dependent corrections to the open string mass, which render open strings between relativistic D-branes surprisingly light. Our analysis has applications to cosmological scenarios in which branes approach each other at very high speeds: pair production of open strings could play an unexpectedly strong role in the brane dynamics.

Next, in Chapter 5, we present a technique for stabilizing the moduli of perturbative heterotic string compactifications on Calabi-Yau threefolds [20]. We show that fractional flux from Wilson lines, in combination with a hidden-sector gaugino condensate [21], generates a potential for the complex structure moduli, Kähler moduli, and dilaton. This potential has a supersymmetric AdS minimum at moderately weak coupling and large volume. In this way we construct the first stabilized heterotic string models. Our solutions have a nonvanishing, although negative, cosmological constant, so our methods are a step toward controllable de Sitter vacua of the heterotic string. Our technique circumvents a well-known problem [21] arising from flux quantization by introducing a Chern-Simons invariant that does not have an integer quantization condition. The necessary Chern-Simons invariant can arise naturally from the GUT-breaking Wilson lines that are already present in most phenomenologically appealing models.

In Chapter 6 we use earlier, fundamental advances [5] in stabilization of type IIB compactifications to build the first concrete model of inflation in a stabilized string compactification [22]. Our construction involves a D3-brane moving down a warped deformed conifold [13] geometry in a Calabi-Yau orientifold stabilized by fluxes [4] and by nonperturbative effects [5]. Condensation of a brane-antibrane tachyon ends inflation, so our model is a string embedding of hybrid inflation. One particularly appealing feature is the possibility of light, stable cosmic strings.

In Chapter 7 we reconsider the effect of nonperturbative volume stabilization on inflation [23], and observe that certain geometric shift symmetries constructed to protect the inflaton mass are broken by threshold corrections [24,25]. We conclude that in typical configurations, some degree of fine-tuning is still required. This presents a mild but relevant challenge for inflationary model-building in such scenarios.

Note on Collaborative Research

Modern theoretical physics is a science built on collaborations. Most progress in string theory, in particular, results from the work of small groups, not of individuals in isolation. The unwritten rule governing this system is that each co-author is expected to contribute in some way to every major aspect of a paper.

I was intimately involved in all the research reported in this dissertation. Furthermore, in each project I was continually involved in the writing and rewriting of our results. My contributions and those of my collaborators have been woven together to create complete works, and there is no meaningful way to partition the finished product.

2. Bouncing Brane Cosmologies

ABSTRACT OF ORIGINAL PAPER

We study the cosmology induced on a brane probing a warped throat region in a Calabi-Yau compactification of type IIB string theory. For the case of a BPS D3-brane probing the Klebanov-Strassler warped deformed conifold, the cosmology described by a suitable brane observer is a bouncing, spatially flat Friedmann-Robertson-Walker universe with time-varying Newton's constant, which passes smoothly from a contracting to an expanding phase. In the Klebanov-Tseytlin approximation to the Klebanov-Strassler solution the cosmology would end with a big crunch singularity. In this sense, the warped deformed conifold provides a string theory resolution of a spacelike singularity in the brane cosmology. The four-dimensional effective action appropriate for a brane observer is a simple scalar-tensor theory of gravity. In this description of the physics, a bounce is possible because the relevant energy-momentum tensor can classically violate the null energy condition.

2.1 Introduction

There has recently been considerable interest in the properties of string theory cosmology. A generic feature of general relativistic cosmologies is the presence of singularities, which is guaranteed under a wide range of circumstances by the singularity theorems [17]. Since string theory has had great success in providing physically sensible descriptions of certain timelike singularities in compactification geometries, one can hope that it will similarly provide insight into the spacelike

This chapter is reprinted from Shamit Kachru and Liam McAllister, "Bouncing Brane Cosmologies from Warped String Compactifications," JHEP **0303** (2003) 018, by permission of the publisher. © 2002 by the Journal of High Energy Physics.

or null singularities which arise in various cosmologies. Proposals in this direction have appeared in e.g. [26,27,28,29,30,31,32,33,34,35,36,37].

In a slightly different direction, the possibility of localizing models of particle physics on three-branes in a higher-dimensional bulk geometry has motivated a great deal of work on brane-world cosmology (see [38,39,40,41,42] and references therein for various examples). Of particular interest to us will be the “mirage” cosmology [38] which is experienced by a D3-brane observer as he falls through a bulk string theory background. In this chapter, we present a simple and concrete example where such an observer would describe a cosmology which evades the singularity theorems: his universe is a flat FRW model which smoothly interpolates between a collapsing phase and an expanding phase.

The background through which the D3-brane moves is a Klebanov-Strassler (KS) throat region [13] of a IIB Calabi-Yau compactification. Compactifications including such throats, described in [4], yield models with 4d gravity and a warp factor which can vary by many orders of magnitude as one moves in the internal space (as in the proposal of Randall and Sundrum (RS) [43]). The backgrounds discussed in [4] would also admit, in many cases, some number of wandering D3-branes. Such a brane can fall down the KS throat and bounce smoothly back out, as the supergravity background has small curvature everywhere. The induced cosmology on this probe, as described by an observer who holds particle masses *fixed*, is a spatially flat Friedmann-Robertson-Walker universe which begins in a contracting phase, passes smoothly through a minimum scale factor, and then re-expands.¹ A D3-brane probe in this background satisfies a “no-force” condition which makes it possible to control the velocity of the contraction; in addition, the background can be chosen so that the universe is large in Planck units at the bounce. For this reason, the calculations which lead the brane observer to see a bounce are controlled and do not suffer from large stringy or quantum gravity corrections. It is important to note that in this scenario, the effective 4d Newton’s constant G_N varies with the scale factor of the universe; this results from the varying overlap of the graviton wavefunction with the D3-brane.

The KS solution is actually a stringy resolution of the singular Klebanov-Tseytlin (KT) supergravity solution [45], which ends with a naked singularity in

¹ A different approach to using the KS model to generate an interesting string theory cosmology recently appeared in [44].

the infrared. A brane falling into a Klebanov-Tseytlin throat would therefore undergo a singular big crunch. In this sense, the cosmology we study involves a stringy resolution of a spacelike singularity, from the point of view of an observer on the brane.

Although one can describe the cosmological history of these universes using the behavior of the induced metric along the brane trajectory, it is also interesting to consider the 4d effective field theory that a brane resident could use to explain his cosmology. We construct a simple toy model of these cosmologies using a 4d scalar-tensor theory of gravity. The scalar can be identified with the open string scalar field Φ_r (corresponding to radial motion down the warped throat) in the Born-Infeld action for the D3-brane. It is well known that such scalar-tensor theories can classically violate the null energy condition, making a bounce possible. Related facts about scalar field theories coupled to gravity have been exploited previously by Bekenstein and several subsequent authors [46,47,48,49].

The organization of this chapter is as follows. In §2.2 we use the construction of [4] to study the cosmology on a brane sliding down the KS throat. In §2.3 we provide a discussion of the effective scalar-tensor theory of gravity a brane theorist would probably use to explain his observations. We close with some thoughts on further directions in §2.4.

Several previous authors have investigated the possibility of bounce cosmologies in scalar-tensor theories and in brane-world models. For FRW models with spherical spatial sections ($k = +1$), examples in various contexts have appeared in [46,47,48]. As we were completing this work, other discussions of bounces in brane-world models appeared in [50,51]. To the best of our knowledge, this chapter provides the first controlled example in string theory of a bouncing, spatially flat FRW cosmology with 4d gravity.

2.2 Brane Cosmology in a Warped Calabi-Yau Compactification

2.2.1 The Compactifications

In [52,4,53], warped string compactifications were explored as a means of realizing the scenario of Randall and Sundrum [43] in a string theory context. It was shown that compactifications of IIB string theory on Calabi-Yau orientifolds

provide the necessary ingredients. In such models, one derives a tadpole condition of the form

$$\frac{1}{4}N_{O3} = N_{D3} + \frac{1}{2(2\pi)^4(\alpha')^2} \int_X H_3 \wedge F_3 . \quad (2.2.1)$$

Here X is the Calabi-Yau manifold, N_{O3} and N_{D3} count the number of orientifold planes coming from fixed points of the orientifold action and the number of transverse D3-branes, and H_3, F_3 are the NSNS and RR three-form field strengths of the IIB theory.² In general, the left-hand side of (2.2.1) is nonzero and can be a reasonably large number, giving rise to the possibility of compactifications with large numbers of transverse D3-branes or internal flux quanta. Since both of these lead to nontrivial warping of the metric as a function of the internal coordinates, (2.2.1) tells us that these Calabi-Yau orientifolds provide a robust setting for finding warped string compactifications [52,4,53].

We can make this somewhat vague statement much more precise in the example of the warped deformed conifold. The conifold geometry is defined in \mathbb{C}^4 by

$$z_1^2 + z_2^2 + z_3^2 + z_4^2 = 0. \quad (2.2.2)$$

It is topologically a cone over $S^2 \times S^3$; we will refer to the direction transverse to the base as the “radial direction” (with small r being close to the tip and large r being far out along the cone). The *deformed* conifold geometry

$$z_1^2 + z_2^2 + z_3^2 + z_4^2 = \epsilon^2 \quad (2.2.3)$$

has two nontrivial 3-cycles, the A -cycle S^3 which collapses as $\epsilon \rightarrow 0$, and the dual B -cycle. Klebanov and Strassler found that the infrared region of the geometry which is holographically dual to a cascading $SU(N+M) \times SU(N)$ $\mathcal{N} = 1$ supersymmetric gauge theory is precisely a warped version of the deformed conifold geometry, with nontrivial 3-form fluxes

$$\frac{1}{(2\pi)^2\alpha'} \int_A F = M, \quad \frac{1}{(2\pi)^2\alpha'} \int_B H = -k \quad (2.2.4)$$

and $N = kM$. In particular, the space (2.2.3) is non-singular and the smooth geometry dual to the IR of the gauge theory reflects the confinement of the Yang-Mills

² In an F-theory description, the left-hand side of (2.2.1) is replaced by $\frac{\chi(X_4)}{24}$, where X_4 is the relevant elliptic Calabi-Yau fourfold.

theory (with the small parameter ϵ mapping to the exponentially small dynamical scale of the gauge theory). In a cruder approximation to the physics, Klebanov and Tseytlin had earlier found a dual gravity description with a naked singularity [45]; this heuristically corresponds to the unresolved singularity in (2.2.2).

In [4], the warped, deformed conifold with flux (2.2.3), (2.2.4) was embedded in string/F-theory compactifications to 4d. The small r region is as in [13], while at some large r (in the UV of the dual cascading field theory), the solution is glued into a Calabi-Yau manifold. The fluxes give rise to a potential which fixes (many of) the Calabi-Yau moduli (and in particular the ϵ in (2.2.3)), while the fluxes plus in some cases wandering D3-branes saturate the tadpole condition (2.2.1). If one considers one of the cases with $N_{D3} > 0$, then it is natural to imagine a cosmology arising on a wandering D3-brane as it falls down towards the tip of the conifold (2.2.3).

2.2.2 The Klebanov-Strassler Geometry

The KS metric is given by (we use the conventions of [54])

$$ds^2 = h^{-1/2}(\tau)\eta_{\mu\nu}dx^\mu dx^\nu + h^{1/2}(\tau)ds_6^2 \quad (2.2.5)$$

where ds_6^2 is the metric of the deformed conifold,

$$ds_6^2 = \frac{1}{2}\epsilon^{4/3}K(\tau)\left(\frac{1}{3K^3(\tau)}[d\tau^2 + (g^5)^2] + \cosh^2\left(\frac{\tau}{2}\right)[(g^3)^2 + (g^4)^2] + \sinh^2\left(\frac{\tau}{2}\right)[(g^1)^2 + (g^2)^2]\right). \quad (2.2.6)$$

Here

$$\begin{aligned} g^1 &= \frac{e^1 - e^3}{\sqrt{2}}, & g^2 &= \frac{e^2 - e^4}{\sqrt{2}} \\ g^3 &= \frac{e^1 + e^3}{\sqrt{2}}, & g^4 &= \frac{e^2 + e^4}{\sqrt{2}} \\ g^5 &= e^5 \end{aligned} \quad (2.2.7)$$

where

$$\begin{aligned} e^1 &= -\sin(\theta_1)d\phi_1, & e^2 &= d\theta_1 \\ e^3 &= \cos(\psi)\sin(\theta_2)d\phi_2 - \sin(\psi)d\theta_2 \\ e^4 &= \sin(\psi)\sin(\theta_2)d\phi_2 + \cos(\psi)d\theta_2 \\ e^5 &= d\psi + \cos(\theta_1)d\phi_1 + \cos(\theta_2)d\phi_2. \end{aligned} \quad (2.2.8)$$

ψ is an angular coordinate which ranges from 0 to 4π , while (θ_1, ϕ_1) and (θ_2, ϕ_2) are the conventional coordinates on two S^2 s. The function $K(\tau)$ in (2.2.5) is given by

$$K(\tau) = \frac{(\sinh(2\tau) - 2\tau)^{1/3}}{2^{1/3}\sinh(\tau)} . \quad (2.2.9)$$

Clearly in (2.2.5) τ plays the role of the “radial” variable in the conifold geometry, with large τ corresponding to large r .

Finally, the function $h(\tau)$ in (2.2.5) is rather complicated; it is given by the expression

$$h(\tau) = (g_s M \alpha')^2 2^{2/3} \epsilon^{-8/3} I(\tau) \quad (2.2.10)$$

where

$$I(\tau) = \int_{\tau}^{\infty} dx \frac{x \coth(x) - 1}{\sinh^2(x)} (\sinh(2x) - 2x)^{1/3} . \quad (2.2.11)$$

It will be useful to note that this reaches a maximum at $\tau = 0$ and decreases monotonically as $\tau \rightarrow \infty$. There are also nontrivial backgrounds of the NSNS 2-form and RR 2-form potential; their detailed form will not enter here, but they are crucial in understanding why the D3-brane propagates with no force in the background (2.2.5).

Since the form of $h(\tau)$ will be important in what follows, we take a moment here to give some limits of the behavior of formulae (2.2.10), (2.2.11) [54]. For very small τ , one finds $I(\tau) \sim a_0 + O(\tau^2)$, with a_0 a constant of order 1. In this limit the complicated metric (2.2.5) simplifies greatly (c.f. equation (67) of [54]):

$$ds^2 \rightarrow \frac{\epsilon^{4/3}}{2^{1/3} a_0^{1/2} g_s M \alpha'} dx_n dx_n + a_0^{1/2} 6^{-1/3} (g_s M \alpha') \left(\frac{1}{2} d\tau^2 + \frac{1}{2} (g^5)^2 + (g^3)^2 + (g^4)^2 + \frac{1}{4} \tau^2 [(g^1)^2 + (g^2)^2] \right) . \quad (2.2.12)$$

This is $R^{3,1}$ times (the small τ limit of) the deformed conifold. In particular, the S^3 has fixed radius proportional to $\sqrt{g_s M}$, and so the curvature can be made arbitrarily small for large $g_s M$. In the opposite limit of large τ , the metric simplifies to Klebanov-Tseytlin form. Introducing the coordinate r via

$$r^2 = \frac{3}{2^{5/3}} \epsilon^{4/3} e^{\frac{2\tau}{3}} \quad (2.2.13)$$

and using the asymptotic behavior $I(\tau) \sim 3 \times 2^{-1/3}(\tau - \frac{1}{4})e^{-\frac{4\tau}{3}}$, one finds

$$ds^2 \rightarrow \frac{r^2}{L^2 \sqrt{\ln(r/r_s)}} dx_n dx_n + \frac{L^2 \sqrt{\ln(r/r_s)}}{r^2} dr^2 + L^2 \sqrt{\ln(r/r_s)} ds_{T^{1,1}}^2 \quad (2.2.14)$$

where $ds_{T^{1,1}}^2$ is the metric on the Einstein manifold $T^{1,1}$ and $L^2 = \frac{9g_s M \alpha'}{2\sqrt{2}}$. This means that up to logarithmic corrections, the large τ behavior gives rise to an AdS_5 metric for the x^μ and τ directions. This is the expected behavior from the field theory dual, since large τ corresponds to the UV, where the theory is approximately the Klebanov-Witten $\mathcal{N} = 1$ SCFT [55].

2.2.3 Trajectory of a Falling Brane

We will start the D3-brane at some fixed $\tau = \tau^*$ and send it flying towards $\tau = 0$ with a small initial proper velocity v in the radial τ direction. Before describing the trajectory we will briefly explain our notation. τ always indicates the radial coordinate in the KS geometry (2.2.5) and is dimensionless in our conventions. We will reserve t for proper time (for the infalling brane) and $\dot{}$ for $\frac{d}{dt}$, while ξ represents the coordinate time, in terms of which the metric is

$$ds^2 = h(\tau)^{-\frac{1}{2}} (-d\xi^2 + \sum_i dx_i^2) + g_{\tau\tau} d\tau^2 + \text{angles} \quad (2.2.15)$$

and thus

$$\left(\frac{dt}{d\xi}\right)^2 = h(\tau)^{-\frac{1}{2}} \left(1 - h(\tau)^{\frac{1}{2}} g_{\tau\tau} \left(\frac{d\tau}{d\xi}\right)^2\right). \quad (2.2.16)$$

To leading order in the velocity we have $\left(\frac{dt}{d\xi}\right)^2 \approx h(\tau)^{-\frac{1}{2}}$.

Proper distance is given by $d = \int d\tau' g_{\tau\tau}^{1/2}$, and proper velocity by $v \equiv \dot{d} = \dot{\tau} g_{\tau\tau}^{1/2}$. The initial values of the position, proper distance, coordinate velocity, and proper velocity are denoted by τ_* , d_* , $\dot{\tau}_0$ and v_0 , respectively.

The D3-brane trajectory is determined by the Born-Infeld action

$$S_{BI} = \frac{-1}{g_s^2 l_s^4} \int d^3\sigma d\xi \left(h(\tau)^{-1} \sqrt{1 - h(\tau)^{\frac{1}{2}} g_{\tau\tau} \left(\frac{d\tau}{d\xi}\right)^2} - h(\tau)^{-1} \right) \quad (2.2.17)$$

where we have neglected contributions from the U(1) gauge field on the brane. At leading order in a low-velocity expansion, rewritten in terms of derivatives with respect to proper time,

$$S_{BI} = \frac{1}{2g_s^2 l_s^4} \int d^3\sigma d\xi h(\tau)^{-1} g_{\tau\tau} \dot{\tau}^2 \quad (2.2.18)$$

where the cancellation of the potential $h(\tau)^{-1}$ is the realization of the no-force condition. Conservation of energy then yields

$$\dot{\tau}(t)^2 = \dot{\tau}_0^2 \frac{h(t)}{h(\tau_*)} \frac{g_{\tau\tau}(\tau_*)}{g_{\tau\tau}(t)} \quad (2.2.19)$$

From the profile of $\frac{h}{g_{\tau\tau}}$ it follows that the brane accelerates gradually toward the tip of the conifold. For large τ we may use the KT radial coordinate r (2.2.13), in terms of which (2.2.19) is $\frac{d^2\tau}{d\xi^2} = 0$, which is another expression of the balancing of gravitational forces and forces due to flux.

2.2.4 The Induced Cosmology

An observer on the brane naturally sees an induced metric

$$ds_{\text{brane}}^2 = -dt^2 + h^{-1/2}(\tau)(dx_1^2 + dx_2^2 + dx_3^2) . \quad (2.2.20)$$

But given that the brane trajectory is a function $\tau(t)$, (2.2.20) gives rise to a standard FRW cosmology

$$ds^2 = -dt^2 + a^2(t)(dx_1^2 + dx_2^2 + dx_3^2) \quad (2.2.21)$$

with $a(t)$ given by

$$a(t) = h^{-1/4}(\tau(t)) . \quad (2.2.22)$$

Notice that the graviton wavefunction has a τ -dependent overlap with a brane located at various points in the metric (2.2.5). This is simply the effect exploited in [43]. The dimensionless strength of gravity therefore scales according to

$$G_N(t)m_{\text{open}}^2 \sim h(\tau(t))^{-\frac{1}{2}} \sim a(t)^2 \quad (2.2.23)$$

where m_{open} is the mass of the first oscillating open string mode. A physicist residing on the brane may choose to fix *one* of the dimensionful quantities G_N , m_{open} in order to set his units of length. Grinstein et al. [56] have shown that a brane observer who uses proper distance to measure lengths on the brane will necessarily find fixed masses and variable G_N . One can argue for the same system of units by stipulating that elementary particle masses should be used to define the units, and should be considered fixed with time. In this model we will use the mass of the first excited open string mode to fix such a frame; in a more realistic model,

one would want other (perhaps “standard model”) degrees of freedom to be the relevant massive modes.

A brane observer following an inward-falling trajectory in the background (2.2.5) would therefore make the following statements.

1. Elementary particle masses, e.g. m_{open} , are considered fixed with time.
2. In these units, the proper distance between galaxies on the brane scales with $a(t)$ as in standard FRW cosmology. In consequence, for the infalling brane (moving towards $\tau = 0$) one observes blueshifting of photons.
3. The gravitational coupling on the brane is time-dependent,

$$G_N(t) \sim a(t)^2 . \quad (2.2.24)$$

Therefore, as the universe collapses, the strength of gravity decreases.

In fact, (2.2.22) together with (2.2.24) imply that in 4d *Planck* units, the size of the universe remains *fixed*. From this “closed string” perspective, the cosmology is particularly trivial; the brane radial position is described by a scalar field Φ_r in the 4d action which is undergoing some slow time variation (and, for small brane velocity, carries little enough energy that backreaction is not an issue). However, in this frame particle masses vary with time. We find it more natural, as in [56], for a brane observer to view physics in the frame specified by 1-3 above; we will henceforth adopt the viewpoint of such a hypothetical brane cosmologist. In §2.3.1 we describe the field redefinition which takes one from the “brane cosmologist” frame to the “closed string” frame in a toy model.

The Bounce

As the brane falls from τ^* towards zero, the scale factor decreases monotonically. It hits $\tau = 0$ in finite proper time. However, as is clear from the metric (2.2.5), there is no real boundary of the space at this point; $\tau = 0$ is analogous to the origin in polar coordinates. The brane smoothly continues back to positive τ , and the scale factor re-expands. Although it is hard to provide an analytical expression for $a(t)$ given the complexity of the expressions (2.2.10) and (2.2.11), we can numerically solve for a ; a plot appears in Figure 1.

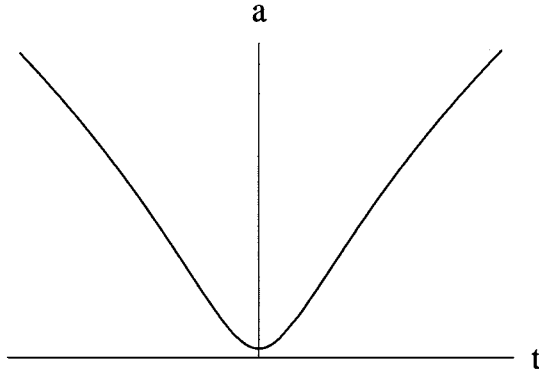


Fig. 1: The scale factor $a(t)$ as a function of proper time for a brane near the tip of the Klebanov-Strassler geometry. This particular bounce begins from radial position $\tau = 4$.

In the approximate supergravity dual to the cascading gauge theory studied in [45], there is instead a naked singularity in the region of small τ , which is deformed away by the fluxes (2.2.4). In the KT approximation to the physics, then, the cosmology on the brane would actually have a spacelike singularity at some finite proper time. The evolution in this background agrees with Figure 1 until one gets close to the tip of the conifold; then, in the “unphysical” region of the KT solution, the brane rapidly re-expands, and a singularity of the curvature scalar of the induced metric arises at a finite proper time. A plot of $a(t)$ for this case appears in Figure 2.

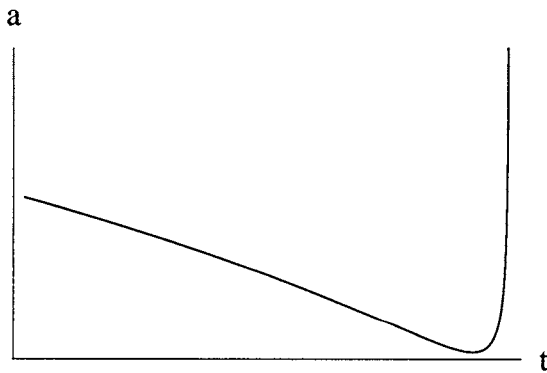


Fig. 2: The scale factor $a(t)$ as a function of proper time for a brane near the singularity of the Klebanov-Tseytlin geometry. The explosive growth of $a(t)$ on the right coincides with a curvature singularity in the induced metric.

Hence, we see that string theory in the smooth KS background gives rise to a bouncing brane cosmology, while the KT approximation would have given rise to a cosmology with a spacelike crunch. There has been great success in understanding the resolution of timelike singularities in string theory, so it is heartening to see that in some special cases one can translate those results to learn about spacelike singularities as well.

Limiting behaviors

In the two asymptotic regimes of $\tau \sim 0$ and very large τ , the formulae simplify [54] and the behavior of $a(t)$ can be given explicitly. For small τ , the geometry is just the product (2.2.12). Hence, in this limit, the brane is effectively falling in an *unwarped* 5d space, and the cosmology is very simple:

$$a(t) = \text{constant} + \mathcal{O}(t^2) . \quad (2.2.25)$$

In the large τ regime, the metric (2.2.14) differs from AdS_5 by logarithmic corrections, and so the brane trajectory deviates very gradually from that of a D3-brane in AdS. For simplicity we present here the induced cosmology on a D3-brane in AdS; the logarithmic corrections require no new ideas but lead to more complicated formulae. From (2.2.18), using the D3-brane form of the AdS_5 metric

$$ds^2 = r^2(-d\xi^2 + dx_1^2 + dx_2^2 + dx_3^2) + \frac{dr^2}{r^2} \quad (2.2.26)$$

we find, in terms of proper time,

$$a^2(t) = a^2(0)\left(1 + 2\frac{\dot{r}_0}{r_0}t\right) \quad (2.2.27)$$

for a brane with initial position and velocity r_0, \dot{r}_0 at $t = 0$. It follows that

$$\left(\frac{\dot{a}}{a}\right)^2 = \frac{C}{a^4} \quad (2.2.28)$$

where $C = a^4(0)\left(\frac{\dot{r}_0}{r_0}\right)^2$. Because the right hand side of (2.2.28) scales like the energy density of radiation, this has been termed “dark radiation” [57,58]. In the language of [38] it might also be called “mirage matter with equation of state $\rho = 3p$.”

The Friedmann equation (2.2.28) has been thoroughly investigated in the context of Randall-Sundrum models. In particular, just such a law was found to arise

on a visible brane which is separated from a Planck brane by an interval whose length varies with time (see [59] and references therein). This is entirely consistent with our scenario, as the Calabi-Yau provides an effective Planck brane and the bulk motion of the probe changes the length of the interval between the branes.

As the brane proceeds to larger τ , eventually it will reach the region where the KS throat has been glued onto a Calabi-Yau space. Beyond that point it is no longer possible for us to say anything universal about the behavior of the brane cosmology.

2.2.5 Issues of Backreaction

There are several issues involving backreaction that merit consideration. To argue that the bounce we have seen in §2.2.4 accurately describes the behavior of the brane as it propagates in from τ_* and back out again, we must ensure that the state with nonzero $\dot{\tau}$ on the brane does not contain enough energy to significantly distort the closed string background geometry. In fact we must check both that a motionless brane in the throat creates a negligible backreaction, and that the kinetic energy on the brane does not undergo gravitational collapse (yielding a clumpy brane) on the relevant timescales. It is also important to understand the extent of the backreaction from semiclassical particle production. Finally, the presence of nonzero energy density on the brane leads to a potential for the Calabi-Yau volume modulus (as in §6 of [60]). We will imagine that this modulus has been fixed and will neglect this effect.

The first concern can be dismissed quickly. In the limit of small g_s the backreaction on the closed string background is small. The second concern needs to be discussed in somewhat more detail. The falling brane necessarily has energy density localized on its worldvolume. After a sufficiently long time this initially uniform energy can become inhomogeneous because of the Jeans instability. In this subsection we demonstrate that, for a suitable choice of the parameters of the KS geometry, this instability is negligible during the bounce portion of the history of the brane universe.

Jeans Instability

For a uniform fluid of density ρ , the Jeans instability appears at length scales greater than $L_{Jeans} \equiv \frac{v_s}{\sqrt{\rho G_N}}$, where v_s is the velocity of sound. Perturbations with

this wavelength could destabilize the brane given a time $t_{instability} \geq L_{Jeans}$. In terms of the volume V_6 of the Calabi-Yau,

$$G_N = g_s^2 l_s^8 V_6^{-1} h(\tau_{UV})^{\frac{1}{2}} h(\tau)^{-\frac{1}{2}} \quad (2.2.29)$$

where we choose τ_{UV} such that r_{UV} (as given in (2.2.13)) is of order one (so the throat extends slightly into the KT regime before gluing into the Calabi-Yau). For the compactifications of interest $V_6 \geq l_s^6$,³ so that for $\tau \leq \tau_{UV}$

$$G_N \leq g_s^2 l_s^2 . \quad (2.2.30)$$

From (2.2.18), (2.2.19), we see that the energy density on the brane is constant,

$$\rho = \frac{1}{2g_s^2 l_s^4} h(\tau_*)^{-1} g_{\tau\tau}(\tau_*) \dot{\tau}_0^2 \quad (2.2.31)$$

so

$$t_{instability} \geq \frac{v_s}{\dot{\tau}_0} h(\tau_*)^{\frac{1}{2}} g_{\tau\tau}(\tau_*)^{-\frac{1}{2}} l_s . \quad (2.2.32)$$

Because the brane accelerates toward the tip of the conifold, to fall from d_* to the tip and rebound requires a time

$$t_{bounce} \leq \frac{2d_*}{v_0} . \quad (2.2.33)$$

This leads to (we now drop numerical factors of order one)

$$\frac{t_{bounce}}{t_{instability}} < \frac{d_*}{l_s} h(\tau_*)^{-\frac{1}{2}} . \quad (2.2.34)$$

Using the asymptotic form of $I(\tau)$, $K(\tau)$ we find

$$\frac{t_{bounce}}{t_{instability}} < \frac{1}{\sqrt{g_s M}} \tau_*^{\frac{3}{4}} l_s^{-2} (\epsilon^2 e^{\tau_*})^{\frac{2}{3}} . \quad (2.2.35)$$

³ In fact, as discussed in [4], warped compactifications really reproduce the RS scenario when the volume is not very large in string units (since the flux and brane backreaction which produce the warping become larger effects at small Calabi-Yau volume). We are assuming we are at the threshold volume where the warping becomes a significant effect, which should justify the estimate (2.2.29).

Because we have glued the KS throat into the Calabi-Yau geometry at a location where $r = r_{UV}$ of (2.2.13) is of order one, we see that $\epsilon^2 e^{\tau_*} = \mathcal{O}(1)$. This leads to

$$\frac{t_{\text{bounce}}}{t_{\text{instability}}} < \frac{1}{\sqrt{g_s M}} \tau_*^{3/4}. \quad (2.2.36)$$

Finally, since the hierarchy between the UV and IR ends of the throat is exponential in τ_* , it is natural to take τ_* to be a number of order 5-10 (in the language of RS scenarios, τ_* controls the length of the interval in AdS radii, up to factors of π). Therefore, in the supergravity regime where $g_s M \gg 1$, (2.2.36) demonstrates that we can neglect the Jeans instability on the brane in discussing the dynamics during the bounce.

Particle Creation

Because the bounce cosmology is strongly time-dependent, it is also important to consider the spectrum of particles created semiclassically by the bounce. We will argue that the energy density due to such particle production is small enough that its backreaction is negligible.

The bounce geometry (2.2.21) is conformally trivial, so massless, conformally coupled scalar fields will not be produced by the cosmological evolution. Massive fields break the conformal invariance. The relevant massive scalar fields on the brane are excited string states with mass $m \geq \frac{1}{l_s}$. Quite generally we expect that modes with frequencies $\omega \gg \frac{\dot{a}}{a} \equiv H$ will not be significantly populated by the bounce, i.e. the probability that a comoving detector will register such a particle long after the bounce is exponentially small in $\frac{\omega}{H}$. The cases of interest involve slow-moving branes, so the maximum value of H is far below the string scale. Thus we expect the energy density due to particle creation should be quite small.

Concrete calculations of the production of massive scalar and fermion fields in a bouncing $k = 0$ FRW cosmology were carried out in [61] (though the system in consideration there did not satisfy Einstein's equations). The scale factor in [61] has the same limiting behaviors as our own, and the results there are consistent with our expectations. It would be interesting to carry out the relevant particle creation calculation directly in string theory. A particle creation calculation in closed string theory was described in worldsheet (2d conformal field theory) language in [62].

2.3 Four-dimensional Lagrangian Description

2.3.1 Effective Lagrangian

In the limit of low matter density on the probe brane, the cosmology is determined entirely by the bulk geometry. The D3-brane trajectory is determined by the Born-Infeld action, and the induced metric along this trajectory provides a time-dependent mirage cosmology. The mirage cosmology proposal of [38] includes another step: one can write down the Friedmann equations for the cosmology and identify the right hand side with mirage density and mirage pressure.

This is not yet an ideal formulation from the perspective of a brane resident. One would like a four-dimensional Lagrangian description of the mirage matter, of the cosmological evolution, and of the variation of G_N . In particular, since a bounce in a flat Friedmann-Robertson-Walker universe necessitates violation of the null energy condition, it would be interesting to understand this violation in terms of a 4d Lagrangian and energy-momentum tensor. In this section we will propose a toy scalar-tensor Lagrangian which admits cosmologies reproducing the basic features of our “bouncing brane” solutions; similar Lagrangians have arisen in the study of RS cosmology [63].

The massless fields in our 4d theory include a 4d graviton and the massless open strings on the D3-brane: a U(1) gauge field A_μ , a scalar Φ_r corresponding to radial motion in the compactified throat, and scalars Φ_i , $i = 1, \dots, 5$ parametrizing motion in the angular coordinates. All other scalar fields are massive. (In fact without a no-force condition there can be a potential and a mass for Φ_r . For simplicity we will work only with the BPS case, but the trajectory of anti-branes in the KS throat would also yield an interesting time-dependent solution.⁴) We will choose to fix the Φ_i , and the requirement of negligible energy density in open string modes on the brane means that A_μ is not relevant for cosmological purposes. This leaves Φ_r and $g_{\mu\nu}$ as the only massless fields entering the 4d Lagrangian.

Our goal in this section is to show explicitly how an observer who sees particle masses which depend on Φ_r could change his units of length and see an FRW cosmology with varying G_N . (In §2.2.4 we provided several arguments motivating

⁴ In particular, anti-branes near the tip of the conifold can annihilate by merging with flux [60]. This could potentially lead to a cosmology which begins or ends with a tunneling or annihilation process.

this choice of frame.) Because the full Lagrangian for a brane observer in the KS background, including all massive fields, is quite complicated, it will be most practical to work with a simpler Lagrangian which has the correct schematic features. In particular, all particle masses depend on Φ_r in the same way, so it will suffice to consider a single massive field χ (which could be, for example, an excited open string mode).

A “mass-varying” Lagrangian with the appropriate features is

$$L = \int d^3x \sqrt{-g} \left(\frac{R}{16\pi G_N} - \frac{R}{12} \Phi_r^2 - \frac{1}{2} g^{\mu\nu} \nabla_\mu \Phi_r \nabla_\nu \Phi_r - \frac{1}{2} g^{\mu\nu} \nabla_\mu \chi \nabla_\nu \chi - \frac{1}{2} m^2(\Phi_r) \chi^2 - V(\chi) \right) \quad (2.3.1)$$

where χ is a matter field on the brane whose mass depends on Φ_r as

$$m^2(\Phi_r) \equiv \Omega^2(\Phi_r) \mu^2 \quad (2.3.2)$$

for fixed μ . The form of the potential for χ and the coupling of χ to the curvature scalar will be unimportant for this analysis, and we will henceforth omit these terms. Note that Φ_r is conformally coupled.

As discussed in §2.2.4, an observer confined to the brane most naturally holds fixed the masses of fields on the brane. This can be accomplished by performing the change of variables

$$\tilde{g}_{\mu\nu} = \Omega^2(\Phi_r) g_{\mu\nu} \quad (2.3.3)$$

$$\tilde{\Phi}_r = \Omega^{-1}(\Phi_r) \Phi_r \quad (2.3.4)$$

$$\tilde{\chi} = \Omega^{-1}(\Phi_r) \chi \quad (2.3.5)$$

The resulting “mass-fixed” Lagrangian is

$$L = \int d^3x \sqrt{-\tilde{g}} \left(\frac{\tilde{R}}{16\pi G_N \Omega^2(\Phi_r)} + \frac{3}{8\pi G_N \Omega(\Phi_r)^4} \tilde{g}^{\mu\nu} \nabla_\mu \Omega \nabla_\nu \Omega - \frac{\tilde{R}}{12} \tilde{\Phi}_r^2 - \frac{1}{2} \tilde{g}^{\mu\nu} \nabla_\mu \tilde{\Phi}_r \nabla_\nu \tilde{\Phi}_r - \frac{1}{2} \tilde{g}^{\mu\nu} \nabla_\mu \tilde{\chi} \nabla_\nu \tilde{\chi} - \frac{1}{2} \mu^2 \tilde{\chi}^2 \right). \quad (2.3.6)$$

We have discarded terms which look like $(\nabla\Omega)^2 \tilde{\chi}^2$ because $\dot{\Omega} \ll \mu$ (at least in our example, where χ represents a massive string mode). Terms which look like $(\nabla\Omega)^2 \tilde{\Phi}_r^2$ cancel due to the conformal coupling of Φ_r .

The effective gravitational coupling is given by

$$G_N^{eff} = G_N \Omega^2(\Phi_r) . \quad (2.3.7)$$

According to the discussion in §2.2.4, we expect that $\Omega^2(\Phi_r) = h(\tau(\Phi_r))^{-\frac{1}{2}}$, so indeed the strength of gravity scales as required by (2.2.24). (We will not need the explicit relation between τ and Φ_r .)

We are interested in the limit where the backreaction due to $\tilde{\Phi}_r, \tilde{\chi}$ is small, so in particular $\tilde{\Phi}_r, \tilde{\chi} \ll m_{Planck}^{eff}$. This means that for the purpose of solving the Einstein equations in the mass-fixed frame we may neglect terms which are suppressed by a factor of G_N . Defining

$$\gamma = \sqrt{\frac{3}{4\pi G_N}} \Omega^{-1}(\Phi_r) \quad (2.3.8)$$

we may write the effective Lagrangian

$$L = \int d^3x \sqrt{-\tilde{g}} \left(\frac{\tilde{R}}{12} \gamma^2 + \frac{1}{2} \tilde{g}^{\mu\nu} \nabla_\mu \gamma \nabla_\nu \gamma + \mathcal{O}\left(\frac{\Phi_r}{m_{Planck}}\right) \right). \quad (2.3.9)$$

Observe that the kinetic energy term is now negative semidefinite (we are using signature $-+++$), so it is easy to violate the null energy condition which is relevant (via the singularity theorems) in constraining the behavior of the metric $\tilde{g}_{\mu\nu}$.⁵

The equation of motion which follows from this Lagrangian is

$$\tilde{g}^{\mu\nu} \nabla_\mu \nabla_\nu \gamma - \frac{\tilde{R}}{6} \gamma = \mathcal{O}\left(\frac{\Phi_r}{m_{Planck}}\right) \quad (2.3.10)$$

Now let us see that this system reproduces our expectations from §2.2.4. Given an FRW cosmology specified by $a(t)$, if we set $\gamma(t) = ca^{-1}(t)$ for some constant c then (2.3.10) is satisfied identically. From (2.3.3), (2.3.4), (2.3.5) it is clear that we should identify

$$a(t) \propto \Omega(\Phi_r(t)). \quad (2.3.11)$$

Then the Einstein equations for (2.3.9) are satisfied if the varying-mass metric $g_{\mu\nu} = \eta_{\mu\nu}$ and the mass-fixed metric $\tilde{g}_{\mu\nu} = a^2(t)\eta_{\mu\nu}$. So as discussed in §2.2.4, we have two complementary perspectives: the brane observer uses the mass-fixed action (2.3.6) and sees an FRW cosmology with varying G_N , while the “closed string” observer sees gravity of fixed strength in Minkowski space.

⁵ Notice that because of the non-minimally coupled scalar, it is also possible to violate the null energy condition which governs the behavior of $g_{\mu\nu}$.

2.3.2 Relation to Warped Backgrounds

We can be slightly more explicit about how the toy model of §2.3.1 would be related to a given warped background. Given any function $a(t)$, we can construct a warped background $h(r)$ such that a no-force brane probe of that geometry experiences an induced cosmology specified by $a(t)$. We simply define $\xi = \int \frac{dt}{a(t)}$, $r = v\xi$ (v constant), and $h(r) = a(r)^{-4}$.

A few comments are in order:

1. Very few backgrounds $h(r)$ will correspond to solutions of IIB supergravity. One which does, and indeed corresponds to a D3-brane in the warped deformed conifold, is given by taking $\tau(t)$ to solve (2.2.19) and setting $a(t) = h^{-\frac{1}{4}}(\tau(t))$ with h given by (2.2.10).
2. The no-force condition is only a convenience. We could instead take $r(\xi)$ to be any function of ξ . This would correspond to a brane which accelerates due to external forces. Again, very few systems of this sort arise from known branes of string theory moving in valid supergravity backgrounds.

2.4 Discussion

As demonstrated in general terms in §2.3, and in a special example in string theory in §2.2, in the presence of scalar fields it is easy to evade the singularity theorems (from the perspective of a reasonable class of observers), even with a $k = 0$ FRW universe. It therefore seems likely that many examples of such constructions, arising both as cosmologies on D-branes and perhaps even as closed string cosmologies, should be possible. The cosmology we presented is just a slice of evolution between some initial time when we join the brane moving down the throat, and a final time when it is heading into the Calabi-Yau region. The later evolution of our model is then non-universal; it depends on the details of the Calabi-Yau model (or in the language of [43], the detailed structure of the Planck brane). It would be very interesting to write down models with 4d gravity whose dynamics can be controlled for an eternity; some controlled, eternal closed string cosmologies were recently described in [62].

The cosmology discussed here is far from realistic. As a first improvement, one would like to study probe branes with a spectrum of massive fields below the scale $\frac{1}{l_s}$ (which could be called “standard model” fields). It may be possible to construct

such examples by using parallel D3-branes which are slightly separated in the radial direction, wrapped Dp-branes with $p > 3$, or anti-branes in appropriate regimes. It is also important to control the time-variation of G_N during/after nucleosynthesis, since this is highly constrained by experiment (see for instance [8]). To improve the situation, one can envision a program of “cosmological engineering.” That is, one could try to design IIB solutions with background fields specifically chosen to give rise to interesting mirage cosmologies (various authors have already proposed mirage models of closed universes [64], inflation with graceful exit [65], asymptotically de Sitter spaces [50], etc., though most of these models do not include 4d gravity). Each desired feature of the cosmology would result in a new condition on the closed string fields. Then one would simply impose these conditions along with the field equations of IIB supergravity.

3. Moduli Trapping at Enhanced Symmetry Points

ABSTRACT OF ORIGINAL PAPER

We study quantum effects on moduli dynamics arising from the production of particles which are light at special points in moduli space. The resulting forces trap the moduli at these points, which often exhibit enhanced symmetry. Moduli trapping occurs in time-dependent quantum field theory, as well as in systems of moving D-branes, where it leads the branes to combine into stacks. Trapping also occurs in an expanding universe, though the range over which the moduli can roll is limited by Hubble friction. We observe that a scalar field trapped on a steep potential can induce a stage of acceleration of the universe, which we call trapped inflation. Moduli trapping ameliorates the cosmological moduli problem and may affect vacuum selection. In particular, rolling moduli are most powerfully attracted to the points with the largest number of light particles, which are often the points of greatest symmetry. Given suitable assumptions about the dynamics of the very early universe, this effect might help to explain why among the plethora of possible vacuum states of string theory, we appear to live in one with a large number of light particles and (spontaneously broken) symmetries. In other words, some of the surprising properties of our world might arise not through pure chance or miraculous cancellations, but through a natural selection mechanism during dynamical evolution.

This chapter is reprinted from Lev Kofman, Andrei Linde, Xiao Liu, Alexander Maloney, Liam McAllister, and Eva Silverstein, “Beauty is Attractive: Moduli Trapping at Enhanced Symmetry Points,” JHEP **0405** (2004) 030, by permission of the publisher. © 2004 by the Journal of High Energy Physics.

3.1 Introduction

3.1.1 Moduli Trapping Near Enhanced Symmetry Points

Supersymmetric string and field theories typically contain a number of light scalar fields, or moduli, which describe low-energy deformations of the system. If the kinetic energy of these fields is large compared to their potential energy then the classical dynamics of the moduli is described by geodesic motion on moduli space.

At certain special points (or subspaces) of moduli space, new degrees of freedom become light and can affect the dynamics of moduli in a significant way [66,67,68,69,70]. These extra species often contribute to an enhanced symmetry at the special point. We will refer to any points where new species become light as ESPs, which stands for extra species points, and also, when applicable, for enhanced symmetry points.

A canonical example is a system of two parallel D-branes. When the branes coincide, the two individual $U(1)$ gauge symmetries are enhanced to a $U(2)$ symmetry, as the strings that stretch between the branes become massless [71]. Similar points with new light species arise in many contexts; examples include the Seiberg-Witten massless monopole and dyon points in $\mathcal{N} = 2$ supersymmetric field theories [72], the conifold point (2.2.3) and ADE singularities in Calabi-Yau compactification [73], the self-dual radius of string compactifications on a torus, small instantons in heterotic string theory [74], and many other configurations with less symmetry.

Classically, there is no sense in which these ESPs are dynamically preferred over other metastable vacuum states of the system. We will argue that this changes once quantum effects are included. In particular, quantum particle production of the light fields alters the dynamics in such a way as to drive the moduli towards the ESPs and trap them there.

The basic mechanism of this trapping effect is quite simple. Consider a modulus ϕ moving through moduli space near an ESP associated to a new light field χ . For example, ϕ could be the separation between a pair of parallel D-branes, and χ a string stretching between the two branes – in this case the ESP $\phi = 0$ is the point where the branes coincide and χ becomes massless. As ϕ rolls through moduli space, the mass of χ changes; χ gets lighter as ϕ moves closer to the ESP and heavier as ϕ moves farther away. This changing mass leads to quantum production of χ particles; as ϕ moves past the ESP some of its kinetic energy will be dumped into χ particles.

As ϕ rolls away from the ESP, more and more of its energy will be drained into the χ sector as the χ mass increases, until eventually ϕ stops rolling. At this point the moduli space approximation for ϕ has broken down, and all of the original kinetic energy contained in the coherent motion of ϕ has been transferred into χ particles, and ultimately into all of the fields interacting with χ (including decoherent quanta $\delta\phi$). As we will see in detail, the χ excitations generate a classical potential for ϕ which drives the modulus back toward the ESP and traps it there.⁶

In the example of the pair of moving D-branes, the consequences of this are simple: two parallel branes that are sent towards each other will collide and remain bound together. The original kinetic energy of the moving branes will be transferred into open string excitations on the branes and eventually into closed string radiation in the bulk.

In §3.3.2 we will describe the general trapping mechanism and study its range of applicability using a few simple estimates. In §3.3 we will write down the equations of motion governing trapping in more detail, and describe the numerical and analytic solutions of these equations in a variety of cases.

It is important to recognize that this trapping effect is in no way special to string theory. Flat space quantum field theory with a moduli space for ϕ and an ESP is an ideal setting for the trapping effect, and it is in this setting that we will perform the analysis of §3.2 and §3.3. In §3.4 we will generalize this to incorporate the effects of cosmological expansion, and in §3.5 we will discuss the possibility of significant effects from string theory. Having established the moduli trapping effect in a variety of contexts, we will then study its applications to problems in cosmology.

The most immediate application is to the problem of vacuum selection. As we will see in §3.6, the trapping effect can provide a dynamical vacuum selection principle, reducing the problem to that of selecting one point within the class of ESPs. This represents significant progress, since the vast majority of metastable vacua are not ESPs. Trapping at ESPs may also help solve the cosmological moduli

⁶ There are also corrections to the effective action for ϕ from loops of χ particles, including both kinetic corrections and a Coleman-Weinberg effective potential. Both effects will be subdominant in the weakly-coupled, supersymmetric, kinetic-energy dominated regimes we will consider.

problem, as we will see in §3.7. In particular, trapping strengthens the proposal of [75] by providing a dynamical mechanism which explains why moduli sit at points of enhanced symmetry.

Finally, as we will explain in §3.8, the trapping of a scalar field with a potential can lead to a period of accelerated expansion, in a manner reminiscent of thermal inflation [76]. This effect, which we will call trapped inflation, can occur in a steeper potential than normally admits such behavior.

From a more general perspective, moduli trapping gives us insight into the celebrated question of why the world is so symmetric. The initial puzzle is that although highly symmetric theories are aesthetically appealing and theoretically tractable, they are also very special and hence, in an appropriate sense, rare. One expects that in a typical string theory vacuum, most symmetries will be strongly broken and most particles will have masses of order the string or Planck mass, just as in a typical vacuum one expects a large cosmological constant. Vacua with enhanced symmetry or light particles should comprise a minuscule subset of the space of all vacua.

Nevertheless, we observe traces of many symmetries in the properties of elementary particles, as spontaneously broken global and gauge invariances. Moreover, all known particles are hierarchically light compared to the Planck mass. Given the expectation that a typical vacuum contains very few approximate symmetries and very few light particles, it is puzzling that we see such symmetries and such particles in our world.

For questions of this nature, moduli trapping may have considerable explanatory power. Specifically, the force pulling moduli toward a point of enhanced symmetry is proportional to the number of particles which become massless at this point, which is often associated with a high degree of symmetry. This means that the most attractive ESPs are typically the ones with the largest symmetry, and rolling moduli are most likely to be trapped at highly symmetric points, where many particles become massless or nearly massless. Moreover, the process of trapping can proceed sequentially: a modulus moving in a multi-dimensional moduli space can experience a sequence of trapping events, each of which increases the symmetry. These effects suggest that the symmetry and beauty we see in our world may have, at least in part, a simple dynamical explanation: beauty is attractive. We will discuss this possibility in §3.6.

3.1.2 Relation to Other Works

Similar effects have been described in the literature. There has been much work on multi-scalar quantum field theory in the context of inflation, especially concerning preheating in interacting scalar field theories. Some of our results will be based on the theory of particle production and preheating developed in the series of papers [66,67,68], which explores many of the basic phenomena in scalar theories of the sort we will consider. Likewise, Chung et al. [69] have explored the effects of particle production on the inflaton trajectory and on the spectrum of density perturbations. Although we will derive what we need here in a self-contained way, many of the technical results in this chapter overlap with those works, as well as with standard results on particle production in time-dependent systems as summarized in e.g. [77]. Although we will not study the case in which χ goes tachyonic for some range of ϕ , our results may nevertheless have application to models of hybrid inflation [78,79], including models based on rapidly-oscillating interacting scalars [80,81,82].

In strong 't Hooft coupling regions of moduli spaces which are accessible through the AdS/CFT correspondence, virtual effects from the large numbers of light species dramatically slow down the motion of ϕ as it approaches an ESP, with the result that the modulus gets trapped there [70]. This also provides a mechanism for slow roll inflation without very flat potentials. In the present work, which applies at weak 't Hooft coupling, it is quantum production of *on-shell* light particles which leads to trapping on moduli space.

Other works in the context of string theory have explored the localization of moduli at ESPs. The authors of [83,84] studied the evolution of a supersymmetric version of the $\phi - \chi$ system arising near a flop transition using an effective supergravity action. They showed that, given nonvanishing initial vevs for both ϕ and χ , the fields will settle at the ESP even if one formally turns off particle production effects. Our proposal, by contrast, is to take into account on-shell quantum effects which dynamically generate a nonzero $\langle \chi^2 \rangle$. In works such as [85] attention was focused on the boundaries of moduli space, while here we focus on ESPs in the interior of moduli space. In [86], production of light strings was studied in the context of D0-brane quantum mechanics; as we explain in §3.2.3, this has some similarities, but important differences, with our case of space-filling branes. Scattering of Dp-branes was also studied in [87].

Dine has suggested that enhanced symmetry points may provide a solution to the moduli problem, as moduli which begin at an enhanced symmetry minimum of the quantum effective potential can consistently remain there both during and immediately after inflation [75]. One would still like to explain why the moduli began at such a point. As we discuss in §3.7, our trapping mechanism provides a natural explanation for this initial configuration.

Horne and Moore [88] have argued that the classical motion on certain moduli spaces is ergodic, provided that the potential energy is negligible. This means that all configurations are sampled given a sufficiently long time, and in particular a given modulus will eventually approach an ESP. We will argue that quantum corrections to the classical trajectory are significant, and indeed lead to trapping, whenever the classical trajectory comes close to an ESP. Combining these two observations, we expect that in the full, quantum-corrected system the moduli are stuck near an ESP at late times. This means that the quantum-corrected evolution is not fully ergodic: the dynamics of [88] (see also [89]) implies that the modulus will eventually approach an ESP, at which point quantum effects will trap it there, preventing the system from sampling any further regions of moduli space.

3.2 Moduli Trapping: Basic Mechanism

We will now describe the mechanism of moduli trapping in more detail. Our discussion in this section will be based on simple estimates of particle production and the consequent backreaction, generalizing the results of [66,67,68] to the case of a complex field. A more complete analysis, along with numerical results, will be presented in §3.3.

We will consider the specific model

$$\mathcal{L} = \frac{1}{2}\partial_\mu\phi\partial^\mu\bar{\phi} + \frac{1}{2}\partial_\mu\chi\partial^\mu\chi - \frac{g^2}{2}|\phi|^2\chi^2 \quad (3.2.1)$$

where a complex modulus $\phi = \phi_1 + i\phi_2$ interacts with a real scalar field χ . We are restricting ourselves to the case of a flat moduli space which has a single ESP at $\phi = 0$, where χ becomes massless, and a particularly simple form for the χ interaction. This simple case illustrates the basic physics and can be generalized as necessary, for example to include supersymmetry.

We will consider the case where ϕ approaches the origin with some impact parameter μ , following a classical trajectory of the form

$$\phi(t) = i\mu + vt. \quad (3.2.2)$$

Classically, if χ vanishes then (3.2.2) is an exact solution to the equations of motion, and the presence of the ESP will not affect the motion of ϕ .

Quantum effects will alter this picture considerably, because the trajectory (3.2.2) will lead to the production of χ particles, as we discuss in §3.2.1. The backreaction of these particles on the motion of ϕ will then lead to trapping, as we will see in §3.2.2. In §3.2.3 we will illustrate this effect with the example of colliding D-branes.

3.2.1 Quantum Production of χ Particles

Let us first study the creation of χ particles without considering how they may backreact to alter the motion of ϕ . In this approximation we may substitute (3.2.2) into the action (3.2.1) to get a free quantum field theory for χ with a time-varying mass

$$m_\chi^2(t) = g^2|\phi(t)|^2. \quad (3.2.3)$$

This time dependence leads to particle production.

Consider a mode of the χ field with spatial momentum k , whose frequency

$$\omega(t) = \sqrt{k^2 + g^2|\phi(t)|^2} \quad (3.2.4)$$

varies in time. This mode becomes excited when the non-adiabaticity parameter $\dot{\omega}/\omega^2$ becomes at least of order one. This parameter vanishes as $t \rightarrow \pm\infty$, indicating that particle creation takes place only while ϕ is near the ESP. It is straightforward to see that, for the trajectory (3.2.2), $\dot{\omega}/\omega^2$ can be large only in the small interval $|\phi| \lesssim \Delta\phi$ near the ESP, where

$$\Delta\phi = \sqrt{\frac{v}{g}}, \quad (3.2.5)$$

and only for momenta

$$\frac{k^2 + g^2\mu^2}{gv} \lesssim 1. \quad (3.2.6)$$

When the quantity on the left hand side is small, particle creation effects are very strong. They are strongest if the modulus passes sufficiently close to the ESP, i.e. if

$$\mu \lesssim \sqrt{v/g}. \quad (3.2.7)$$

In this case χ modes whose momenta k fall in the range (3.2.6) will be excited.⁷ Qualitatively, we expect that the occupation numbers n_k of such modes will vary from zero (no real particles) for modes with vanishing non-adiabaticity to of order unity for modes with very large non-adiabaticity. The full computation of n_k given in Appendix 3.A yields

$$n_k = \exp\left(-\pi \frac{k^2 + g^2 \mu^2}{gv}\right), \quad (3.2.9)$$

which agrees with this qualitative expectation. Note that even when (3.2.7) is not satisfied, there is generically a nonvanishing, though exponentially suppressed, number density of created particles; even in this case we will find a nontrivial trapping effect.

Before discussing the backreaction due to the production of χ particles, it is crucial to control other effects from the χ field. In particular, there is another important quantum effect which arises in motion toward the origin: loops of light χ particles give corrections to the effective action. These include both kinetic corrections and the Coleman-Weinberg potential energy. The latter we will subtract by hand, as we will explain in §3.3.1. This gives a good approximation to the dynamics in any situation where kinetic energy dominates.

The kinetic corrections are organized in an expansion in v^2/ϕ^4 [70]. The parameters controlling both remaining effects – the nonadiabaticity controlling particle production and the kinetic factor v^2/ϕ^4 controlling light virtual χ particles –

⁷ This may be checked as follows. We have argued that unsuppressed particle production occurs only when the modulus is sufficiently close to the ESP, $|\phi| \lesssim \sqrt{v/g}$. The modulus remains within this window for a time

$$\Delta t \sim \frac{\sqrt{v/g}}{v} \sim (gv)^{-1/2}. \quad (3.2.8)$$

The uncertainty principle implies in this case that the created particles will have typical energy $E \sim (\Delta t)^{-1}$ and thus momenta $k \sim (gv - g^2 \mu^2)^{1/2}$. This agrees with the estimate (3.2.6).

diverge as we approach the origin. However, at weak coupling, the nonadiabaticity parameter is parametrically enhanced relative to the kinetic corrections, i.e. $v^2/g^2\phi^4 \gg v^2/\phi^4$, so we can sensibly focus on the effects of particle production. More specifically, we can ensure that the kinetic corrections are insignificant by including a sufficiently large impact parameter μ .

We will also analyze the case of small μ , including $\mu = 0$. This relies on the plausible assumption that the effects of the kinetic corrections remain subdominant as we approach very close to the origin, and that in particular in our weak coupling case they do not by themselves stop ϕ from progressing through the origin. It would be interesting to develop theoretical tools to analyze this issue more directly and check this hypothesis.

3.2.2 Backreaction on the Motion of ϕ

One might expect *a priori* that any description of the motion of ϕ which fully incorporates backreaction from particle production would be immensely complicated. Fortunately, this turns out not to be the case, and a simple description is possible. The key simplification is that creation of χ particles happens primarily in a small vicinity of the ESP $\phi = 0$, so one can treat this as an instant event of particle production. These particles induce a very simple linear, confining potential acting on ϕ , $V \sim |\phi|$. The motion of ϕ in this potential between successive events of particle production can be described rather simply.

Let us now explore this in more detail. We have seen that as ϕ moves in moduli space, some of its energy will be transferred into excitations of χ . This leads to a quantum vacuum expectation value $\langle \chi^2 \rangle \neq 0$. As ϕ rolls away from the ESP, the mass of the created χ particles increases, further increasing the energy contained in the χ sector. At this point the backreaction of the χ field on the dynamics of ϕ becomes important, and the moduli space approximation breaks down.

We will concentrate on the backreaction of the created particles on the motion of the field ϕ far away from the small region of non-adiabaticity, i.e. for $\phi \gg \Delta\phi \sim \sqrt{v/g}$. At this stage the typical momenta are such that the χ particles are nonrelativistic, $k \lesssim \sqrt{g\bar{v}} \ll g|\phi|$. Therefore the total energy density of the gas of χ particles is easily seen to be

$$\rho_\chi(\phi) = \int \frac{d^3k}{(2\pi)^3} n_k \sqrt{k^2 + g^2|\phi(t)|^2} \approx g|\phi(t)| n_\chi, \quad (3.2.10)$$

where n_χ is the number density of χ particles,

$$n_\chi = \int \frac{d^3k}{(2\pi)^3} n_k = \frac{(gv)^{3/2}}{(2\pi)^3} e^{-\pi g\mu^2/v} \quad (3.2.11)$$

As ϕ continues to move away from the ESP $\phi = 0$, the number density of χ particles remains constant, as particles are produced only in the vicinity of $\phi = 0$. However, the energy density of the χ particles grows as $g|\phi(t)|n_\chi$. This leads to an attractive force of magnitude gn_χ , which always points towards the ESP $\phi = 0$.

This force of attraction slows down the motion of ϕ , and eventually turns ϕ back toward the ESP. This reversal occurs in the vicinity of the point ϕ_* at which the initial kinetic energy density $\frac{1}{2}\dot{\phi}^2 \equiv \frac{1}{2}v^2$ matches the energy density ρ_χ contained in χ particles. We find

$$\phi_* = \frac{4\pi^3}{g^{5/2}} v^{1/2} e^{\pi g\mu^2/v}. \quad (3.2.12)$$

Observe that for $g \ll 1$ the trapping length on the first pass is always much greater than the impact parameter μ , which means that the motion of the moduli after the first impact is effectively one-dimensional.

After changing direction at ϕ_* , ϕ falls back toward the origin. On this second pass by the ESP, more χ particles are produced, leading to a stronger attractive force. This process repeats itself, leading ultimately to a trapped orbit of ϕ about the ESP, in a trajectory determined by the effective potential and consistent with angular momentum conservation on moduli space.

We conclude that, in this simplified setup, a scalar field which rolls past an ESP will oscillate about the ESP with an initial amplitude given by (3.2.12).

In fact, in many cases the amplitude of these oscillations will rapidly decrease due to the effect of parametric resonance, similar to the effects studied in the theory of preheating [66], and the field ϕ will fall swiftly towards the ESP. This important result will be described in more detail in §3.3.3.

So far we have not incorporated the effects of scattering and decay of the χ particles. These could weaken the trapping potential (3.2.10) by reducing the number of χ particles. Specifically, the energy density ρ_χ contained in a fixed number of χ particles (3.2.10) grows at late times, since the χ mass increases as ϕ rolls away from the ESP. However, if the number density of χ particles decreases due to annihilation or decay into lighter modes, this mass amplification effect is

lost. It is therefore important to determine the rate of decay and annihilation of the χ particles.

In Appendix 3.B we address these issues and demonstrate that the trapping effect is robust for certain parameter ranges, provided that the light states are relatively stable. This stability can easily be arranged in supersymmetric models, and in fact occurs automatically in certain D-brane systems.

Rescattering effects, in contrast, may actually strengthen the trapping effect. Once χ particles have been created, they will scatter off of the homogeneous ϕ condensate, causing it to gradually decay into inhomogeneous, decoherent ϕ excitations [66,90,91]. However, we will not consider this potentially beneficial effect here.

3.2.3 The Example of Moving D-branes

Before proceeding, it may be illustrative to discuss these results in terms of a simple, mechanical example – a moving pair of D-branes. The moduli space of a system of two D-branes is the space of brane positions. In terms of the brane worldvolume fields the separation between the two branes can be regarded as a Higgs field ϕ . The off-diagonal components of the $U(2)$ gauge field are the W bosons. At the ESP of this system, $\phi = 0$, the W bosons are massless. Away from $\phi = 0$ the W bosons acquire a mass by the Higgs mechanism, breaking the symmetry group from $U(2)$ down to $U(1) \times U(1)$. If we identify χ with the W field⁸ and $g^2 \sim g_{YM}^2 \sim g_s$ with the string coupling, then we find that the brane worldvolume theory contains a term like (3.2.1). We therefore expect this system to exhibit moduli trapping.

The trapping effect is a quantum correction to the motion of D-branes. As the D-branes approach each other, the open strings stretched between them become excited. When the D-branes pass by each other and begin moving apart the stretched open strings become massive and pull the D-branes back together. We depict this in Figure 3.

This effect can be a significant correction to the dynamics of any system with a number of mobile, mutually BPS D-branes. Consider, for example, N D3-branes which fill spacetime and are transverse to a compact six-manifold M . Let us take these branes to begin with small, random, classical velocities in M . The classical

⁸ For simplicity we ignore the superpartner of the χ boson.

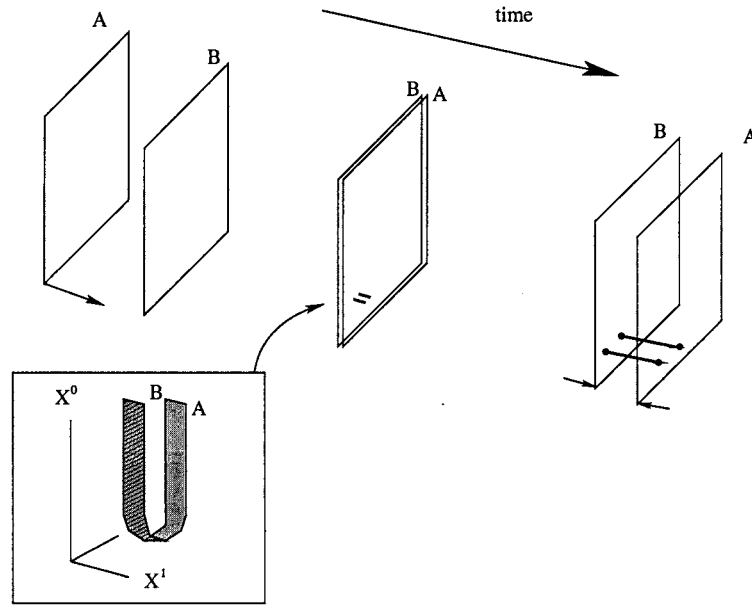


Fig. 3: This figure illustrates the creation of open strings as two D-branes pass near each other. The left corner shows the target space picture of the creation of the open strings.

dynamics of this system is similar to that of a nonrelativistic, noninteracting, classical gas. When we include quantum production of light strings, the branes begin to trap each other, pairwise or in small groups, then gradually agglomerate until only a few massive clumps of many branes remain.

One interesting consequence is that such a system will tend to exhibit enhanced gauge symmetry, with gauge group $U(N)$ if the final state consists of a single clump. (Hubble friction may bring the branes to rest before the aggregation is complete, in which case the gauge group will be a product of smaller factors; we will address related issues in §3.4.1.) Another important effect of massive clumps is their gravitational backreaction: a large cluster of D-branes will produce a warped throat region in M , which may be of phenomenological interest [92].

There are additional corrections to the classical moduli space approximation of the D-brane motion which come from velocity-dependent forces. These correspond in the D-brane worldvolume field theory to higher-derivative corrections generated by virtual effects. When this field theory is at weak 't Hooft coupling, open string production is the dominant effect as one approaches an ESP. However, sufficiently

large clusters of branes will be described by gauge theories at strong 't Hooft coupling, where the dynamics of additional probe branes is governed instead by the analysis of [70].⁹

A similar interaction was studied in the context of the scattering of D0-branes in [86]. There is a crucial difference between that system and the case of interest here, in which the branes are extended along 3 + 1 dimensions. In the D0-brane problem, there is a nontrivial probability for the D0-branes to pass by each other without getting trapped: because the D0-brane is pointlike, there is some probability for no open strings between them to be created or for those created to annihilate rapidly. This is the leading contribution to the S-matrix. In our case, there is always a nonzero number *density* of particles created. As we argue in Appendix 3.B, for certain ranges of parameters these particles do not annihilate rapidly enough to prevent trapping.

3.3 Moduli Trapping: Detailed Analysis

In the previous section we gave an intuitive explanation of the trapping effect, which we will now describe in more detail. In §3.3.1 we will present the equations of motion which govern the trajectory of the modulus ϕ , including the backreaction due to production of light particles. These equations are difficult to solve exactly, so in §3.3.2 we will integrate the system numerically. In §3.3.3 we focus on the special case $\mu = 0$, where the modulus rolls directly through the ESP. In this case analytic techniques are available, and as we will see the trapping effect is considerably stronger than in the $\mu \neq 0$ case.

3.3.1 Formal Description of Particle Production Near an ESP

The full equations of motion are found by coupling the classical motion of ϕ to the time-dependent χ quantum field theory defined by (3.2.1).¹⁰

In general, the presence of an ESP will alter the moduli dynamics in two ways. First, any χ excitations produced by the mechanism described above will backreact on the classical evolution of ϕ . In particular, as we saw in (3.2.10), a non-zero

⁹ A further correction to our dynamics could arise if, as we will discuss in §3.5, the branes keep moving until the system is beyond the range of effective field theory.

¹⁰ We remain in flat space quantum field theory, reserving gravitational effects for §3.4.

expectation value $\langle \chi^2 \rangle \neq 0$ arising from particle production effectively acts like a linear potential for ϕ and drives the moduli towards the origin. This is the effect we wish to describe. Second, virtual χ particles generate quadratic and higher-derivative contributions to the effective action as well as an effective potential for a spacetime-homogeneous ϕ .

As we discussed in §3.2.1, we can neglect the kinetic corrections in our weakly-coupled situation. The interaction in (3.2.1) also induces important radiative corrections to the effective potential. Specifically, it leads to a Coleman-Weinberg effective potential and three UV-divergent terms:

$$V_{eff}(\phi) = \Lambda_{eff} + g^2 m_{eff}^2 \phi^2 + g^4 \lambda_{eff} \phi^4. \quad (3.3.1)$$

These UV divergences could be subtracted by hand using appropriate counterterms. In a supersymmetric system these divergences are absent.

In order to isolate the effects of particle production at the order we are working, we will subtract by hand the entire Coleman-Weinberg effective potential for ϕ that is generated by one loop of χ particles. This mimics the effect of including extended supersymmetry, which is a toy case of interest in string theory and supergravity. For the more realistic $\mathcal{N} = 1$ supersymmetry in four dimensions, radiative corrections do generically generate a nontrivial potential energy. Nevertheless, particle production effects can still dominate the virtual corrections to the potential after spontaneous supersymmetry breaking. The reason is that bosons and fermions contribute with opposite signs in loops, but on-shell bosons and fermions, such as those produced by the changing mass of χ , contribute with the same sign to backreaction on ϕ .

To describe the production of χ particles, we first expand the quantum field χ in terms of Fock space operators as

$$\chi = \sum_k a_k \chi_k + a_k^\dagger \chi_k^* \quad (3.3.2)$$

where the χ_k are a complete set of positive-frequency solutions to the Klein-Gordon equation with mass

$$m_\chi^2(t) = g^2 |\phi(t)|^2. \quad (3.3.3)$$

Expanding in plane waves

$$\chi_k = u_k(t) e^{ik \cdot x} \quad (3.3.4)$$

the equation of motion is

$$\left(\partial_t^2 + k^2 + g^2|\phi(t)|^2\right)u_k = 0. \quad (3.3.5)$$

The modes (3.3.4) are normalized with respect to the Klein-Gordon inner product, which fixes

$$u_k^* \dot{u}_k - \dot{u}_k^* u_k = -i. \quad (3.3.6)$$

The wave equation (3.3.5) has two linearly-independent solutions for each k , so in general there will be many inequivalent choices of positive-frequency modes χ_k . Each such choice of mode decomposition defines a set of Fock space operators via (3.3.2), which in turn define a vacuum state of the theory. The wave equation depends explicitly on time, so there is no canonical choice of Poincaré invariant vacuum. Instead, there is a large family of inequivalent vacua for χ .

We can choose a set of positive frequency modes u_k^{in} that take a particularly simple form in the far past,

$$u_k^{in} \rightarrow \frac{1}{\sqrt{2\sqrt{k^2 + g^2|\phi|^2}}} e^{-i \int^t \sqrt{k^2 + g^2|\phi(t')|^2} dt'} \quad \text{as } t \rightarrow -\infty. \quad (3.3.7)$$

This choice of mode decomposition defines a vacuum state $|in\rangle$. In the far past the phases of the solutions (3.3.7) are monotone decreasing with t , indicating that the state $|in\rangle$ has no particles in the far past. This state, known as the adiabatic vacuum, evolves into a highly excited state as the modulus ϕ rolls past the ESP.

We can now write down the classical equation of motion for ϕ including the effects of χ production. Including a subtraction δ_M , to be determined shortly, it is

$$\left(\partial^2 + g^2(\langle\chi^2\rangle - \delta_M)\right)\phi = 0. \quad (3.3.8)$$

The expectation value $\langle\chi^2\rangle$ depends on time and is calculated in the adiabatic vacuum $|in\rangle$. At time t

$$\langle in|\chi^2(t)|in\rangle = \int \frac{d^3k}{(2\pi)^3} |u_k^{in}(t)|^2. \quad (3.3.9)$$

where the u_k^{in} are determined by the boundary condition (3.3.7) in the far past.

In order to subtract the Coleman-Weinberg potential, we must remove the contribution to $\langle \chi^2 \rangle$ coming from one loop of χ particles, replacing the χ mass-squared with $g^2|\phi(t)|^2$. That is, the subtraction δ_M can be written as

$$\delta_M \equiv \int \frac{d^3k}{(2\pi)^3} \frac{1}{2\sqrt{k^2 + g^2|\phi|^2}}. \quad (3.3.10)$$

With this form it is straightforward to see that when the impact parameter is very large, $(\langle \chi^2 \rangle - \delta_M)$ is negligible and ϕ follows its original trajectory (3.2.2).

To summarize, the effects of quantum production of χ particles on the classical motion of the modulus ϕ are governed by:

$$\begin{aligned} (\partial^2 + g^2(\langle \chi^2 \rangle - \delta_M))\phi &= 0 \\ (\partial_t^2 + k^2 + g^2|\phi(t)|^2)u_k^{in} &= 0 \\ \langle \chi^2(t) \rangle &= \int \frac{d^3k}{(2\pi)^3} |u_k^{in}(t)|^2. \end{aligned} \quad (3.3.11)$$

The above equations of motion can be reformulated in terms of the energy transferred between the two systems. In particular, it is straightforward to show that the coupled equations (3.3.11) are equivalent to the statement

$$\frac{d}{dt}H_\phi = -\frac{d}{dt}\langle in|H_\chi|in \rangle. \quad (3.3.12)$$

The left-hand side of (3.3.12) involves the classical energy of the rolling $\phi(t)$ fields, whereas the right hand side is an expectation value of the time-dependent χ Hamiltonian calculated in quantum field theory. This is the more precise form of energy conservation which applies to our rough estimate in §3.2.2.

Furthermore, the angular momentum on moduli space is conserved, since the action (3.2.1) is invariant under phase rotations $\phi \rightarrow \phi e^{i\theta}$. In the present case (3.2.1), the χ particles do not carry angular momentum, so the orbit of ϕ around the ESP will have fixed angular momentum. The result is an angular momentum barrier which keeps the modulus at a finite distance from the ESP.

More complicated scenarios allow for the exchange of angular momentum between ϕ and χ . This includes the case of colliding D-branes, where the strings stretching between the two D-branes can carry angular momentum. Moreover, as we will see in §3.4, the situation changes once gravitational effects are included, as angular momentum is redshifted away by cosmological expansion. This leads to scenarios where the moduli are trapped exactly at the ESP, rather than orbiting around it at some finite distance.

3.3.2 Moduli Trapping: Numerical Results

The coupled set of integral and differential equations (3.3.11) governing the trapping trajectory is hard to solve in general. Some analytic results can be obtained through an expansion in the non-adiabaticity parameter $\dot{\omega}/\omega^2$, combined with a systematic iteration procedure. However, as time goes on, the mass amplification of the χ particles makes higher-order terms as well as non-perturbative terms in the adiabatic expansion crucial for the motion of the moduli. This makes it very hard to proceed analytically to obtain the detailed evolution of the system.

We have therefore numerically integrated the coupled equations (3.3.11) in Mathematica, using a discrete sum to approximate the momentum integral k , and implementing the subtraction of the Coleman-Weinberg potential described above.

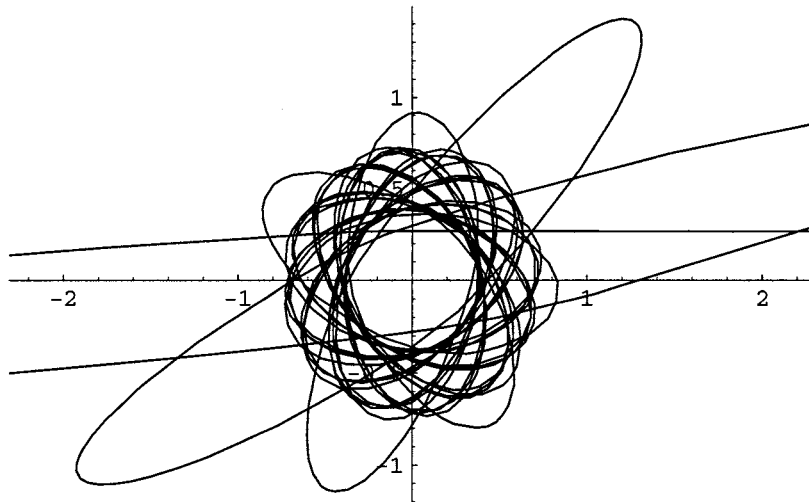


Fig. 4: This figure shows the evolution, in the complex ϕ plane, of a system with parameters $g^2 = 20, \mu = 0.3, v = 1$. The field rolls in from the right and gets trapped into the precessing orbit exhibited in the plot. The orbit is initially an elongated ellipse, but gradually becomes more circular. In an expanding universe, the field would lose its angular momentum, so that the radius of the circle would eventually shrink to zero.

In Figure 4 we plot a trajectory for the case $\mu > 0$, where ϕ becomes trapped in a spiral orbit around the ESP. The radius of the orbit varies with the parameters, but the qualitative features shown are typical.

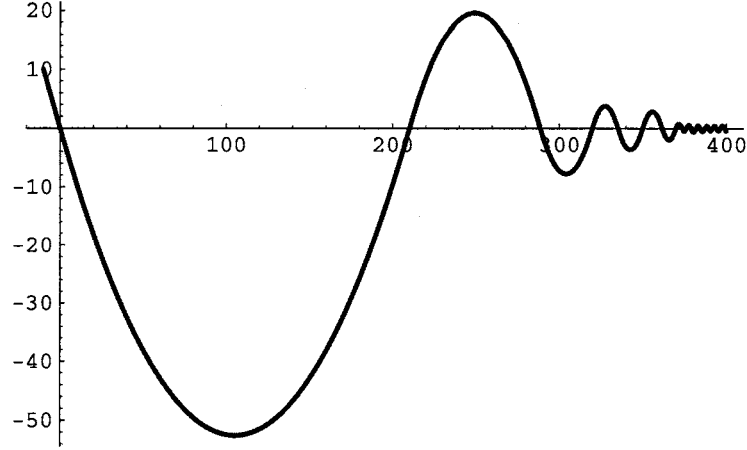


Fig. 5: This shows one-dimensional trapping, in which ϕ passes directly through the ESP $\phi = 0$. The vertical axis is the real part of ϕ , and the horizontal axis is time. The amplitude of the oscillations decreases exponentially as a result of parametric resonance, as we explain in §3.3.3.

In Figure 5 we plot the trajectory of a modulus which is aimed to pass directly through an ESP, with vanishing impact parameter. In this case the motion becomes effectively one-dimensional, and the field moves directly through the ESP $\phi = 0$. The trapping effect in this case is especially strong, and can be understood analytically to come from resonant production of χ particles, as we will now explain.

3.3.3 The Special Case of One-Dimensional Motion

In this section we will concentrate on the interesting and important special case of one-dimensional motion, i.e. vanishing impact parameter μ . Perhaps surprisingly, this is a good approximation to the general case. Indeed, the results of §3.2 demonstrate that trapping becomes exponentially suppressed when the impact parameter μ (the imaginary part of the moduli field) becomes greater than $\sqrt{\frac{v}{\pi g}}$. On the other hand, for $\mu \ll \sqrt{\frac{v}{\pi g}}$ the motion of the field ϕ stops at $\phi_* \sim \frac{4\pi^3 v^{1/2}}{g^{5/2}}$. The ratio of ϕ_* to μ in the regime where trapping is efficient (i.e. for $\mu < \sqrt{\frac{v}{\pi g}}$) is therefore

$$\frac{\phi_*}{\mu} > \frac{4\pi^{7/2}}{g^2} . \quad (3.3.13)$$

Thus, in the case of efficient trapping and weak coupling, the ellipticity of the moduli orbit is very high, so that the motion is effectively one-dimensional.

In the case $\mu = 0$ the number density of χ particles created when the field ϕ passes the ESP is

$$n_\chi = \frac{(gv)^{\frac{3}{2}}}{(2\pi)^3} . \quad (3.3.14)$$

At $|\phi| \gg \sqrt{\frac{v}{g}}$, when the χ particles are nonrelativistic, the mass of each particle is equal to $g|\phi|$, and their energy density is given by [67]

$$\rho_\chi(\phi) = gn_\chi|\phi| = \frac{g^{\frac{5}{2}}v^{3/2}}{(2\pi)^3} |\phi| \quad (3.3.15)$$

We have written $|\phi|$ because this energy does not depend on the sign of the field ϕ . This will be very important for us in what follows.

One should note that, strictly speaking, the χ particles have some kinetic energy even at $\phi = 0$, but for $g \ll 1$ this energy is much smaller than the kinetic energy of ϕ [67]:

$$\rho_\chi(\phi = 0) \sim \frac{g^2}{4\pi^{7/2}} \frac{v^2}{2} = \frac{g^2}{4\pi^{7/2}} \rho_\phi^{\text{kin}} . \quad (3.3.16)$$

This means that the energy of ϕ decreases only slightly when it passes through the ESP $\phi = 0$. Although the initial energy in χ particles is small, this energy increases with $|\phi|$, $\rho_\chi \sim gn_\chi|\phi|$, and creates an effective potential for ϕ . The equation of motion for ϕ in this potential is [66]:

$$\ddot{\phi} + gn_\chi \frac{\phi}{|\phi|} = 0 . \quad (3.3.17)$$

The last term means that ϕ is attracted to the ESP $\phi = 0$ with a constant force proportional to n_χ .

At some location ϕ_1^* the χ energy density ρ_χ equals the initial kinetic energy density $\frac{1}{2}\dot{\phi}^2 \equiv \frac{1}{2}v^2$; at this point ϕ stops and then falls back toward $\phi = 0$.

On this second pass by the origin, the energy density of the χ particles again becomes much smaller than the kinetic energy of ϕ . Energy conservation implies that ϕ will pass the point $\phi = 0$ at almost exactly the initial velocity v . Since the conditions are almost the same as on the first pass, new χ particles will be created, i.e. n_χ will increase. The field ϕ will continue moving for a while, stop at some point ϕ_2^* , and then fall back once more to the ESP, creating more particles. Because each new collection of particles is created in the presence of previous generations of

particles, the process occurs in the regime of parametric resonance, as in the theory of preheating.

A detailed theory of this process was considered in [66]; see in particular Eqs. (59),(60). By translating the problem into a one-dimensional quantum mechanics system (as in Appendix 3.A) with a particle scattering repeatedly across an inverted harmonic potential, [66] calculated the multiplicative increase of the Bogoliubov coefficients during each pass in terms of the reflection and transition amplitudes. In application to our problem, the equations describing the occupation numbers of χ particles with momentum k produced when the field passes through the ESP $j + 1$ times look as follows:

$$n_k^{j+1} = n_k^j \exp(2\pi\mu_k^j), \quad (3.3.18)$$

where

$$\mu_k^j = \frac{1}{2\pi} \ln \left(1 + 2e^{-\pi\xi^2} - 2 \sin \theta^j e^{-\frac{\pi}{2}\xi^2} \sqrt{1 + e^{-\pi\xi^2}} \right). \quad (3.3.19)$$

Here $\xi^2 = \frac{k^2}{gv}$ and θ^j is a relative phase variable which takes values from 0 to 2π . In a cyclic particle creation process in which the parameters of the system change considerably during each oscillation (which is our case, as will become clear shortly), the phases θ^j change almost randomly. As a result, the coefficient μ_j for small k takes different values, from 0.28 to -0.28 , but for 3/4 of all values of the angle θ^j the coefficient μ_j is positive. The average value of μ_j is approximately equal to 0.15. This means that, on average, the number density of χ particles grows by approximately a factor of two or three each time that ϕ passes through the ESP $\phi = 0$.

But this means that with each pass, the coefficient n_χ in (3.3.15) grows by a factor of two or three. It follows that the effective potential becomes two to three times more steep with each pass. Correspondingly, the maximal deviation $|\phi_i^*|$ from the point $\phi = 0$ exponentially decreases with each new oscillation. Since the velocity of the field at the point $\phi = 0$ remains almost unchanged until ϕ loses its energy to the created particles, the duration of each oscillation decreases exponentially as well. Therefore the whole process takes a time $\mathcal{O}(10)\phi_1^*/v$, after which the backreaction of the created particles becomes important, and the field falls to the ESP.

This process is very similar to the last stages of preheating, as studied in [66]. The main difference is that in the simplest models of preheating the field

oscillates near the minimum of its classical potential. In our case the effective potential is initially absent, but a potential is generated due to the created particles. This is exactly what happens at the late stages of preheating, when the effective potential (with an account taken of the produced particles) becomes dominated by the rapidly-growing term proportional to $|\phi|$; see the discussion in Section VIII B of [66].

We would like to emphasize that until the very last stages of the process, the backreaction of the created particles can be studied by the simple methods described above. At this stage the total number of created particles is still very small, but their number grows exponentially with each new oscillation. This leads to an exponentially rapid increase of the steepness of the potential energy of the field ϕ (3.3.15) and, correspondingly, to an exponentially rapid decrease of the amplitude of its oscillations. This extremely fast trapping of ϕ happens despite the fact that at this first stage of oscillations the total energy of ϕ , including its potential energy, remains almost constant.

Once the amplitude of oscillations becomes smaller than the width of the nonadiabaticity region, $|\phi(t)| \lesssim \Delta\phi \sim \sqrt{v/g}$, one can no longer assume that the number of particles will continue to grow via a rapidly-developing parametric resonance. The amplitude of the oscillations is given by $\frac{v^2}{2g|\phi|n_\chi}$, so the amplitude becomes $\mathcal{O}(\sqrt{v/g})$ when the total number of the produced particles grows to

$$n_\chi \sim v^{3/2} g^{-1/2} . \quad (3.3.20)$$

Note that the typical energy of each χ particle at $|\phi(t)| \sim \sqrt{v/g}$ is of the same order as its kinetic energy $\mathcal{O}(\sqrt{gv})$. One can easily see that the total energy density of particles χ at that stage is roughly $\sqrt{gv}n_\chi \sim \mathcal{O}(v^2)$, i.e. it is comparable to the initial kinetic energy of ϕ .

Thus, our estimates indicate that the regime of the broad parametric resonance ends when a substantial part of the initial kinetic energy of ϕ is converted to the energy of the χ particles, and the amplitude of the oscillating field ϕ becomes comparable to the width of the nonadiabaticity region,

$$|\phi| \sim \Delta\phi = \sqrt{v/g} . \quad (3.3.21)$$

We will use these estimates in our discussion of the cosmological consequences of moduli trapping. In order to obtain a more complete and reliable description of

the last stages of this process one should use lattice simulations, taking into account the rescattering of created particles [90,91]. An investigation of a similar situation in the theory of preheating has shown that rescattering makes the process of particle production more efficient. This speeds up the last stages of particle production and leads to a rapid decay of the field ϕ [93], which in our case corresponds to a rapid descent of ϕ toward the enhanced symmetry point.

3.4 Trapped Moduli in an Expanding Universe

3.4.1 Rapid Trapping

In this section we will study the conditions under which the trapping mechanism in quantum field theory survives the effects of coupling to gravity in an expanding universe.

First, we should point out one very beneficial effect of cosmological expansion. The field-theoretic mechanism presented above often leads to moduli being trapped in large-amplitude fluctuations (3.2.12) around an ESP when $\mu \neq 0$. On timescales where the expansion is noticeable, Hubble friction will naturally extract the energy from this motion, drawing the modulus inward and leading the modulus to come to rest at the ESP.

Let us now ask whether the expansion of the universe can impede moduli trapping. Consider a system of moduli coupled to gravity, with the fields arranged to roll near an ESP. For simplicity we will consider FRW solutions with flat spatial slices,

$$ds^2 = dt^2 - a(t)^2 d\vec{x}^2. \quad (3.4.1)$$

The Friedman equation determining $a(t)$ is

$$3H^2 = \frac{1}{M_p^2} \rho \quad (3.4.2)$$

where $H = \dot{a}/a$ and ρ is the energy density of the moduli.

The trapping effect will be robust against cosmological expansion if the timescale governing trapping is short compared to H^{-1} , i.e. if $H \ll v/\phi_*$, where ϕ_* is given by (3.2.12). Assuming that the potential energy of the moduli is non-negative, this implies that

$$\phi_* \ll \sqrt{6}M_p \rightarrow \frac{4\pi^3}{6^{1/2}g^{5/2}} \frac{v^{1/2}}{M_p} e^{\pi g \mu^2/v} \ll 1. \quad (3.4.3)$$

This condition suffices to ensure that trapping is very rapid.

If this condition is satisfied, trapping occurs in much less than a Hubble time, in which case the analysis of §3.2 and §3.3 remains valid. We will show in §3.4.3 that even when (3.4.3) is not satisfied, trapping does still occur, although with somewhat different dynamics.

3.4.2 Scanning Range in an Expanding Universe

An important effect of the gravitational coupling is that during the expansion of the universe, the energy density in produced χ particles dilutes like $1/a^3$ if they are non-relativistic and like $1/a^4$ if they are relativistic. The energy in coherent motion of ϕ , however, has the equation of state $p = \rho$ and therefore dilutes much faster, as $1/a^6$.

This effect reduces the range of motion for the moduli even before they encounter any ESPs. Hubble friction slows the progress of any rolling scalar field, and if the distance between ESPs is sufficiently large then a typical rolling modulus will come to rest without ever passing near an ESP. In order to apply our results to the vacuum selection problem, we will need to know how large a range of ϕ we can scan over in the presence of Hubble friction. This can be obtained as follows [94].

If we are in an FRW phase,

$$a(t) = a_0 t^\beta \quad (3.4.4)$$

then the equation of motion for ϕ (ignoring any potential terms)

$$\ddot{\phi} + 3H\dot{\phi} = 0 \quad (3.4.5)$$

has solutions of the form

$$\dot{\phi}(t) = v \left(\frac{t_0}{t} \right)^{3\beta}. \quad (3.4.6)$$

We can integrate this to determine how far the field rolls before stopping.

Let us first consider the case $\beta = 1/3$, which corresponds to the equation of state $p = \rho$. This includes the case where the coherent, classical kinetic energy of ϕ drives the expansion. The value of ϕ ,

$$\phi(t) = vt_0 \log \left(\frac{t}{t_0} \right) \quad (3.4.7)$$

diverges at large t . Thus ϕ can travel an arbitrarily large distance in moduli space.

In the more general case $\beta > 1/3$ the field will travel a distance

$$\phi(t) - \phi(t_0) = \frac{v}{H(t_0)} \frac{\beta}{3\beta - 1} \quad (3.4.8)$$

before stopping.

In order to be in a phase with $\beta > 1/3$, the kinetic energy of ϕ must not be totally dominant; that is, we must have $\frac{1}{2}\dot{\phi}^2 < \rho$, where $\rho \equiv 3M_p^2 H^2$ is the total energy density appearing on the right hand side of the Friedman equation. Plugging this into (3.4.8) we obtain the constraint

$$\phi(t) - \phi(t_0) < \sqrt{6}M_p \frac{\beta}{3\beta - 1}. \quad (3.4.9)$$

Let us consider a specific example. Suppose that we start at t_0 with kinetic energy domination: $K_0/\rho_0 = 1 - \epsilon$, $\epsilon \ll 1$, in some region of the universe that can be modelled as an expanding FRW cosmology. The kinetic energy drops like $K \sim \rho_0(a_0/a)^6 \sim \rho_0(t_0/t)^2$, while the other components of the energy dilute like

$$\rho(t) = \epsilon\rho_0(t_0/t)^{1+w}, \quad (3.4.10)$$

with $w < 1$. The universe will stop being kinetic-energy dominated at the time $t_c = t_0\epsilon^{-1/(1-w)}$, at which point, according to (3.4.7), the modulus has travelled a distance

$$\phi(t_c) - \phi(t_0) = -\frac{1}{1-w}vt_0 \log \epsilon. \quad (3.4.11)$$

After this the field keeps moving and covers an additional range

$$\phi(t_*) - \phi(t_c) = \sqrt{3}M_p \frac{2}{3(1-w)}. \quad (3.4.12)$$

To get a feel for the numbers, consider the case where $vt_0 \sim M_p$, $\epsilon \sim 10^{-2}$, and $w = 0$. Then ϕ will travel a total distance $\phi(t_*) - \phi(t_0) \sim 6M_p$ in field space, which is not particularly far. However, as we will discuss in §3.6, certain moduli spaces of interest have a rich structure on sub-Planckian scales, so in these cases there is a good chance that the modulus will encounter an ESP and get trapped before Hubble friction brings the system to rest.

There is another natural possibility if we assume low-energy $\mathcal{N} = 1$ supersymmetry. If the moduli acquire their potentials from supersymmetry breaking then

there is a large ratio between the Planck scale and the scale of these potentials, leading to significant scanning ranges. Specifically, consider a contribution to the energy density coming from a potential energy V at the supersymmetry-breaking scale. If the initial kinetic energy of the moduli is Planckian and the supersymmetry-breaking scale is TeV then there will be a prolonged phase in which kinetic energy dominates, since $\epsilon = V/M_p^4 \sim 10^{-64}$. This allows ϕ to scan a significantly super-Planckian range in field space.

3.4.3 Trapping in an Expanding Universe

We are now in a position to combine all the relevant effects and consider trapping during expansion of the universe. For simplicity, we will concentrate on the case of effectively one-dimensional motion, $\mu \ll \sqrt{v/g}$. Suppose that, taking into account Hubble friction, the modulus field passes in the vicinity of the ESP at some moment t_0 , so that χ particles are produced, with $n_\chi(t_0) = \frac{(gv)^{3/2}}{(2\pi)^3}$. We will now determine the remaining evolution including both our trapping force and Hubble friction. After the particles have been produced, the field ϕ becomes attracted toward $\phi = 0$ by a force gn_χ , so taking into account the dilution of the produced particles, for $\phi > 0$ the equation of motion is

$$\ddot{\phi} + 3H\dot{\phi} = -gn_\chi(t_0) \left(\frac{a(t_0)}{a(t)} \right)^3 \quad (3.4.13)$$

For the general power law case, $a(t) \propto t^\beta$, this becomes

$$\ddot{\phi} + 3\frac{\beta}{t}\dot{\phi} = -gn_\chi(t_0)(t_0/t)^{3\beta} . \quad (3.4.14)$$

The general solution of this equation is

$$\phi(t) = \phi(t_0) + c(t_0^{-3\beta+1} - t^{-3\beta+1}) + \frac{gn_\chi(t_0)t_0^2}{(2-3\beta)} - \frac{gn_\chi(t_0)}{(2-3\beta)}(t_0/t)^{3\beta}t^2 \quad (3.4.15)$$

where c is some constant. In the important case $\beta = 2/3$, which corresponds to a universe dominated by pressureless cold matter, the general solution is

$$\phi = \phi(0) + c(t_0^{-1} - t^{-1}) - gn_\chi t_0^2 \log \frac{t}{t_0} . \quad (3.4.16)$$

According to these solutions, in a universe dominated by matter with non-negative pressure (i.e. $\beta \leq 2/3$) the field ϕ moves to $-\infty$ as $t \rightarrow \infty$.

Of course, as soon as the field reaches the point $\phi = 0$, this solution is no longer applicable, since the attractive force changes its sign (the potential is proportional to $|\phi|$). The result above simply means that the attractive force is always strong enough to bring the field back to the point $\phi = 0$ within finite time. Then the field moves further, with ever decreasing speed, turns back again, and returns to $\phi = 0$ once again. The amplitude of each oscillation rapidly decreases due to the combined effect of the Hubble friction and of the (weak) parametric resonance. This means that once ϕ passes near the ESP, its fate is sealed: eventually it will be trapped there.

3.4.4 Efficiency of Trapping

It is useful to determine what fraction of all initial conditions for the moving moduli lead to trapping. There are several constraints to be satisfied. First of all, if the impact parameter μ is much larger than $\sqrt{v/g}$, the number of produced particles will be exponentially small, and the efficiency of trapping will be exponentially suppressed. Of course, eventually ϕ will fall to the enhanced symmetry point, but if this process takes an exponentially large time, the trapping effect will be of no practical significance. Thus one can roughly estimate the range of interesting impact parameters to be $\mathcal{O}(\sqrt{v/g})$.

Another constraint is related to the fact that even if initially the energy density of the universe was dominated by the moving moduli, as discussed in §3.4.2, these fields can only move the distance given by (3.4.11),(3.4.12). This distance depends on the initial ratio $1 - \epsilon$ of kinetic energy to total energy, leading to a scanning range CM_p in field space, where the prefactor C is logarithmically related to ϵ .

Thus, the field becomes trapped only if there is an enhanced symmetry point inside a rectangle with sides of length CM_p along the direction of motion and width $\mathcal{O}(\sqrt{v/g})$ in the direction perpendicular to the motion.

Interestingly, the total area (phase space) of the moduli trap

$$S_{\text{trap}} \sim CM_p \sqrt{\frac{v}{g}} \quad (3.4.17)$$

increases as the coupling decreases. This implies that the efficiency of trapping grows at weak coupling. Although this may seem paradoxical, it happens because the mass of the χ particles is proportional to the coupling constant and (fixing the

other parameters) it is easier to produce lighter particles. On the other hand, if g becomes too small, the trapping force $gn_\chi \sim g^{5/2}v^{3/2}$ becomes smaller than the usual forces due to the effective potential, which we assumed subdominant in our investigation.

So far we have studied the simplest model where only one scalar field becomes massless at the enhanced symmetry point. Let us suppose, however, that N fields become massless at the point $\phi = 0$. If these fields interact with ϕ with the same coupling constant g , then particles of each of these fields are produced, and the trapping force becomes N times stronger. In other words, the trapping force is proportional to the degree of symmetry at the ESP.

3.5 String Theory Effects

It is interesting to ask if there is any controlled situation where string-theoretic effects become important for moduli trapping. Here we will simply list several circumstances in which stringy and/or quantum gravity effects might come into play, as well as some constraints on these effects. In Chapter 4 we will revisit this subtle and interesting situation.

3.5.1 Large χ Mass

One way stringy and quantum gravity effects could become important in the colliding D-brane case is if the χ mass at the turnaround point is greater than string scale, $g\phi_* > m_s$. This can happen even if the velocity is so small that during the non-adiabatic period near the origin only unexcited stretched strings are created. Then, as in our above field theory analysis, we have

$$g\phi_* = \frac{4\pi^3}{g^{3/2}}v^{1/2}e^{\pi g\mu^2/v}. \quad (3.5.1)$$

In this case, the full system includes modes, namely the created χ strings, which are heavier than the string oscillator mode excitations on the individual branes. This means that the system as a whole cannot consistently be captured by pure effective field theory. However, it may still happen that the created stretched strings are relatively stable against annihilation or decay into the lighter stringy modes. Their annihilation cross section is suppressed by their large mass, as discussed in Appendix

3.B.¹¹ Furthermore, an individual stretched string will not directly decay if it is the lightest particle carrying a conserved charge.

This latter situation happens in the simplest version of a D-brane collision. The created stretched string cannot decay into lighter string or field theory modes because it is charged and they are not.

3.5.2 Large v and the Hagedorn Density of States

If we increase the field velocity $\dot{\phi} = v$, then we may obtain a situation in which excited string states are produced as ϕ passes the ESP. The number of string states produced in this process is enhanced by the Hagedorn density of states, so the Bogoliubov coefficients have the structure

$$|\beta_k|^2 = \sum_n e^{\frac{\sqrt{n}}{2\pi\sqrt{2}}} e^{-\pi(k^2 + nm_s^2 + g^2\mu^2)/(gv)} \quad (3.5.2)$$

where in the D-brane context, $g = \sqrt{g_s}$ is the Yang-Mills coupling on the D-branes. Because of the $e^{-\pi nm_s^2/(gv)}$ suppression in the second factor, this effect is only significant if $gv \gg m_s^2$.

However, in the case of colliding D-branes, and any situation dual to it, there is a fundamental bound on the field velocity from the relativistic speed limit of the branes. That is, for large velocity one must include the full Dirac-Born-Infeld Lagrangian for ϕ , which takes the form

$$S = -\frac{1}{(2\pi)^3 g_s \alpha'^2} \int d^4x \sqrt{1 - g^2 \frac{\dot{\phi}^2}{m_s^4}}. \quad (3.5.3)$$

This action governs the nontrivial dynamics of ϕ for velocities approaching the string scale, and in particular, it reflects the fact that the brane velocity $g\dot{\phi}\alpha'$ must be less than the speed of light in the ambient space. Applied to our situation, (3.5.3) implies that the D-brane velocity cannot be large enough for the Hagedorn enhancement (3.5.2) to substantially increase the trapping effect.

However, in the presence of a large velocity, the effective mass of the stretched string also has important velocity-dependent contributions [70]. As we will explain in Chapter 4, this will increase the non-adiabaticity near the origin and dramatically enhance the particle production effect.

¹¹ For stringy densities of stretched strings, there could be additional corrections to the annihilation rate, but we will not consider this possibility.

3.5.3 Light Field-Theoretic Strings

A further possibility is to formally reduce the tension of strings by considering strings in warped throats, strings from branes partially wrapped on shrinking cycles, and the like. In these situations, the strings are essentially field-theoretic, though string theory techniques such as AdS/CFT and “geometric engineering” of field theories may provide technical help in analyzing the situation.

3.6 The Vacuum Selection Problem

We can now apply the ideas of the previous five sections to the cosmology of theories with moduli.

A natural application of the moduli trapping effect is to the problem of vacuum selection. One mechanism of vacuum selection is based on the dynamics of light scalars during inflation. Moduli fields experience large quantum fluctuations during inflation and can easily jump from one minimum (or valley) of their effective potential to another. It was suggested long ago that such processes may be responsible, e.g., for the choice of the vacuum state in supersymmetric theories [95] and for the smallness of the cosmological constant [96]. The probability of such processes and the resulting field distribution depends on the details of the inflationary scenario and the structure of the effective potential [97].

The mechanism that we consider in this chapter is, in a certain sense, complementary to the inflationary mechanism discussed above. During inflation the average velocities of the fields are very small, but quantum fluctuations tend to take the light scalar fields away from their equilibrium positions. On the other hand, after inflation, the fields often find themselves not necessarily near the minima of their potentials or in the valleys corresponding to the flat directions, but on a hillside. As they roll down, they often acquire some speed along the valleys, see e.g. [68]. At this stage (as well as in a possible pre-inflationary epoch) the moduli trapping mechanism may operate.

This mechanism may reduce the question of how one vacuum configuration is selected dynamically out of the entire moduli space of vacua to the question of how one ESP is selected out of the set of all ESPs. This residual problem is much simpler because ESPs generically comprise a tiny subset of the moduli space.

3.6.1 Vacuum Selection in Quantum Field Theory

In pure quantum field theory, discussed in §3.2, we saw that if a scalar field ϕ is initially aimed to pass near an ESP, then ϕ gets drawn toward the ESP and is ultimately trapped there. This appears to be a basic phenomenon in time-dependent quantum field theory: moduli which begin in a coherent classical motion typically become trapped at an ESP. This leads to a dynamical preference for ESPs.

In many of the supersymmetric quantum field theories that have been studied rigorously [72], the moduli space contains singular points at which light degrees of freedom emerge. We have seen that moduli can become trapped near these points given suitable initial conditions.

3.6.2 Vacuum Selection in Supergravity and Superstring Cosmology

Compactifications of M/string theory which have a description as a low energy effective supersymmetric field theory can have a natural separation of scales: the string or Planck scale can be much larger than the energy scales in the effective field theory potential. Thus, the intrinsically stringy effects of §3.5 are unimportant in this limit. On the other hand, the effects of coupling to gravity given in §3.4 continue to provide a crucial constraint, as we will now discuss.

First of all, as in the case of pure quantum field theory, there exist very instructive toy models with extended supersymmetry, for which there is no potential at all on the moduli space. For these examples, in situations where higher-derivative corrections to the effective action are suppressed, a rolling scalar field has the equation of state $p = \rho$. This corresponds to the $\beta = 1/3$ case (3.4.7) of §3.4, for which one can scan an arbitrarily large distance in field space. Therefore, in this case, the trapping effect applies in a straightforward way to dynamically select the ESPs for regimes in which (3.4.3) is also satisfied.

More generally, however, one may wish to implement cosmological trapping in theories with some potential energy. In this case the requirement that the scanning range of ϕ (as constrained by Hubble friction in §3.4) should be large enough to cover multiple vacua is an important constraint. The absolute minimum requirement is that the scanning range is sufficient for the moduli to reach one ESP before stopping from Hubble friction; but to address the vacuum selection problem one should ideally scan a number of ESPs.

One context in which this can happen is in a phase in which the kinetic energy of the rolling scalar fields dominates the energy density of the universe so that the $\beta = 1/3$ result (3.4.7) applies. This may occur in a pre-inflationary phase in some patches of spacetime, though it is subject to the stringent limitation in duration given in (3.4.11). Given such a phase, the field will roll around until it gets trapped at an ESP.

During the ordinary radiation-dominated ($\beta = 1/2$) and matter-dominated ($\beta = 2/3$) eras, the more stringent constraint (3.4.9) applies. As we indicated in §3.4, this scanning range is not large in Planck units, so we can usefully apply moduli trapping to the problem of vacuum selection in these eras only if the vacuum has appropriately rich structure on sub-Planckian scales. In other words, the average distance in moduli space between ESPs should be sub-Planckian.

Gravitationally-coupled scalars ϕ generically have a potential energy $V(\phi/M_p)$ which has local minima separated by Planck-scale distances. In this cases, the limited scanning range during the $\beta \neq 1/3$ cosmological eras prevents our mechanism from addressing the vacuum selection problem. However, it is generic for compactification moduli to have special ESPs where the gravitationally-coupled system is enhanced to a system with light field theory degrees of freedom. Given a rich enough effective field theory in this ESP region, there will generically be interesting vacuum structure on sub-Planckian distances. In this sort of region moduli trapping will pick out the ESP vacua of the system.

3.6.3 Properties of the Resulting Vacua

Let us now consider the qualitative features of the vacua selected by moduli trapping, assuming that the constraint imposed by Hubble friction has been evaded in one of the ways described above.

First of all, it is important to recognize that what we have called ESPs may well be subspaces of various dimensions, not points. For example, in toroidal compactification of the heterotic string, there is one enhanced symmetry locus for each circle in the torus – new states appear when the circle is at the self-dual radius. Each of these loci is codimension one in the moduli space, but of course their intersections, where multiple radii are self-dual, have higher codimension.

When moduli trapping acts in such a system of intersecting enhanced symmetry loci, we expect that the moduli will first become trapped on the locus of lowest

codimension, but retain some velocity parallel to this locus. Further trapping events can then localize the modulus to subspaces of progressively higher codimension. The final result is that the moduli come to rest on a locus of maximally enhanced symmetry.

The simplest examples of this phenomenon are toroidal compactification, in which all circles end up at the self-dual radius, and the system of N D-branes discussed in §3.2.3, in which the gauge symmetry is enhanced to $U(N)$.¹²

Quite generally, we expect that within the accessible range in field space, taking into account Hubble friction and the form of the potential, moduli trapping will select the ESPs with the largest number of light states, which often corresponds to the highest degree of symmetry.¹³

In some very early epoch the rolling moduli can have large velocities, so trapping can occur even at points where the “light” states χ have a relatively large mass, and the enhanced symmetry is strongly broken. However, Hubble friction inevitably slows the motion of the moduli. Thus, trapping at late times is possible only at ESPs with weakly-broken symmetries and very light particles. One could speculate about a possible relation of this fact to the mass hierarchy problem.

Note that even though we emphasized the natural role of enhanced symmetry in moduli trapping, in fact the only strict requirement was the appearance of new light particles at the trapping points. In some of the many vacua of string theory, particles may be light not because of symmetry but because of some miraculous cancellations. Invoking such unexplained cancellations to produce a small mass is highly undesirable. However, moduli trapping may ameliorate this problem, as those rare points in moduli space where the cancellation does happen are actually dynamical attractors.

¹² A toy model for this situation, in the case of three D-branes, has the potential $\frac{g^2}{2} [\chi_1^2 |\phi_2 - \phi_3|^2 + \chi_2^2 |\phi_1 - \phi_3|^2 + \chi_3^2 |\phi_1 - \phi_2|^2]$, where ϕ_i and χ_i are six different fields. Suppose that ϕ_2 moves through the point $\phi_2 - \phi_3 = 0$. This creates χ_1 particles and traps the system at $\phi_2 = \phi_3$, where χ_1 is massless. Subsequent motion of ϕ_1 can trap it at the point $\phi_1 = \phi_2 = \phi_3$, making the remaining fields χ_2 and χ_3 massless.

¹³ Moreover, as we discuss in Appendix 3.B, the trapping effect is far more effective at ESPs for which the χ particles do not decay rapidly. We therefore expect moduli trapping to select ESPs which have relatively stable light states.

Thus, the attractive power of symmetry and of light particles may have implications for questions involving the distribution of vacua in string theory [3,98,5,99]. Given the strong preference we have seen for highly-enhanced symmetry, the distribution of all string vacua obtained by a naive counting, weighted only by multiplicity, may be quite different from the distribution of vacua produced by the dynamical populating process discussed in this chapter. It is therefore very tempting to speculate that some of the surprising properties of our world, which might seem to be due to pure chance or miraculous cancellations, in fact may result from dynamical evolution and natural selection.

3.7 The Moduli Problem

One aspect of the moduli problem is that reheating and nucleosynthesis can be corrupted by energy locked in oscillations of the moduli. The source of the problem is that the true minima of the low-temperature effective potential applicable after inflation do not coincide with the minima of the Hubble-temperature effective potential which is valid during inflation. It follows that moduli which sit in minima of the latter during inflation will find themselves displaced from their true, low-temperature minima once inflation is complete. The energy stored in this displacement, and in the resulting oscillations about the true minimum, poses problems for nucleosynthesis.

One way to address this problem is to permit initial displacements of the moduli, as described above, but somehow arrange that the oscillating moduli decay very rapidly to Standard Model particles. Alternatively, one could fix the moduli at a scale high enough that the Hubble temperature during inflation does not destabilize them. This may work in string models with stabilized moduli such as [98,100,5,20].

Another approach to this problem [75] is to posit that the moduli sit at an enhanced symmetry point minimum of the finite-temperature effective potential during inflation. Then, when inflation ends, the moduli are still guaranteed to be at an extremum of the effective potential. If this extremum is a minimum then the moduli have no problematic oscillations after inflation. Our trapping mechanism allies nicely with this idea by providing a preinflationary dynamical mechanism which explains the initial condition assumed in this scenario. That is, in parts of the universe where ϕ kinetic energy dominates well before inflation, the trapping effect can explain why the moduli find themselves in ESP minima at the onset of inflation.

3.8 Trapped Inflation and Acceleration of the Universe

The main motivation of our investigation was to study the behavior of moduli in quantum field theory and string theory. However, the results we have obtained have more general applicability. To give an example, in this section we will study the cosmological implications of the trapping of a scalar field ϕ with a relatively steep potential.

Consider the theory of a real scalar field ϕ with the effective potential $m^2\phi^2/2$. In the regime $\phi < M_p$ the curvature of the effective potential is greater than H^2 , with H the Hubble parameter, so ϕ falls rapidly to its minimum, and inflation does not normally occur.

We will assume that ϕ gives some bosons χ a mass $g|\phi - \phi_1|$. Let us assume that ϕ falls from its initial value $\phi_0 = \phi_1(1 + \alpha) < M_p$ with vanishing initial speed. If we take $\alpha \ll 1$ and neglect for the moment the expansion of the universe, then ϕ arrives at ϕ_1 with the velocity $v = \sqrt{2\alpha} m \phi_1$.

As ϕ passes ϕ_1 , it creates χ particles with number density $n_\chi = (gv)^{3/2}/8\pi^3$. After a very short time these particles become nonrelativistic, and further motion of ϕ away from ϕ_1 requires an energy $g|\phi - \phi_1|n_\chi$. In other words, the effective potential becomes

$$V(\phi) \approx \frac{1}{2}m^2\phi^2 + gn_\chi|\phi - \phi_1| = \frac{1}{2}m^2\phi^2 + g^{5/2}\frac{v^{3/2}}{8\pi^3}|\phi - \phi_1|. \quad (3.8.1)$$

For $g^{5/2}\frac{v^{3/2}}{8\pi^3 m^2} > \phi_1$, the minimum of the effective potential is not at $\phi = 0$, but at the point ϕ_1 , where the particle production takes place. The condition $g^{5/2}\frac{v^{3/2}}{8\pi^3 m^2} > \phi_1$ implies that

$$m < 2^{-9/2}\pi^{-6}g^5\alpha^{3/2}\phi_1. \quad (3.8.2)$$

Thus, if the mass of ϕ is sufficiently small, the field will be trapped near the point ϕ_1 .

To give a particular example, take $\phi_1 \sim M_p/2$, $\alpha \sim 1/4$. Then ϕ is trapped near ϕ_1 if

$$m < 10^{-6}g^5M_p. \quad (3.8.3)$$

For a very light field, such as a modulus with $m \sim 10^2$ GeV $\sim 10^{-16}M_p$, this condition is readily satisfied unless g is very small.

Once the field is trapped, it starts oscillating around ϕ_1 with ever-decreasing amplitude, creating new χ particles in the regime of parametric resonance. Eventually ϕ transfers a large fraction of its energy to χ particles. One can easily check that in this model the fall of ϕ to the point ϕ_1 and the subsequent process of creation of χ particles occurs within a time smaller than H^{-1} , so one can neglect expansion of the universe at this stage. This process is therefore governed by the theory described in §3.3. In particular, we may use the estimate (3.3.20) of the total number of χ particles produced in the process. At the end of the particle production, the correction to the effective potential becomes much larger than at the beginning of the process:

$$\Delta V = g|\phi - \phi_1|n_\chi \sim v^{3/2}g^{1/2}|\phi - \phi_1|, \quad (3.8.4)$$

Subsequent expansion of the universe dilutes the density of χ particles as a^{-3} , which eventually makes the correction to the effective potential small, so that ϕ starts moving down again. The field ϕ remains trapped at $\phi = \phi_1$ until the scale factor of the universe grows by a factor

$$a \sim \alpha^{1/4} \left(\frac{g\phi_1}{m} \right)^{1/6} \quad (3.8.5)$$

since the beginning of the trapping process.

In the beginning of the first e-folding, the kinetic energy of the χ particles and of the oscillations of ϕ is comparable to the potential energy of ϕ . However, the kinetic energy rapidly decreases, and during the remaining time the energy is dominated by the potential energy $V(\phi_1)$. This means that the trapping of ϕ may lead to a stage of inflation or acceleration of the universe, even if the original potential $V(\phi)$ is too steep to support inflation.

Let us consider various possibilities for the scales in the potential, to get some simple numerical estimates for the duration of inflation. For example, if we take $\alpha, g = \mathcal{O}(1)$, $\phi_1 \sim M_p$ and $m \sim 10^2$ GeV, then the scale factor during a single trapping event will grow by a factor of e^6 . If one considers a model with $m \sim 10^{-30}M_p$, which can arise in a radiatively stable manner (as in the “new old inflation” model [81]), the scale factor during a single trapping event can grow by a factor of e^{11} . Finally, if the moduli mass is of the same order as a typical mass taken in theories of quintessence, $m \sim 10^{-60}M_p$, we can have an accelerated expansion of the universe

by a factor e^{23} , in a sub-Planckian regime of field space, just from trapping. (In this last case, as in ordinary quintessence models, tuning is required.)

Thus, the stage of inflation in this simple model is shorter than the usual 60 e-folds, but it may nevertheless be very useful for initiating a first stage of inflation in theories where this would otherwise be impossible, or for diluting unwanted relics at the later stages of the evolution of the universe. Moreover, this scenario can easily describe the present stage of acceleration of the universe.

One can also make the effect more substantial by constructing a more complicated scenario, consisting of a chain of N particle production events at locations $\phi = \phi_i$, where some fields χ_i become light. The field ϕ may be trapped and enter the stage of parametric resonance near each of these points. Correspondingly, the universe enters the stage of inflation many times. One could arrange for 60 e-folds of inflation by taking, for example, $m \sim 10^2$ GeV, $N \sim 10$.

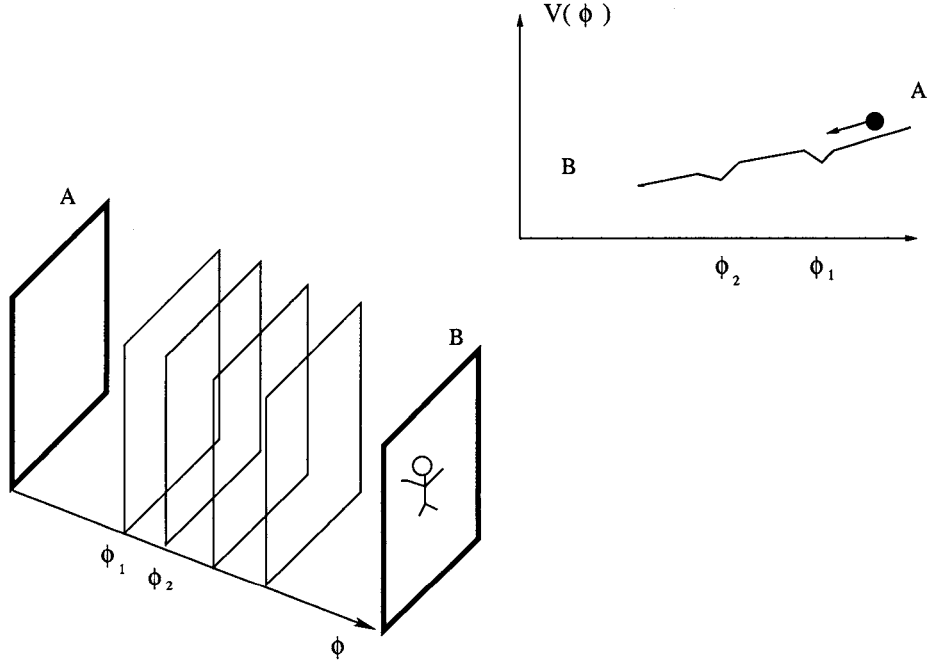


Fig. 6: The D-brane picture of a series of trapping events.

A D-brane example provides a useful geometrical model of this process. Suppose we have an observable brane B and another brane A approaching it. Suppose also that there are a number of other branes in between A and B . Each time the moving brane passes through one of the standing intermediate branes, stretched strings are created and slow the motion of A . The cumulative effect of a number of standing branes is perceived on the observable brane as a slowing-down of the motion of A due to the interactions.

One should note that inflation in our scenario is rather unusual: the inflaton ϕ rolls a short distance, then oscillates for a long time, but with period much smaller than H^{-1} , then rolls again, etc. This may lead to peculiar features in the spectrum of density perturbations. One can avoid these features if the points ϕ_i are very close to each other, and each of them does not stop the rolling of ϕ but only slows it down. In this case, particle production will not lead to parametric resonance, so it is not very important to us whether the fields χ_i are bosons or fermions, as long as their masses vanish at ϕ_i .

This scenario is similar to the string-inspired thermal inflation considered in [76] (see also [101]), but our proposal does not require thermal equilibrium. The main effect which supports inflation in our scenario is based on particle production and has a nonperturbative origin. (A closely-related mechanism uses the corrections to the kinetic terms in the strong coupling regime, where the particle production is suppressed [70].) We hope to return to a discussion of this possibility in a separate publication.

3.9 Conclusion

We have argued that the dynamics of rolling moduli is considerably modified due to quantum production of light fields. In flat space quantum field theory, moduli typically become trapped in orbits around loci which have extra light degrees of freedom. In the presence of gravity, Hubble friction limits the field range the system samples, but any trapping events which do occur are enhanced by Hubble friction, which rapidly brings the modulus to rest at an ESP. Moduli trapping may aid in solving the cosmological moduli problem by driving moduli to sit at points of enhanced symmetry. Furthermore, the trapping of a scalar field which has a potential can lead to a short period of accelerated expansion in situations with

steeper potentials than would otherwise allow this. Finally, the trapping effect has important consequences for the problem of vacuum selection, as it can reduce the problem to that of selecting one point within the class of ESPs. An intriguing feature of this process is that the trapping is more efficient near points with a large number of unbroken symmetries.

3.A Particle Production Due to Motion on Moduli Space

In this section we will calculate the quantum production of χ particles, ignoring the effect of backreaction on the motion of ϕ .

A mode of χ with spatial momentum k obeys the wave equation

$$\left(\partial_t^2 + k^2 + g^2(\mu^2 + v^2 t^2)\right)u_k = 0. \quad (3.A.1)$$

There are two solutions to this equation, u_k^{in} and u_k^{out} , associated to vacuum states with no particles in the far past and no particles in the far future, respectively. These two sets of modes are related by a Bogoliubov transformation

$$u_k^{in} = \alpha_k u_k^{out} + \beta_k u_k^{out*}. \quad (3.A.2)$$

If we start in the state with no particles in the far past, then one can calculate the number density of particles in the far future to be

$$n_k = |\beta_k|^2 \quad (3.A.3)$$

in the k^{th} mode. This may be evaluated by solving equation (3.A.1) in terms of hypergeometric functions (see e.g. §3.5 of [77]), but we will present here a more physical argument.

One can view (3.A.1) as a one dimensional Schrödinger equation for particle scattering/penetration through an inverted parabolic potential. If we send in a wave ψ_k^{in} from the far right of the potential, part of it will penetrate to the far left, with an asymptotic amplitude $T_k \psi_k^{out}$, and part of it will be reflected back to the right, with an asymptotic amplitude $R_k \psi_k^{in*}$, where T_k and R_k are the transmission and reflection amplitudes.¹⁴

¹⁴ The modes in the two problems are related by $u_k^{in}(t \rightarrow -\infty) = T_k^* \psi_k^{out*}$, etc.

The Bogoliubov coefficient in (3.A.2) is determined in terms of these transmission and reflection amplitudes via

$$\beta_k = \frac{R_k^*}{T_k^*}. \quad (3.A.4)$$

Now we use a trick from quantum mechanics to relate R and T using the WKB method. If we are moving along the real time coordinate, the WKB form of the solution $u_k^{in}(t)$ will be violated at small t , due to non-adiabaticity. However, if we take t to be complex then we can move from $t = -\infty$ to $t = +\infty$ along a complex contour in such a way that the WKB approximation

$$u_k^{in}(t) \sim \frac{1}{\sqrt{2\sqrt{k^2 + g^2(\mu^2 + v^2 t^2)}}} e^{-i \int^t \sqrt{k^2 + g^2(\mu^2 + v^2 t'^2)} dt'} \quad (3.A.5)$$

is valid. Here the integral $\int^t dt'$ becomes a contour integral along a semicircle of large radius in the lower complex t plane. For large $|t|$, we can estimate the phase integral in (3.A.5) by expanding

$$\sqrt{k^2 + g^2(\mu^2 + v^2 t^2)} \sim gvt + \frac{k^2 + g^2 \mu^2}{2gvt}. \quad (3.A.6)$$

As we go around half of the circle, this term generates a factor

$$(e^{-i\pi})^{-i(k^2 + g^2 \mu^2)/2gv - 1/2} = ie^{-\pi(k^2 + g^2 \mu^2)/2gv}. \quad (3.A.7)$$

This is exactly the ratio between R^* and T^* , so we find

$$n_k = |\beta_k|^2 = e^{-\pi(k^2 + g^2 \mu^2)/gv}. \quad (3.A.8)$$

It is important to note that this result applies much more generally than for

$$\phi = i\mu + vt. \quad (3.A.9)$$

In many cases the nonadiabaticity is only appreciable near the origin $\phi = 0$, so that the near-origin trajectory can be approximated by (3.A.9) with some appropriate near-origin velocity v , even if the evolution away from the origin is very different from (3.2.2).

Moreover, in analogous circumstances (T-dual in the brane context) with a nontrivial electric field, we obtain a similar expression due to Schwinger pair production; a related point was made in [87]. In addition, formula (3.A.8) applies not only to scalar fields, but also to fields of arbitrary spin. From this universal behavior, it is tempting to speculate that (3.A.8) could provide an effective model for string theory effects, but we will not pursue this direction here.

The result (3.A.8) is nonperturbative in g (with g , not g^2 , appearing in the denominator of the exponent); it is interesting to ask whether there is a simple interpretation of this nonanalytic, nonperturbative effect. Similarly, it is interesting to note that as discussed in §3.3, the potential for ϕ induced by particle production is linear, so that if extended to the origin it would have a nonanalytic cusp there.

Our results correspond to the low-velocity limit of the D-brane calculation by Bachas [87]. Bachas obtains an imaginary part to the action for moving D3-branes of the form

$$\text{Im } S \propto \sum_{n=1}^{\infty} \frac{(-1)^{(n+1)}}{n} \left(\frac{gv}{\pi n} \right)^{3/2} \exp(-n\pi g\mu^2/v) \quad (3.A.10)$$

where we have translated his results into our variables. The first term in this expansion is proportional to the overlap $\int d^3\vec{k} |\beta_k|^2$ giving the number density (3.3.14) of produced particles; this agrees with what we expect from unitarity. More generally, backing away from this low-velocity limit, the calculation in [87] combined with unitarity provides a generalization of our results to the string case, as we will explain in Chapter 4.

3.B Annihilation of the χ Particles

In this section we study the effects of collisions and direct decays of the created χ particles, and demonstrate that for suitably chosen parameters the trapping effect receives only small corrections. More specifically, we place limits on the reduction of the χ number density through processes like $\chi\chi \rightarrow \phi\bar{\phi}$ and $\chi \rightarrow \eta\bar{\eta}$, where η is some light field.

Direct decays, if present, could easily ruin the trapping mechanism: if the χ particles decay too rapidly into light fields then the energy stored in created χ particles will not suffice to stop ϕ . In this case the modulus will roll past the ESP,

feel a transient tug toward the ESP while the χ particles remain, and then gradually break free and glide off to infinity at a reduced speed.

We will therefore consider only models in which couplings of the form $\chi\bar{\psi}\psi$, with $\bar{\psi}, \psi$ very light, are negligible. As an example, one can easily exclude such decays in a supersymmetric model with a superpotential of the form $\mathcal{W} \sim g\Phi X^2$. Here X is a chiral superfield with scalar component χ and fermion ψ_χ , and Φ is a chiral superfield with scalar component ϕ and fermion ψ_ϕ . This generates Yukawa couplings of the form $\chi\psi_\chi\psi_\phi$ and $\phi\psi_\chi\psi_\chi$, which do not allow decays from a component of X to purely Φ particles. Thus, if all components of X are heavy, the X -particle energy density we produce cannot decrease by direct decays. In some of the simplest brane setups, exactly this situation is realized: a string which is heavy because it stretches between two branes separated in a purely closed string bulk space cannot decay perturbatively into two light, unstretched strings.

On the other hand, a priori we cannot ignore the coupling $\frac{g^2}{2}\chi^2\phi^2$ as it is this which gives rise to the desired trapping effect. This means that we must tolerate a certain rate of annihilation (as opposed to direct decay). We will now review the cross section for this process and determine its effect on the number density n_χ appearing in (3.2.10).

The Lorentz-invariant cross section for the annihilation process $\chi\chi \rightarrow \phi\bar{\phi}$ is, written in terms of center of mass variables,

$$\sigma = \frac{g^4 k'}{4\pi k E^2}, \quad (3.B.1)$$

where k and k' are the momenta of the ingoing and outgoing particles and E is the energy of the ingoing χ particles. The reverse process $\phi\bar{\phi} \rightarrow \chi\chi$ tends to enhance the trapping effect. As we are in search of a lower bound on the number of χ particles, we will simply omit this reverse process.

We now determine the annihilation rate to find the rate at which χ particles are lost. If we assume that all the χ 's are produced at $t = 0$, we find

$$\frac{\dot{n}(\vec{k}_1, t)}{n(\vec{k}_1, t)} = - \int d\vec{k}_2 n(\vec{k}_2, t) \frac{\sqrt{(k_1 k_2)^2 - m_\chi^4}}{E_1 E_2} \sigma(\vec{k}_1, \vec{k}_2). \quad (3.B.2)$$

Here $u = \sqrt{(k_1 k_2)^2 - m_\chi^4}/E_1 E_2$ is the Lorentz-invariant relative velocity of the initial χ 's and $\sigma(\vec{k}_1, \vec{k}_2)$ is the cross section, to be calculated using (3.B.1) in the center of mass frame.

We can simplify (3.B.2) to get an upper bound on how fast χ decays. Ignoring the momentum dependence on the right hand side of (3.B.2), which amounts to taking the non-relativistic limit, and ignoring the mass of ϕ produced by the χ particles, we have

$$\frac{\dot{n}(\vec{k}_1, t)}{n(\vec{k}_1, t)} \geq -\frac{g^4}{2\pi m_\chi^2} \int d\vec{k}_2 n(\vec{k}_2, t). \quad (3.B.3)$$

We can bound the integral in the second term on the right hand side by n_χ , the total number of χ 's produced, as given in (3.3.14). To approximate the time-dependence of the mass m_χ , we take $m_\chi^2 = \mu^2 + v^2 t^2$, which is what the uncorrected motion for ϕ would give. So we have finally

$$\frac{\dot{n}(\vec{k}_1, t)}{n(\vec{k}_1, t)} \geq -\frac{g^4 n_\chi}{2\pi(\mu^2 + v^2 t^2)}, \quad (3.B.4)$$

which yields

$$\frac{n(\vec{k}, t)}{n(\vec{k}, 0)} \geq \exp\left(-\frac{g^4 n_\chi}{2\pi\mu v} \arctan \frac{vt}{\mu}\right). \quad (3.B.5)$$

This is clearly bounded from below by

$$\exp\left(-\frac{g^4 n_\chi}{2\pi\mu v}\right). \quad (3.B.6)$$

so that the number density is reduced over time by at worst the factor (3.B.6).

The total energy density in the χ particles at a given time is therefore

$$\begin{aligned} E &= \int d\vec{k} n(\vec{k}, t) \sqrt{k^2 + g^2(\mu^2 + v^2 t^2)} \\ &\geq n_\chi \sqrt{g^2(\mu^2 + v^2 t^2)} \exp\left(-\frac{g^4 n_\chi}{2\pi\mu v} \arctan \frac{vt}{\mu}\right). \end{aligned} \quad (3.B.7)$$

From this we see that the mass amplification effect of the χ particles inevitably prevails and stops ϕ from rolling arbitrarily far past the enhanced symmetry point.

This reduction of the number density softens, but does not ruin, the trapping effect. Using the energy density (3.B.7) in the simple estimate leading to (3.2.12), we find a new estimate for ϕ_* :

$$\phi_* = \frac{4\pi^3}{g^{5/2}} v^{1/2} e^{\pi g \mu^2 / v} e^{g^4 n_\chi / 4\mu v} \quad (3.B.8)$$

Thus, although collisions never lead to an escape, they do lead to a somewhat increased stopping length ϕ_* .

For suitably chosen parameters we can arrange that the effect of collisions is unimportant and the estimates (3.2.12), (3.B.8) approximately agree. For example, the final exponential factor, which encodes the consequences of annihilations, will be less important than the factor $e^{\pi g \mu^2 / v}$ as long as $g^3 v \ll \mu^2$.

We conclude that direct decays can be forbidden using symmetry, whereas collisions increase the stopping length (3.B.8) but do not ruin the trapping effect.

3.C Classical Trapping Versus Quantum Trapping

In this section we will compare our quantum trapping mechanism with the purely classical trapping proposed in [102].

Consider for simplicity a theory of two real scalar fields, ϕ and χ , with the interaction $\frac{g^2}{2} \phi^2 \chi^2$. In our discussion in the main text we assumed the initial conditions $\langle \chi \rangle = 0$, $\langle \phi \rangle \neq 0$, $\dot{\chi} = 0$, $\dot{\phi} = v$. Potentially interesting classical dynamics arises in the more general case in which the initial velocity of χ is nonzero [102].

Let us therefore consider the classical behavior of these fields, ignoring particle production entirely. If we define $v \equiv \sqrt{\dot{\chi}^2 + \dot{\phi}^2}$, then energy conservation implies that the trajectory of ϕ and χ is bounded by the surface $g^2 \phi^2 \chi^2 = v^2$. The fields will evidently start bouncing off the curved walls of the potential. This bouncing will be highly random.

Naively, one would expect that on average the fields become confined in the region

$$\langle \phi^2 \rangle = \langle \chi^2 \rangle \sim \frac{v}{g}. \quad (3.C.1)$$

This result would coincide with our estimate for the amplitude of the oscillations of ϕ at the end of the stage of parametric resonance, cf. (3.3.21).

However, the situation is more complicated. As we are going to show, the fields spend most of the time not at $|\phi| \sim |\chi| \sim \sqrt{\frac{v}{g}}$, but exponentially far away from this region, moving along one of the flat directions of the potential.

To see this, note that because of the chaotic nature of the bouncing, it will occasionally happen that the fields enter the valley $\chi \ll \phi$ at a small angle to the flat direction, i.e. with velocities obeying $|\dot{\chi}| \ll \dot{\phi}$. Defining $|\dot{\chi}| \equiv \alpha v$, we are interested in the case that the angle α happens to be small.

Energy conservation implies that the amplitude of the oscillations of χ at the initial stage of this process is approximately $\frac{\alpha v}{g\phi}$. Because of the interaction term $\frac{g^2}{2}\phi^2\chi^2$, these oscillations act on the field ϕ with an average returning force $\sim \frac{\alpha^2 v^2}{\phi}$, which corresponds to the logarithmic potential $V(\phi) \sim \alpha^2 v^2 \log \phi$ [102]. Clearly, this potential will eventually pull the field ϕ back to the ESP $\phi = 0$. However, this happens at exponentially large ϕ : the field starts moving back only after its value approaches

$$\phi_{\text{class}}^* \sim \sqrt{\frac{v}{g}} e^{c/\alpha}, \quad (3.C.2)$$

where $c = \mathcal{O}(1)$.

Once again, because the bouncing process is highly random, we do not expect that the probability to enter the valley at a small angle α is exponentially suppressed. This means that after bouncing back and forth near the point $\phi = \chi = 0$, the fields ϕ and χ eventually enter one of the valleys at a small angle, and subsequently spend a very long time there. In general, the fields will spend an exponentially long time at an exponentially large distance from the origin. Thus, the classical trapping mechanism, unlike the particle production mechanism described in this chapter, does not lead to a permanent trapping of the fields in the vicinity of the point $\phi = \chi = 0$.

4. Relativistic D-brane Scattering

ABSTRACT OF ORIGINAL PAPER

We study the effects of quantum production of open strings on the relativistic scattering of D-branes. We find strong corrections to the brane trajectory from copious production of highly-excited open strings, whose typical oscillator level is proportional to the square of the rapidity. In the corrected trajectory, the branes rapidly coincide and remain trapped in a configuration with enhanced symmetry. This is a purely stringy effect which makes relativistic brane collisions exceptionally inelastic. We trace this effect to velocity-dependent corrections to the open string mass, which render open strings between relativistic D-branes surprisingly light. We observe that pair-creation of open strings could play an important role in cosmological scenarios in which branes approach each other at very high speeds.

4.1 Introduction

Thought experiments involving the scattering of strings or of D-branes provide the key to understanding certain essential phenomena in string theory. The discovery of strings in the theory is perhaps the most striking case, but other examples include the elucidation of the sizes of strings under various conditions and the appreciation of another length-scale in the dynamics of slow-moving D-branes.

Despite much early interest in the scattering of D-branes, certain important aspects of the dynamics have remained unexplored. In particular, the simplest treatments involve parameter regimes governed either by supergravity or by the

This chapter is reprinted from Liam McAllister and Indrajit Mitra, “Relativistic D-Brane Scattering is Extremely Inelastic,” JHEP **0502** (2005) 019, by permission of the publisher.
© 2005 by the Journal of High Energy Physics.

effective worldvolume field theory of massless open strings. In the latter case, there can be significant quantum corrections arising from loops of light open strings or from pair-production of on-shell open strings.

A key consequence of the pair-production of open strings is the *trapping* of D-branes [18], which we now briefly review. Consider two D_p -branes, $p > 0$, moving with a small relative velocity. As the branes pass each other, the masses of stretched open strings vary with time. This leads to pair production, in a direct analogue of the Schwinger pair-creation process for charged particles [103] or strings [104] in an electric field. Because the velocities are low, the production of stretched strings with oscillator excitations is highly suppressed. The resulting unexcited stretched strings introduce an energy cost for the branes to separate; unless these strings can rapidly annihilate, the branes will be drawn close together. In collisions with a nonzero impact parameter, the brane pair carries angular momentum; in this case the branes spiral around their center of mass, radiating closed strings, until eventually they fall on top of each other. The final outcome is that the open strings trap the branes in a configuration with enhanced symmetry. Because this process involves the production of only unexcited open strings, it falls within the purview of effective field theory.

Our goal is to explore related processes which are not describable in the low-energy effective field theory but which instead involve intrinsically stringy physics. We will show that the ultrarelativistic scattering of D-branes is a suitable laboratory for such an investigation, as corrections from the massive string states turn out to be essential. In particular, we will demonstrate that production of highly-excited open strings generates crucial corrections to the brane dynamics and leads to spectacular trapping of the branes over distances which can be of order the string length. As we will show, these corrections are much stronger than a naive application of effective field theory would predict; hence this is a setting where the importance of purely stringy effects is a surprise. The explanation of such a huge production of highly excited strings is that these states effectively become quite light – the mass receives velocity dependent corrections. The fact that open string masses are in principle velocity-dependent is well-known, but we have not found any explicit computations of these masses in the literature. Our result leads to a formula for the masses of open strings between moving D-branes.

The intuition underlying this result is that in relativistic D-brane scattering, it should be possible to pair-produce highly-excited open strings. The density of string states at high excitation levels grows exponentially with energy; this is the well-known Hagedorn density of states. For this reason, even if the production of a given excited string state is exponentially suppressed compared to production of a massless string state, the competition of the growing and decaying exponentials will typically cause highly-excited strings to dominate the process, in terms of both their number and their share of the total energy. Thus, one expects pair production of a huge number of highly excited strings. This is indeed the case, as was first explained by Bachas in the important work [87]. Our further observation is that because the energy transferred into these open strings can easily be comparable to the initial kinetic energy of the D-brane pair, the massive open strings are absolutely central to the dynamics. This means that the backreaction arising from purely stringy effects is crucial.

We will study the effect on the dynamics of this explosive pair-production of massive modes. Our conclusion is that for a large range of velocities and impact parameters, almost all the initial kinetic energy of the branes is transferred to open strings and to closed string radiation. After the collision the branes are drawn together and come to rest. In near-miss scattering events with an impact parameter b , the branes revolve around their center of mass in a roughly circular orbit whose initial radius is of order b ; this orbit swiftly decays via radiation of closed strings. This is to be contrasted to the much weaker trapping of nonrelativistic branes, which typically proceeds via very elliptical orbits, i.e. the stopping length is much greater than the impact parameter.

To recap, the dynamics of ultrarelativistic D-branes is strikingly inelastic: copious production of highly-excited stretched open strings rapidly drains the brane kinetic energy and traps the branes into a tight orbit, eventually leading the branes to coincide.

In this simple and controllable example it proves possible to understand aspects of the backreaction of open string production on the dynamics of colliding D-branes. The lessons of our analysis could be extended to cosmological models in which other sorts of fast-moving branes approach each other and collide. As we will discuss, these include the ekpyrotic/cyclic universe scenario, brane-antibrane scenarios, and the DBI model.

It is useful to indicate the various regions of parameter space that we will probe. We will outline this now to apprise the reader of our strategy; later, in §4.5.3, we will provide a more complete discussion.

The dimensionless quantities of interest are the impact parameter b measured in units of the string length; the string coupling g_s , which determines the mass of the D-branes in string units; and the initial relative velocity of the branes v . We will find it more convenient to convert this velocity into the rapidity, $\eta \equiv \operatorname{arctanh}(v)$. We will usually set $\alpha' = 1$, except for a few cases where we will retain explicit factors of the string length for clarity.

Our goal in this work is to understand open string effects in *relativistic* dynamics; the nonrelativistic case is already well-understood [105,18]. We will therefore impose $1 - v \ll 1$ so that $\eta \gg 1$. Another important consideration is that the D-branes should have Compton wavelengths small compared to the impact parameter. Because the D-branes grow light at strong string coupling, this amounts to a requirement that the coupling should be sufficiently weak. Another obvious advantage of weak coupling is the suppression of string loop effects; our primary computation is a one-loop open string process. A further requirement is that the D-brane Schwarzschild radius should be much smaller than the impact parameter. This too can be achieved with a suitably small string coupling, as we will demonstrate in §4.5.3. Furthermore, although energy loss through closed string radiation can be an important effect in a system of moving branes, there is a wide range of string coupling, depending on η , for which this effect is subleading compared to open string production. Although all these considerations show that weak coupling is desirable for control, it is important to recognize that as the coupling decreases, the D-branes grow heavy and hence stretch the strings farther before coming to rest.

In summary, there is a range of values of the string coupling in which the backreaction of open strings is significant and competing effects are suppressed.

The organization of this chapter is as follows. First, in §4.2, we review the trapping of nonrelativistic branes, which provides the basic intuition for the more complicated, stringy process which we aim to study. Then, in §4.3, we study the interaction amplitude for moving branes. We compute the brane interaction via an annulus diagram and examine its imaginary part, which corresponds to open string pair production. This result is well-known, but we include it for logical

completeness and to set our notation. Our primary result appears in §4.4, where we study the backreaction of open string production on the brane trajectory and estimate the stopping length on energetic grounds. In §4.5 we discuss potential corrections and additional effects, in particular the production of closed strings, and explain how they affect our considerations. We conclude with a few comments in §4.6. In Appendix 4.A we give a detailed check of our formula for the velocity-dependent string mass. Finally, we collect useful identities about the theta functions in Appendix 4.B.

4.2 Overview of the Trapping of Nonrelativistic Branes

We will now briefly review the trapping of D-branes in nonrelativistic motion, which was studied in [18]. (See also [106,107] for earlier work on related mechanisms in field theory and cosmology.) This process is governed by pair production of massless open strings and hence is describable in effective field theory. It provides the basic framework for understanding corrections to the brane dynamics, and so is a useful background for the stringy trapping which we will study in §4.3.

Because the field theory description is entirely sufficient, we can abstract the relevant properties of the worldvolume gauge theory and represent the system with a simplified model,

$$\mathcal{L} = \frac{1}{2} \partial_\mu \phi \partial^\mu \bar{\phi} + \frac{1}{2} \partial_\mu \chi \partial^\mu \chi - \frac{1}{8\pi^2} |\phi|^2 \chi^2 \quad (4.2.1)$$

in which a complex scalar field ϕ couples to a real scalar field χ . We have normalized the cross-coupling term so that the mass of χ is precisely the mass of a stretched string whose length is $|\phi|$ in string units. At the origin $\phi = 0$, χ becomes massless.

Let us consider the trajectory

$$\phi(t) = ib + vt \quad (4.2.2)$$

in which ϕ is separated from the origin by the impact parameter b . This is a solution to the classical equations of motion of (4.2.1) provided that $\chi = 0$. Along this trajectory, the mass of χ changes: in the limit where we impose (4.2.2) and ignore the effect of the coupling to χ , we may rewrite (4.2.1) as

$$\mathcal{L} = \frac{1}{2} \partial_\mu \phi \partial^\mu \bar{\phi} + \frac{1}{2} \partial_\mu \chi \partial^\mu \chi - \frac{1}{8\pi^2} (b^2 + v^2 t^2) \chi^2 \quad (4.2.3)$$

so that the effective mass of χ varies with time. This results in production of χ quanta.

This effect is easily understood in the quantum mechanics example of a harmonic oscillator whose frequency changes over time from ω_i to ω_f . If the oscillator begins in its ground state at frequency ω_i but the frequency changes nonadiabatically then the final state will not be the ground state of an oscillator of frequency ω_f .

One can readily compute the occupation numbers n_k of modes with momentum k . The result [18] is

$$n_k = \exp\left(-\frac{4\pi^2 k^2 + b^2}{2v}\right). \quad (4.2.4)$$

If instead we consider a model in which the mass of χ is nowhere zero,

$$\mathcal{L} = \frac{1}{2}\partial_\mu\phi\partial^\mu\bar{\phi} + \frac{1}{2}\partial_\mu\chi\partial^\mu\chi - \left(\frac{m^2}{2} + \frac{1}{8\pi^2}|\phi|^2\right)\chi^2 \quad (4.2.5)$$

the result is instead

$$n_k = \exp\left(-\frac{4\pi^2 k^2 + 4\pi^2 m^2 + b^2}{2v}\right). \quad (4.2.6)$$

The crucial, though intuitive, observation is that production of a massive species is exponentially suppressed. For this reason, production of massive string modes is entirely negligible when the velocity is small.

We may now apply the result of the simplified model to a pair of D-branes. Suppose that two Dp-branes, $p > 0$, are arranged to pass near each other. The brane motion changes the masses of stretched string states and induces pair production of unexcited stretched strings. As the branes begin to separate, these strings stretch and pull the branes back together.

This process can be followed in detail by numerically integrating the quantum-corrected equations of motion which follow from (4.2.1). Such an analysis was presented in [18]. However, analytical estimates are more readily generalized to the case of interest in this chapter, which is the stringy scattering of relativistic branes. We will therefore explain how one can use energetics to estimate the stopping length in the system (4.2.1). (It was shown in [18] that such estimates are in excellent agreement with the numerical results, although only the nonrelativistic case was studied there.)

After the branes have passed each other, the stretched open strings grow in mass. Even though pair production has ceased, the energy contained in open strings grows with time, because the strings are being stretched:

$$\rho_{open} \approx |\phi(t)| n_{open} \quad (4.2.7)$$

When the energy in open strings is of the same order as the initial brane kinetic energy, the backreaction of the open strings is of order one and the brane motion slows down significantly. We therefore define the ‘stopping length’ ϕ_* via $\rho_{open}(\phi_*) \approx \frac{1}{2} T_p v^2$ where T_p is the tension of a Dp-brane.

A few qualitative features of low-velocity trapping are worth mentioning. First, the greater the number density of produced strings, the shorter the stopping length. On the other hand, the stopping length increases if the brane velocity increases or the string coupling decreases (making the branes heavier in string units).

The behavior in the limit $v \rightarrow 1$ is not obvious *a priori*. To estimate the total number density ν_{total} of all string modes, we could take the nonrelativistic result (4.2.6) for the occupation numbers of a massive species and sum it over the levels n in the string spectrum, including a factor of the density of states $N(n)$. The result (which was also presented in [18]) is

$$\nu_{total} \propto \sum_{n=0}^{\infty} N(n) \exp\left(-\frac{2\pi^2}{v} \left(n + \frac{b^2}{4\pi^2}\right)\right). \quad (4.2.8)$$

As we explain in §4.4.1, the density of states at high levels n obeys

$$N(n) \sim n^{-11/4} \exp\left(\sqrt{8\pi^2 n}\right) \quad (4.2.9)$$

This does not grow rapidly enough to compete with the exponential suppression (4.2.6) of high levels, so the limit $v \rightarrow 1$ does not display strong production of excited strings.

However, we will show in detail in §4.3, following [87], that the actual number density of produced strings is very much larger than the nonrelativistic estimate (4.2.8) suggests. We will find instead

$$\nu_{total} \propto \sum_{n=0}^{\infty} N(n) \exp\left(-\frac{2\pi^2}{\eta} \left(n + \frac{b^2}{4\pi^2}\right)\right) \quad (4.2.10)$$

where $\eta = \text{arctanh}(v) \gg 1$. This result does not follow from special relativity alone; it is instead a stringy effect arising from velocity-dependent corrections to the stretched string masses, as we will show.

4.3 The Interaction Amplitude for Moving D-branes

We will now derive the interaction potential for two D-branes in relative motion with arbitrary velocity. Although this result is well-known [87], we include the calculation for completeness and to set notation.

4.3.1 Interaction Potential from the Annulus Diagram

We will derive the interaction potential by computing the open string one-loop vacuum energy diagram. This diagram is an annulus whose two boundaries correspond to the two D-branes. By the optical theorem, twice the imaginary part of this amplitude is the rate of pair production of on-shell open strings. Thus, our goal is to determine the imaginary part of the vacuum energy.

Several equivalent methods can be used to compute the vacuum energy. The original treatment [87] involves a direct computation of the spectrum of open strings between the moving branes; that is, it is possible to impose appropriate boundary conditions and solve for the mode expansion. The vacuum energy is then the sum of the zero-point energies of these oscillators.

We choose instead to review the perhaps more transparent computation given in [108]. Let us stress that in this subsection we follow the treatment of [108] in detail, with very minor modifications.

By double Wick rotation, a pair of branes in relative motion, separated by a transverse distance b , can be mapped to a stationary pair of branes at an imaginary relative angle, again separated by a distance b . We will make this precise below. Because the partition function for branes at angles is very well understood, the vacuum energy is easily computed in this approach.

Following [108], we begin with two D4-branes which are parallel to each other, extended along the directions 0, 1, 3, 5, 7, and separated by a distance b (the impact parameter) along X^9 . (To regulate the computation we compactify the spatial dimensions on a T^9 of radius R .) Now let one brane move towards the other along the direction X^8 with velocity v . That is, the coordinates of the moving brane are $X^8 = vX^0, X^9 = b$ while the other brane has $X^8 = X^9 = 0$. This is our actual problem.

We now perform the Wick rotation $X^0 \rightarrow -iX'^7, X^7 \rightarrow iX'^0$. This transforms the moving branes into static branes which are misaligned by an angle ϕ in the

$(7', 8)$ plane. The angle ϕ is given by $X'^7 \tan \phi = X^8$. The brane velocity v and rapidity η are related to this angle by $\phi = -i \operatorname{arctanh}(v) \equiv -i\eta$.

Next, it is useful to combine the coordinates into complex pairs Y_a , where $Y_1 = X^1 + iX^2, Y_2 = X^3 + iX^4, Y_3 = X^5 + iX^6, Y_4 = X'^7 + iX^8$. Define also the angles $\phi_1 = \phi_2 = \phi_3 = 0, \phi_4 = \phi$. The rotation then takes $Y_4 \rightarrow \exp(i\phi)Y_4$. It is now a simple matter to set up the boundary conditions satisfied by strings which stretch between the branes:

$$\begin{aligned} \sigma_1 = 0 : \quad & \partial_1 \operatorname{Re}[Y_a] = \operatorname{Im}[Y_a] = 0 \\ \sigma_1 = \pi : \quad & \partial_1 \operatorname{Re}[\exp(i\phi_a)Y_a] = \operatorname{Im}[\exp(i\phi_a)Y_a] = 0. \end{aligned} \quad (4.3.1)$$

The solutions to the wave equation which satisfy these boundary conditions are:

$$Y_a(w, \bar{w}) = i\sqrt{\frac{\alpha'}{2}} \left(\sum_{r=\mathbf{Z}+\phi_a/\pi} \frac{\alpha_r^a}{r} \exp(irw - 2i\phi_a) - \sum_{r=\mathbf{Z}+\phi_a/\pi} \frac{\alpha_r^{a*}}{r} \exp(ir\bar{w}) \right), \quad (4.3.2)$$

where $w = \sigma_1 + i\sigma_2$. We can readily write down the partition function for these four scalars:

$$Z_{\text{scalar}}(\phi_a) = -i \frac{\exp(\phi_a^2 t / \pi) \eta(it)}{\theta_{11}(i\phi_a t / \pi, it)} \quad (4.3.3)$$

so that the resulting bosonic partition function is

$$Z_{\text{boson}} = \prod_{a=1}^4 Z_{\text{scalar}}(\phi_a) \quad (4.3.4)$$

In a similar way, one can compute the fermionic partition function, keeping in mind the various spin structures:

$$Z_{\text{ferm}} = \prod_{a=1}^4 Z_1^1(\phi_a/2, it), \quad (4.3.5)$$

where

$$Z_1^1(\phi_a/2, it) \equiv \frac{\theta_{11}(i\phi_a t / 2\pi, it)}{\exp(\phi_a^2 t / 4\pi) \eta(it)} \quad (4.3.6)$$

We conclude that the one-loop potential is

$$V = - \int_0^\infty \frac{dt}{t} \frac{1}{\sqrt{8\pi^2 \alpha' t}} \exp\left(-\frac{tb^2}{2\pi\alpha'}\right) \prod_{a=1}^4 \frac{\theta_{11}(i\phi_a t / 2\pi, it)}{\theta_{11}(i\phi_a t / \pi, it)}. \quad (4.3.7)$$

This potential governs D4-branes at a relative angle. To map into the case of interest, we T-dualize as many times as needed, each time introducing the replacement $\theta_{11}(i\phi_a t/\pi, it) \rightarrow i\sqrt{8\pi^2\alpha't}\eta^3(it)/R$, where R is the size of the spatial torus.

This finally brings us to the potential for p-branes at an angle ϕ :

$$V = -iR^p \int_0^\infty \frac{dt}{t} (8\pi^2\alpha't)^{-p/2} \exp\left(-\frac{tb^2}{2\pi\alpha'}\right) \frac{\theta_{11}(i\phi t/2\pi, it)^4}{\theta_{11}(i\phi t/\pi, it)\eta(it)^9}. \quad (4.3.8)$$

Our final interest is in the number density and energy density of open strings, so the spatial volume $R^p \equiv iV_p$ will eventually cancel.

To read off the desired result for moving branes, we set $\phi = -i\eta$ to get

$$V = V_p \int_0^\infty \frac{dt}{t} (8\pi^2\alpha't)^{-p/2} \exp\left(-\frac{tb^2}{2\pi\alpha'}\right) \frac{\theta_{11}(\eta t/2\pi, it)^4}{\theta_{11}(\eta t/\pi, it)\eta(it)^9}. \quad (4.3.9)$$

One can easily show that this agrees precisely with the result of [87], equation (11). To see this, use (4.B.2) and (4.B.8), define $t_{there} = 2t$, $\epsilon = \frac{\eta}{\pi}$, and set $\alpha' = \frac{1}{2}$.

A useful equivalent form for (4.3.9) is

$$V = V_p \int_{-\infty}^\infty d\tau \int_0^\infty \frac{dt}{t} (8\pi^2\alpha't)^{-p/2} \frac{\theta_{11}(\eta t/2\pi, it)^4}{\theta_{11}(\eta t/\pi, it)\eta(it)^9} \times \exp\left(-\frac{t}{2\pi\alpha'} (b^2 + v^2\tau^2)\right) \frac{v}{\pi} \sqrt{\frac{t}{2\alpha'}} \quad (4.3.10)$$

In this form the time-dependence of the stretched string masses is manifest.

4.3.2 Imaginary Part and Pair-Production Rate

The above expression from the interaction potential is rich in information. The real part tells us about the velocity-dependent forces from closed string exchange, while twice the imaginary part is equal to the rate of production of open strings.

The potential (4.3.9) would be real if the integrand had no poles. However, $\theta_{11}(\eta t/\pi, it)$ has a zero for integral values of $\eta t/\pi \equiv k$, so we can compute the imaginary part of the integral by summing the residues at the corresponding poles.

$$\text{Im}[V] = \frac{V_p}{2(2\pi)^p} \sum_{k=1}^\infty \frac{1}{k} \left(\frac{\eta}{\pi k}\right)^{p/2} \exp\left(-\frac{b^2 k}{2\eta}\right) Z(ik\pi/\eta) \left(1 - (-1)^k\right), \quad (4.3.11)$$

where we have defined the partition function $Z(\tau) \equiv \frac{1}{2}\theta_{10}^4(0|\tau)\eta(\tau)^{-12}$. (The factor projecting out even values of k arises because of Jacobi's 'abstruse identity'.)

This expression, which was first derived in [87], will be essential to our investigation. By extracting its behavior in various limits we will be able to study the effect of open string production on the brane dynamics.

First of all, we can check the normalization of (4.3.11) by taking the low-velocity limit, in which $\eta \rightarrow v$. The result is

$$\text{Im}[V] = \frac{8V_p}{(2\pi)^p} \sum_{k=1,3,5,\dots}^{\infty} \frac{1}{k} \left(\frac{v}{\pi k}\right)^{p/2} \exp\left(-\frac{b^2 k}{2v}\right). \quad (4.3.12)$$

This is identical to Schwinger's classic result (4.3.12) for the pair-production rate of electrons in a constant electric field. In the present case, the interpretation is of pair production of massless open strings between the branes, which was also obtained by the method of Bogoliubov coefficients in [18].

Our interest is in the case of velocities approaching the speed of light. We expect that the dominant contribution to pair production in this limit will come from highly-excited string states. Because the density of states grows exponentially (4.2.9) at high levels, we anticipate copious production of massive strings and, as a result, dramatic backreaction on the brane motion.

To investigate this, we begin with the high-velocity limit $\eta \gg 1$ of (4.3.11):

$$\text{Im}[V] = \frac{V_p}{2(2\pi)^p} \sum_{k=1,3,5,\dots}^{\infty} \frac{1}{k} \left(\frac{\eta}{\pi k}\right)^{p/2-4} \times \exp\left(\frac{\eta}{k} - \frac{b^2 k}{2\eta}\right) \left(1 + \mathcal{O}(e^{-\eta/k})\right) \quad (4.3.13)$$

where we have used the asymptotics (2.B.5).

Keeping the dominant contribution, which comes from $k = 1$, and expressing the result as a number density ν_{open} of open strings stretching between the branes, we find

$$\nu_{open} \approx c_p \eta^{\frac{p}{2}-4} \times \exp\left(\eta - \frac{b^2}{2\eta}\right) \quad (4.3.14)$$

where $c_p = \left(2(2\pi)^p \pi^{p/2-4}\right)^{-1}$.

There are three important differences between the low-velocity effect in (4.3.12) and the high-velocity relation of (4.3.14). The first is that production of strings is exponentially suppressed at low velocities: this can be understood from the fact that the amount of strings produced at a given energy falls off exponentially

with energy, while the density of states for such low energies is a simple power law. At high energies, however, the density of states grows exponentially and these two competing exponentials lead to copious string production if the initial velocity of the branes is sufficiently high.

The second important difference is that at low velocities, the efficacy of the trapping process is strongly dependent on the impact parameter. For large impact parameters, $b \gg 1$ (recall that b is measured in string units), the trapping is exponentially weak. For ultrarelativistic branes, however, the trapping weakens only when $b \gg \eta$. The effective range of strong trapping is evidently much increased in the ultrarelativistic limit.

Finally, in the low-velocity limit, the energy of produced open strings is a negligible fraction of the D-brane energy [18] until the branes separate far enough to stretch the open strings significantly. The associated distance, the ‘stopping length’, is generically much larger than the impact parameter. In the ultrarelativistic limit, in contrast, the energy carried by the open strings can be comparable to the brane kinetic energy even before any stretching. This occurs because high speeds make possible the production of highly-excited strings with significant oscillator energy. This consideration suggests that the backreaction of open strings is much more dramatic for relativistic branes than for nonrelativistic ones. We undertake a careful study of this in the following section.

4.4 Backreaction from Energetics

We have seen in the previous section that relativistic brane motion leads to the production of a tremendous number density (4.3.14) of stretched open strings. We would now like to estimate the effect of this process on the brane motion, and to do so we must estimate the energy density carried by the produced open strings.

4.4.1 Open String Energy

An open string stretched between two moving branes receives velocity-dependent corrections to its mass. The change in mass is understood to be due to a rescaling of the effective tension, and in the limit that the branes move towards each other at the speed of light, the strings must become massless. This rescaling can also be understood from the T-dual electric field perspective: as the electric

field approaches a critical value, the strings can no longer hold themselves together, so their effective tension goes to zero [104]. We will now determine this rescaling in a simple way; in Appendix 4.A we will provide a detailed consistency check of this result.

The factor depending on b in (4.3.14) indicates that the effective area of a brane moving with rapidity η is [87]

$$r_{eff}^2 \approx \eta \alpha'. \quad (4.4.1)$$

This corresponds precisely to the logarithmic growth in cross-sectional area of a highly-boosted fundamental string, $r_{eff}^2 \sim \alpha' \ln(\alpha' s)$, where \sqrt{s} is the center-of-mass energy. The explanation for this growth is that a Regge probe of an ultrarelativistic string is sensitive to rather high-frequency virtual strings, whose considerable length creates a large cloud of virtual strings [109]. We conclude that a D-brane with rapidity η has an apparent radius $r_{eff} = \sqrt{\eta \alpha' / v}$, where we have inserted the factor of v to produce the correct behavior in the zero-velocity limit.

We therefore propose that the effective string tension is:

$$T(\eta) = \frac{v}{2\pi \alpha' \eta}. \quad (4.4.2)$$

This rescaling of the effective tension of the string means that the energy of a string excited at level n is:

$$E(n)^2 = \frac{nv}{\alpha' \eta} + \frac{(b^2 + r^2)v^2}{4\pi^2 \alpha'^2 \eta^2}. \quad (4.4.3)$$

In this expression b is the usual impact parameter, while r is the brane separation along the direction of motion.

In Appendix 4.A we demonstrate that precisely this dependence of mass on velocity explains the dramatic difference between the naive result (4.2.8) and the complete annulus computation (4.3.14) for the number density. Note also that the mass formula (4.4.3) does reduce to the usual formula for low speeds ($\eta \rightarrow v$).

We now proceed to calculate the energy density of the produced open strings. This energy is easily computed if we first rewrite the partition function Z as a sum over string states. This is conveniently parametrized in terms of the excitation level n and the number of states $N(n)$ at each level.

$$Z(ik\pi/\eta) \equiv \frac{1}{2} \theta_{10}(0, ik\pi/\eta)^4 \eta (ik\pi/\eta)^{-12} = \sum_{n=0}^{\infty} N(n) \exp\left(-\frac{2\pi^2 nk}{\eta}\right). \quad (4.4.4)$$

We would first like to determine the behavior of $N(n)$ at high excitation levels n . Taking the ansatz

$$N(n) \approx c_N n^a \exp(b\sqrt{n}), \quad (4.4.5)$$

approximating the sum by an integral, evaluating this integral by stationary phase, and demanding the asymptotics (2.B.5), we find

$$N(n) \approx (2n)^{-11/4} \exp(\pi\sqrt{8n}). \quad (4.4.6)$$

The numerical prefactor was chosen for convenience; strictly speaking, the approximate evaluation of the integral does not determine constant prefactors of order unity, but for our purposes it suffices to choose the factor now as in (4.4.6).

With this result in hand, we can rewrite (4.3.11) as

$$\text{Im}[V] = \frac{V_p}{(2\pi)^p} \sum_{k=1,3,\dots}^{\infty} \frac{1}{k} \left(\frac{\eta}{\pi k}\right)^{p/2} \exp\left(-\frac{b^2 k}{2\eta}\right) \sum_{n=0}^{\infty} N(n) \exp\left(-\frac{2\pi^2 n k}{\eta}\right). \quad (4.4.7)$$

An equivalent form for this relation is

$$\text{Im}[V] = \frac{\sqrt{2}vV_p}{(2\pi)^{p+1}} \int_{-\infty}^{\infty} d\tau \sum_{k=1,3,\dots}^{\infty} \frac{1}{k} \left(\frac{\eta}{\pi k}\right)^{\frac{p-1}{2}} \sum_{n=0}^{\infty} N(n) \exp\left(-\frac{2\pi^2 k \mu^2(\tau)}{\eta}\right). \quad (4.4.8)$$

where

$$\mu^2(\tau) \equiv \frac{n}{\alpha'} + \frac{b^2 + v^2 \tau^2}{4\pi^2 \alpha'^2}. \quad (4.4.9)$$

We can now express the energy density of produced open strings as

$$\rho_{open} = \frac{1}{(2\pi)^p} \sum_{k=1,3,\dots}^{\infty} \frac{1}{k} \left(\frac{\eta}{\pi k}\right)^{p/2} \exp\left(-\frac{b^2 k}{2\eta}\right) \sum_{n=0}^{\infty} E(n) N(n) \exp\left(-\frac{2\pi^2 n k}{\eta}\right), \quad (4.4.10)$$

where (4.4.3) is used for $E(n)$. Because of the competition of the growing and decaying exponential factors, this sum is dominated by terms near some $n_{peak} \gg 1$. As indicated above, we approximate the sum on levels using the relation

$$\sum_{n=0}^{\infty} N(n) n^a \exp\left(-\frac{2\pi^2 n}{\eta}\right) \approx 2^{-11/4} \int_{n_0}^{\infty} dn n^{a-11/4} \exp\left(\pi\sqrt{8n} - \frac{2\pi^2 n}{\eta}\right) \quad (4.4.11)$$

where the lower bound $n_0 > 0$ is chosen so that the integral is dominated by $n \approx n_{peak}$, not $n \approx 0$. We have kept the leading term in the sum on k . By the method

of stationary phase we find that the integral is dominated by $n \approx n_{peak} = \eta^2(2\pi^2)^{-1}$, leading to

$$2^{-11/4} \int_{n_0}^{\infty} dn n^{\alpha-11/4} \exp\left(\pi\sqrt{8n} - \frac{2\pi^2 n}{\eta}\right) \approx \frac{1}{2} e^{\eta} \left(\frac{\pi}{\eta}\right)^4 \left(\frac{\eta^2}{2\pi^2}\right)^{\alpha}. \quad (4.4.12)$$

For $\alpha = 0$ this reproduces the asymptotic behavior (4.B.5); we normalized (4.4.6) to arrange this.

This approximate result provides an important physical lesson: the primary contribution to the open string energy comes from strings at levels $2\pi^2 n \approx \eta^2$. For such a string,

$$E(n) = \sqrt{\frac{nv}{\eta} + \frac{(b^2 + r^2)v^2}{4\pi^2\eta^2}} \approx \frac{1}{2\pi} \sqrt{2\eta + \frac{b^2 + r^2}{\eta^2}}. \quad (4.4.13)$$

Let us now examine this result in the parameter ranges of interest. If the stretched string length is large compared to $\eta^{3/2}$, $\sqrt{b^2 + r^2} \gg \eta^{3/2}$, then the sum (4.4.10) is simply

$$\rho_{open} \approx \frac{\sqrt{b^2 + r^2}}{2\pi\eta} \nu_{open}. \quad (4.4.14)$$

On the other hand, when $\eta^{3/2} \gg \sqrt{b^2 + r^2}$, we have instead

$$\rho_{open} \approx \frac{\sqrt{\eta}}{\pi\sqrt{2}} \nu_{open} \quad (4.4.15)$$

where we have used (4.4.12) with $\alpha = 1/2$.

The key observation which follows from (4.4.15) is that the energy density carried by produced pairs of stretched open strings can be a significant fraction of the kinetic energy density of the Dp-brane. The backreaction from open string production is therefore an important contribution to the dynamics of relativistic D-branes. We will now examine this in detail.

4.4.2 Estimate of the Stopping Length

It will be very important to recognize three length-scales which arise in the problem: the effective size $r_{eff}(\eta) = \sqrt{\eta}\alpha'$ of a relativistic brane, the critical impact parameter $b_{crit}(\eta)$ beyond which the trapping rapidly weakens, and the size $r_{nad}(\eta)$ of the region in which the stretched open string masses change nonadiabatically.

To find the critical impact parameter, we note that the open string energy density obeys

$$\rho_{open} \propto \exp\left(\eta - \frac{b^2}{2\eta}\right), \quad (4.4.16)$$

so that for $\eta \gg 1$, the critical distance is evidently $b_{crit} \sim \eta$. For impact parameters less than b_{crit} , the open string energy density is generically large. The trapping effect is therefore very strong for impact parameters of order b_{crit} and smaller. (Nevertheless, trapping still occurs for impact parameters much larger than b_{crit} .)

The nonadiabaticity is characterized by how rapidly the frequency changes with time. Quantitatively, it is measured by the dimensionless quantity $\xi \equiv \frac{\dot{\omega}}{\omega^2}$, where ω is the frequency. Using (4.4.3) with $r = vt$ we find

$$\xi = \frac{2\pi\eta v^4 t}{(4\pi^2 n v \eta + (b^2 + r^2)v^2)^{3/2}} \approx \frac{2\pi\eta r}{(4\pi^2 n \eta + b^2 + r^2)^{3/2}} \quad (4.4.17)$$

which reaches its peak at $r^2 = \frac{1}{2}b^2 + 2\pi^2 n \eta$. For the energetically-dominant levels, $2\pi^2 n \approx \eta^2$, so that the effective region of nonadiabaticity has size $r_{nad} \sim \eta^{\frac{3}{2}}$ for $\eta \gg b$. Open strings are produced in large quantities when $-r_{nad} \lesssim r \lesssim r_{nad}$.

In summary, for relativistic speeds the critical impact parameter is $b_{crit} \sim \eta$, and is smaller than the size of the nonadiabatic region. The effective radius of a moving D-brane, i.e. the size of the stringy halo, is much smaller, $r_{eff} \sim \sqrt{\eta} \ll b_{crit}$. For any fixed, large η we can require

$$r_{eff} \ll b \ll b_{crit} \quad (4.4.18)$$

so that the trapping is very strong but the stringy halos are small enough to be unimportant. The case of a head-on collision, $b \lesssim r_{eff}$, is also interesting, particularly for the question of string production in the cyclic universe models, but we will first explore the better-controlled regime (4.4.18).

With these estimates in hand we can at last compute the stopping length for a scattering event. Taking one brane to be at rest and the other to have velocity v , we define as before

$$\eta \equiv \text{arctanh}(v). \quad (4.4.19)$$

Working instead in the center of mass frame, the branes approach each other with velocities

$$u = \tanh(\omega) = \tanh(\eta/2) \quad (4.4.20)$$

so that the center-of-mass γ factor for either brane is

$$\gamma = \frac{1}{\sqrt{1-u^2}} \sim \frac{1}{2}e^\omega \quad (4.4.21)$$

when $\omega \gg 1$. The energy density of the brane pair is then

$$E_{tot} = 2T_{Dp}\gamma \sim T_{Dp}e^\omega = T_{Dp}e^{\eta/2}. \quad (4.4.22)$$

We therefore find that for $\eta \rightarrow \infty$,

$$\rho_{Dp} = T_{Dp}e^{\eta/2} = \frac{1}{g_s(2\pi)^p}e^{\eta/2}. \quad (4.4.23)$$

In the case of strong trapping, $b \ll b_{crit} \approx \eta$, the open string energy at the minimum brane separation is

$$\rho_{open} \approx \frac{c_p}{\pi\sqrt{2}}\eta^{\frac{p-7}{2}}\exp(\eta) \quad (4.4.24)$$

whereas for weak trapping, $b \gg b_{crit}$, the open string energy is instead

$$\rho_{open} \approx \frac{c_p}{2\pi}\eta^{\frac{p}{2}-5}\sqrt{b^2+r^2}\exp\left(\eta - \frac{b^2}{2\eta}\right), \quad (4.4.25)$$

where $c_p = \left(2(2\pi)^p\pi^{p/2-4}\right)^{-1}$. Of course, the open string energy depends on r even in the case of strong trapping, but this dependence is relatively unimportant until $r \sim \eta$.

Comparing (4.4.23), (4.4.24) we conclude that if an external force compels the branes to pass each other at constant, ultrarelativistic velocity, then, unless the string coupling is exponentially small, the energy stored in open strings at the point of closest approach is considerably larger than the initial kinetic energy of the branes. This means that without an artificial external force, the branes will *not* pass each other with undiminished speed, as this is energetically inconsistent.

We expect instead that as open strings are produced, the branes slow down gradually, leading to diminished further production of strings. The final result, of course, will be consistent with conservation of energy. (In §4.4.3 we will address the production of open strings between decelerating branes, and in §4.5.1 we will explain that the emission of closed string radiation also serves to reduce the rate of production of open strings.)

Although the open string energy in (4.4.24) is an overestimate for the reason just mentioned, we will nevertheless use it now to find an estimate of the stopping length. This will serve to illustrate our technique in a manageable setting; it will then be a simple matter to repeat the analysis including the corrections of §4.4.3 and §4.5.1, which will not alter the form of our result.

We define the stopping length r_* by $\rho_{open}(r_*) = \rho_{Dp}$, so that at $r = r_*$ all the initial energy has been stored in stretched open strings. Equating (4.4.23) and (4.4.25), we find the stopping length

$$r_* \approx \frac{4\pi^2}{g_s} \exp\left(-\frac{\eta}{2} + \frac{b^2}{2\eta}\right) \left(\frac{\eta}{\pi}\right)^{5-p/2}. \quad (4.4.26)$$

This is our main result. It manifests the surprising property that for sufficiently large rapidity, the stopping length *decreases* as the rapidity increases. (More precisely, for any fixed g_s, b there exists a rapidity η_{min} such that the stopping length decreases as η increases past η_{min} .) To understand this unusual property, it is useful to keep in mind the behavior of D-branes scattering at even greater speeds, so great that the stringy halos themselves collide. For any b there is an η such that $r_{eff} \gtrsim b$; the scattering of the branes is then described by the collision of absorptive disks of radius r_{eff} [87]. Moreover, for a suitable range of g_s the brane Schwarzschild radii are so large that black hole production is an important consideration. We have carefully chosen our parameter ranges to exclude these effects and focus instead on the more controllable regime of strong stringy trapping; however, the black disk collisions and black hole production serve to illustrate that the limit of arbitrarily high rapidity involves very hard scattering and high inelasticity, in good agreement with the large- η behavior of (4.4.26).

The stopping length (4.4.26) is large in string units only when

$$g_s \ll 4\pi^2 \exp\left(-\frac{\eta}{2} + \frac{b^2}{2\eta}\right) \left(\frac{\eta}{\pi}\right)^{5-p/2} \quad (4.4.27)$$

which is an exponentially small value of the coupling provided $\eta \gg b, \eta \gg 1$. Thus, although backreaction from open string production is a higher-order correction to the dynamics [110] which one might suppose is unimportant at moderately weak coupling, we have shown that for relativistic branes with $b \ll \eta$ the backreaction of open strings is crucial unless the string coupling is extraordinarily small.

4.4.3 Corrections from Deceleration

All of our computations so far have applied exclusively to a pair of branes approaching each other at constant velocity. On the other hand, we have demonstrated that the backreaction from open string production, as computed along this trajectory, necessarily causes the branes to decelerate. Clearly, the next step is to understand how the amount of string production changes when the branes follow a decelerating trajectory.

The analysis of string production during deceleration turns out to be tractable in the nonrelativistic limit. However, we have not found an exact answer for the relativistic case. Upon double Wick rotation the amount of string production between decelerating branes is mapped to the interaction between curved branes, which is not obviously solvable with conformal field theory techniques.

Even though we will not find an exact result for the string production, we will be able to place bounds on the resulting number density. This suffices to reveal the qualitative features of the trapping process: copious production of excited strings and very high inelasticity.

First, however, we will examine the limit of instantaneous deceleration. Take the branes to move with a velocity v_0 for all $t < 0$, but to come to rest for $t > 0$. This problem can be solved exactly by matching the parabolic cylinder functions (and their derivatives) to the plane wave solutions at $t = 0$. However, this setup clearly involves enormous non-adiabaticity and so there would be an extremely large amount of pair-production, far greater even than in the case of constant velocity. This is readily computed, but it is not useful; we would like a more conservative estimate.

A more realistic picture is one in which the relative velocity of the branes varies as a function of time, for example as $v(t) = v_0(1 - \tanh(t/f))$, where f measures how abruptly the brane slows down. (Note also that in this setup the initial velocity is $v(-\infty) = 2v_0$.) The wave equation governing the stretched strings is therefore

$$\left(\partial_t^2 + k^2 + \frac{b^2}{4\pi^2} + \frac{v_0^2}{4\pi^2}[t - \log(\cosh(t/f))]^2\right)\chi = 0. \quad (4.4.28)$$

It is instructive to consider the non-adiabaticity parameter $\xi \equiv \dot{\omega}/\omega^2$, where

$$4\pi^2\omega^2(t) = 4\pi^2k^2 + b^2 + v_0^2[t - \log(\cosh(t/f))]^2. \quad (4.4.29)$$

Let us first take $f \ll 1$, which is the case of very rapid deceleration. In this limit the deceleration is concentrated at $t = 0$, so that for slightly later times, when the branes have come to a halt, we have $\xi = 0$ and hence no particle production. Comparing this scenario to that of branes moving with uniform velocity $2v$ and no deceleration, we see that an abrupt stop reduces the effective time available for particle production by a factor of two. Thus, for branes which come to a halt very rapidly, the total number of particles produced is approximately half the number produced when the branes move with uniform velocity.

We can analytically solve the problem in the opposite limit of very gentle deceleration, $f \gg \sqrt{4\pi^2 k^2 + b^2}/v_0$. Using the steepest descent method to determine the Bogoliubov coefficients [111,39,112] and observing that in this limit there is a branch point very near the imaginary axis, at $-i\sqrt{4\pi^2 k^2 + b^2}/v_0$, we find

$$|\beta_k|^2 = \exp\left(-\frac{1}{2v_0}(4\pi^2 k^2 + b^2)\right). \quad (4.4.30)$$

This coincides with the exact result for the constant-velocity problem with velocity $v(t) = v_0$. However, as we already noted, in the present case the initial velocity is $v(-\infty) = 2v_0$. Our very simple conclusion is that this gradually decelerating trajectory leads to the same amount of string production as an unaccelerated trajectory in which the branes move at a uniform velocity which is smaller by a factor of two. The effective velocity, for purposes of particle production, is thus the average velocity $\frac{1}{2}(v(-\infty) + v(\infty))$.

We conclude that very gradual deceleration results in significantly reduced string production. In particular, comparing the limits of large and small f , we see that the reduction in number density is much greater for gradual than for rapid deceleration.

The above result applies to nonrelativistic motion. The string computation which would be analogous to the annulus partition function but incorporate deceleration is considerably more complicated. In particular, the acceleration of the branes breaks conformal invariance, so it is difficult to use conventional techniques to compute the string production in this case.

Fortunately, it is possible to estimate the stopping length without an exact result for the string production during deceleration. The simple argument relies only on energetics and on the constant-velocity result (4.3.14).

Suppose that open string production slows a moving brane, bringing it from an initial kinetic energy $E_i = \gamma_i T_p$ to an energy (at the point of closest approach) $E_f = \gamma_f T_p$, where γ_i, γ_f are the usual relativistic factors. The stopping length, defined again by $E_i = E_{open}(r_*)$, is easily seen to be

$$r_* \approx \frac{2\pi\eta E_i}{\nu_{open}} = \sqrt{2}\eta^{3/2} \frac{E_i}{E_i - E_f}, \quad (4.4.31)$$

where we have used (4.4.14), (4.4.15).

Consider first the case $\gamma_f \gg 1$. If the stopping length is large compared to the size r_{nad} of the nonadiabatic region, $r_* \gg \eta^{3/2}$, then the branes are moving quickly as they leave the region of nonadiabaticity. This means that the result (4.3.14) applies directly, and we return to an apparent inconsistency: the open string energy is large compared to the initial energy. This is a clear signal that the stopping length cannot be much larger than $r_{nad} \sim \eta^{3/2}$.

A stopping length of order $\eta^{3/2}$ or smaller is indicative of strong trapping: the branes come to rest around the time that the nonadiabaticity grows small, which means that a few strings are still being produced.

On the other hand, in the case $\gamma_f \sim 1$, we have $E_f \ll E_i$, so that (4.4.31) yields the stopping length $r_* \approx \sqrt{2}\eta^{3/2}$.

We conclude that no matter how the deceleration affects open string production, if the only process acting to slow the branes is loss of energy to open strings, then the stopping length is no more than of order $\eta^{3/2}$, i.e. the size of the nonadiabatic region. Thus, the trapping is very strong: very little stretching is required before the branes are brought to rest.

Given a good estimate of the open string production along a decelerating path, we could give a more accurate estimate of the stopping length. However, we have just demonstrated through energetics and the result (4.3.14) that in any event this stopping length is no larger than $\eta^{3/2}$. In fact, we expect that it is actually considerably smaller than this, as suggested by (4.4.26).

It remains a possibility that loss of energy through closed string radiation could modify this result. We now proceed to show that this is not the case.

4.5 Further Considerations

4.5.1 Production of Closed Strings

By incorporating the effects of open string production we have seen that relativistic D-branes decelerate abruptly as they pass each other. This deceleration will lead to radiation of closed strings, in a process analogous to bremsstrahlung. This drains energy from the brane motion, and, unlike the transfer of energy into stretched open strings, this energy is forever lost from the brane system. Closed string radiation therefore serves to increase the inelasticity of a brane collision. Now, the end state of a near-miss is a spinning ‘remnant’, i.e. two D-branes orbiting rapidly around each other, connected by a high density of strings. Loss of energy and angular momentum to closed string radiation will swiftly reduce the rotation of this remnant, at least until the velocities become nonrelativistic.

One potential worry is that the energy loss to radiation might be so large that the quantity of open strings produced during a near-miss is quite small, leading to weak trapping and a large stopping length. This is an example of the more general concern that string production could be highly suppressed if any other effect caused the branes to decelerate to nonrelativistic speeds before reaching each other. We will show that the radiation of massless closed strings can be energetically significant but, even so, does not alter our conclusion that the stopping length is not large in string units.

To estimate the energy emitted as massless closed strings, we will make use of the close analogy of this process to gravitational bremsstrahlung [113] and to gravitational synchrotron radiation [114]. Of course, one of the massless closed string modes is the graviton, but we also expect radiation of scalars, including the dilaton and, when present, the compactification moduli. Even so, it will not be at all difficult to convert results from general relativity to the case at hand, because in practice, relativists often use the far simpler scalar radiation to estimate the basic properties of gravitational radiation. We will do the same.

Consider a small mass m moving rapidly past a large mass M in a path which is, to first approximation, a straight line. A burst of gravitational radiation will be emitted in a very short time, at the moment of closest approach. This is called gravitational bremsstrahlung. The peak radiated power is approximately [113]

$$P \sim \frac{G^3 M^2 m^2}{b^4} \gamma^4 \quad (4.5.1)$$

where G is the Newton constant, b is the impact parameter, and γ is the relativistic factor. For the remainder of this section we omit numerical prefactors: it will suffice to have the dimensional factors and the powers of γ .

The case of interest to us is extremely strong binding by open strings, for if the acceleration caused by the open strings is small then the closed string radiation should not play a key role, and the argument for trapping given in §4.4.3 suffices. Thus, we model the brane scattering by a gravitational scattering event in which the impact parameter is not much larger than the Schwarzschild radius of the larger mass. This gives

$$P \sim \frac{Gm^2}{b^2} \gamma^4. \quad (4.5.2)$$

Another useful case is that of gravitational synchrotron radiation from a mass m moving in a circular orbit with period ω_0 . The power is [114]

$$P \sim Gm^2 \omega_0^2 \gamma^4 \sim \frac{Gm^2}{b^2} \gamma^4 \quad (4.5.3)$$

where we have identified the inverse frequency with the minimum expected orbital radius, which is of order the impact parameter. This result will be very useful for understanding the decay of the initial circular orbit.

Furthermore, one can directly compute, in the supergravity limit, the radiation from an accelerated D-brane. The result for circular motion with radius b is [115]

$$P = \frac{Gm^2}{b^2} \gamma^4 \quad (4.5.4)$$

The results (4.5.3), (4.5.2), and (4.5.4) are thus in good agreement.

Knowing now the power lost to closed strings for a given decelerating trajectory, we also wish to compute the quantity of open strings which would be required to produce this trajectory. Stated more generally, given an object being accelerated by an external force, we are interested in the ratio of the radiated power to the power associated with the driving force. For an accelerating electron this is a textbook problem; see e.g. [116], chapter 14.

The result is that there is a characteristic length $L_e = \frac{2}{3} \frac{e^2}{mc^2}$ governing radiation by electrons, and unless an electron's energy changes by of order its rest energy during acceleration over a distance of order L_e , the radiation is negligible compared to the external power. More specifically,

$$\frac{E_{\text{radiated}}}{E_{\text{driving}}} \equiv \Omega_e \approx \frac{\Delta E}{\Delta x} \frac{L_e}{mc^2} \quad (4.5.5)$$

where the total change in energy, from all causes, is ΔE over a distance Δx .

One can readily estimate the corresponding characteristic length L_D for massless closed string radiation from a D-brane by comparing to the power (4.5.4). The outcome is that $L_D \sim g_s l_s$.

Let us now consider a brane whose initial kinetic energy is $E_i = \gamma_i T_p$, where $\gamma_i \gg 1$. Suppose that the brane decelerates over a distance Δx to a new kinetic energy $E_f = \gamma_f T_p$, $\Delta\gamma \equiv \gamma_i - \gamma_f$. The ‘driving force’ here is loss of energy through open string production; we will now compare this to the energy lost to radiation.

$$\Omega_D \equiv \frac{E_{\text{closed}}}{E_{\text{open}}} \approx \frac{\Delta E}{T_p} \frac{L_D}{\Delta x} = g_s \Delta\gamma \frac{l_s}{\Delta x} \quad (4.5.6)$$

If $\Omega_D \ll 1$ then our previous conclusions hold automatically, as the closed strings are energetically negligible. If $\Omega_D \gg 1$, there are two cases to consider. First, if $\gamma_f \sim 1$, so that $\Delta\gamma \sim \gamma_i \gg 1$, the branes have slowed down to nonrelativistic motion. In this case the energy in open strings can be estimated to be

$$E_{\text{open}} \approx \frac{\Delta E}{\Omega_D} \approx \frac{T_p}{g_s} \frac{\Delta x}{l_s}. \quad (4.5.7)$$

To arrive at this rough estimate we did not need the Bogoliubov coefficients derived from the annulus amplitude; we have used instead the fact that the external driving force (open string production) can be determined based on the postulated trajectory. Proceeding to estimate the stopping length, we find

$$\frac{r_*}{l_s} \approx \frac{2\pi\eta E_f}{\nu_{\text{open}}} \approx \frac{\sqrt{2}\eta^{3/2} E_f}{E_{\text{open}}} \ll \frac{\eta^{3/2} T_p}{E_{\text{open}}} = \eta^{3/2} g_s \frac{l_s}{\Delta x}. \quad (4.5.8)$$

The distance Δx is roughly order $\eta^{3/2}$, because that is the size of the nonadiabatic region in which open strings are created. (Two branes approaching each other will begin to decelerate when they enter this region.) To make a very conservative estimate, however, we will use $\Delta x \gtrsim l_s$. Then, because we are working at weak string coupling, the stopping length is

$$\frac{r_*}{l_s} \ll \eta^{3/2} g_s \frac{l_s}{\Delta x} \ll \eta^{3/2} \quad (4.5.9)$$

so that the stopping length is *much* smaller than $\eta^{3/2} l_s$.

The second case is $\Omega_D \gg 1$, $\gamma_f \gg 1$, so that the brane is moving relativistically even after decelerating, and the relative velocity is large when the branes pass each

other. Our general conclusion will be invalid only if the branes do not rapidly trap in this final case. However, if the branes separate to a considerable distance while moving rapidly, our annulus amplitude computation of open string production applies directly. In other words, by assuming that the branes can separate, we are arranging that they leave the region of nonadiabaticity, so that the number density of open strings is accurately given by (4.3.14), and the trapping length by (4.4.26). Thus, the assumption that the branes separate at high speed is not consistent.

We conclude that closed string emission can slow the motion of the brane pair, but it does not substantially increase the stopping length. In fact, radiation helps considerably to bring the branes to rest: once the branes are trapped and are spiraling around each other, rapid radiation losses will slow their rotation. This is enhanced by the familiar fact that, for relativistic objects, radiation losses are greater in circular motion than in rectilinear accelerated motion. Once the branes are trapped they slow down through this closed string synchrotron radiation. From the power (4.5.3) we conclude that the branes lose energy so rapidly that they would require only a few orbits to come to rest. In practice the spin-down process is prohibitively complicated, but this result suffices to show that the lifetime of the highly-excited, rapidly revolving remnant is in any case very short.

One important additional point is that the closed string radiation is strictly negligible only when the coupling is so small that the branes are rather heavy, and hence stretch the open strings farther before stopping. There is consequently a tradeoff between computability and control, which are best at extremely weak coupling, and the strength of the trapping, which is best for couplings above the bound (4.4.27). It is essential to recognize that for any nonzero coupling, the collision is inelastic and trapping eventually does occur; however, the stopping length increases when the coupling grows very small.

A further question which we have not addressed is the production of massive closed strings. In the case of very abrupt deceleration we would expect nonvanishing production of these modes. We will leave a precise computation of this effect within string theory as an interesting problem for future work.

For the present analysis, we can make a very crude estimate of massive string production by using a result on the spectrum of gravitational synchrotron radiation. For a mass in an orbit with period ω_0 , the power per unit frequency is [114]

$$\frac{dP}{d\omega} \propto \exp\left(-\frac{\omega}{\omega_{crit}}\right) \quad (4.5.10)$$

where $\omega_{crit} = \frac{6}{\pi}\gamma^2\omega_0$. Thus, for $\omega_{crit} \ll l_s^{-1}$, massive closed strings should play a negligible role, but when gravitons of frequency l_s^{-1} are being produced, it is natural to expect massive modes as well. We therefore expect some emission of massive closed strings in processes where $\gamma^2 \gg \frac{b}{l_s}$. This will further increase the rate of energy loss from the revolving brane pair, speeding the trapping and increasing the effective inelasticity of the collision.

4.5.2 Summary of the Argument

For clarity, we will now briefly review our argument that the trapping of relativistic D-branes is powerful and abrupt.

The annulus partition function for open strings between moving D-branes indicates that the density of produced open strings is given, in the relativistic limit, by (4.3.14). The characteristic impact parameter below which the backreaction of these strings is strong can then be seen to be $b_{crit} \sim \eta l_s$. If the D-branes are assumed to separate to a distance larger than of order $\eta^{3/2}$, they have left the region of nonadiabaticity, so that (4.3.14) applies. The energy (4.4.15) in open strings then exceeds the initial brane energy, so that the assumption of significant separation was inconsistent.

The same argument applies when closed string radiation is taken into account. A straightforward estimate of the energy lost to radiation over a distance $\eta^{3/2}$ shows that the energy transferred to open strings is still sufficient to stop the branes before their separation exceeds $\eta^{3/2}$.

We expect that a detailed computation of the string production along a decelerating trajectory would show that the stopping length is at most of order b , which can be much smaller than $\eta^{3/2}$. In particular, we expect that in a head-on collision with negligible impact parameter the stopping length would be of order the string length. However, estimates involving (4.3.14) are strictly valid only when the branes eventually leave the window of nonadiabaticity, leading to the *very* conservative estimate $r_* \sim \eta^{3/2}l_s$.

A few potential objections remain. First of all, one might worry that the branes somehow slow down before reaching each other, so that at the moment of closest approach the velocities are nonrelativistic. In this case excited open strings would not be produced and we would simply have field theory trapping. We have already explained in §4.4.3 that if the branes slow down exclusively due to open

string production, then they will still experience rapid trapping. Then, we showed in §4.5.1 that additional loss of energy through closed string radiation also does not ruin the trapping.

A final worry is that the branes could interact by creating string pairs at extremely high excitation levels. A vanishingly small number density of arbitrarily highly excited strings (with level much higher than η^2) could absorb all the initial kinetic energy and yet not generate a strong attractive force between the branes. However, we have seen that in fact string production peaks around level $n_{peak} \approx \eta^2(2\pi^2)^{-1}$, which is sufficiently small to ensure that the trapping is strong.

We therefore conclude that D-branes in relativistic motion generically trap each other through copious production of open strings, with a trapping length no larger than the size $\eta^{3/2}l_s$ of the nonadiabatic region. A sizeable fraction of the initial energy is eventually emitted in the form of massless closed string radiation.

The limitations to our argument which we have discussed above make it challenging to precisely and controllably compute the stopping length in an ultrarelativistic D-brane collision. However, these issues, and others – such as massless and massive closed string radiation, annihilation of the produced strings, and dilution of the produced strings in a cosmological background – do not in any way weaken our argument that the brane collision is inelastic. In fact, it is easy to see that radiation, annihilation, and dilution all extract energy from the brane system, slowing the brane motion. (See [18] for an analysis of these issues in the nonrelativistic context.) Happily, for applications to cosmological models, it is the inelasticity rather than the stopping length which is most immediately relevant.

4.5.3 Regime of Validity and Control

We will now examine the characteristics of the trapping process as a function of the dimensionless parameters g_s, b, η .

First of all, we will never work at strong string coupling ($g_s > 1$), since then we would have to include higher string loop effects. Furthermore, at strong coupling the D-branes become very light, and their Compton wavelength λ_D grows. We require $\lambda_D \ll b$ so that we can neglect these quantum effects.

Secondly, we should require that the Schwarzschild radius R_s of the D-brane is negligibly small compared to b . To estimate this, we treat the Dp -brane as a point

source in $10 - p$ dimensions. The black hole solution in $(10 - p)$ dimensions for a p -dimensional extended object of tension T and zero charge is [117]

$$T = \left(\frac{8-p}{7-p} \right) \frac{R_s^{7-p}}{(2\pi)^7 d_p g_s^2} \quad (4.5.11)$$

where $d_p = 2^{5-p} \pi^{\frac{5-p}{2}} \Gamma\left(\frac{7-p}{2}\right)$.

We are interested in the limit of zero charge because the highly-boosted branes have far greater effective mass than the BPS bound requires. Note that in fact the metric for one of these moving branes is of a shock-wave form, not a static black hole. We are imagining that the branes collide inelastically and then asking whether the Schwarzschild radius of the excited remnant, seen in the center of mass frame, is comparable to the initial impact parameter.

In this scheme, the effective tension is the center-of-mass energy $2T_p \gamma \approx T_p e^{\eta/2}$. We therefore find, using the tension of a p -brane,

$$\left(\frac{R_s}{l_s} \right)^{7-p} = g_s \left(\frac{7-p}{8-p} \right) (2\pi)^{7-p} d_p e^{\eta/2} \quad (4.5.12)$$

from which we conclude that for $p < 7$, the Schwarzschild radius can be made parametrically less than any given impact parameter by reducing the string coupling.

Let us now fix b and η and take the string coupling to be small enough so that string loops, the brane Schwarzschild radius, and the brane Compton wavelength can be neglected. As we further decrease the coupling, the brane becomes heavier and the stopping length becomes greater. Now, recall that when we examined the open string production along a constant-velocity path, we found an energetic inconsistency: unless the coupling was exponentially small, the open string energy exceeded the initial kinetic energy of the system. Of course, deceleration reduces string production, so for any controllable coupling the energy in open strings will not exceed the initial energy. However, we can still define a value of g_s at which the energetics is consistent even before we incorporate the deceleration which arises from backreaction. Comparing (4.4.23) and (4.4.24), we find that the energetics are automatically consistent provided that

$$g_s < 2^{3/2} \pi^{p/2-3} \eta^{\frac{7-p}{2}} e^{-\eta/2}. \quad (4.5.13)$$

Thus, only for exponentially small string coupling are the branes so heavy that they stretch the open strings substantially before coming to rest.

4.6 Discussion

We have argued that the relativistic scattering of Dp-branes, $p > 0$, at small impact parameters is almost completely inelastic as a result of pair production of excited open strings. The time-dependence induces production of an extremely high density of highly-excited, stretched open strings, which rapidly draw the branes into a tight orbit. The resulting acceleration results in significant closed string radiation, which acts to further brake the motion.

Powerful stringy trapping of this sort occurs whenever the impact parameter, measured in string units, is small compared to the rapidity η . This is a much larger range of distances than that controlled by collision of the stringy halos of the two branes, whose radius grows as $\sqrt{\eta}$. Moreover, the strength of this stringy trapping was a surprise: it does not follow from summing the low-velocity result of [18] over the string spectrum. Instead, the velocity-dependence of stretched string masses enters in a crucial way to enhance the production effect.

Our result, which is essentially a simple observation about the quantum-corrected dynamics of D-branes, has obvious implications for scenarios involving branes in relativistic motion. One example¹⁵ is the stage of reheating in cosmological models with fast-moving branes and antibranes. Brane-antibrane inflation models typically end with the condensation of the open string tachyon, leaving a dust of closed strings in the bulk as well as excited open strings on any remaining branes [118]. Despite much effort, this process is not fully understood [119]. Suppose, however, that the antibrane is moving relativistically toward the end of its evolution, and then passes by or collides with a stack of branes. (Ultrarelativistic brane motion is natural in the DBI models [120,121], for example, and could occur elsewhere.) In this case tachyon condensation governs only a small fraction of the energy released; most of the kinetic energy goes into open string pair production. Thus, reheating in such a model proceeds by stringy trapping (for related work, see [122]).

More speculatively, moduli trapping may be a useful mechanism for vacuum selection [18], as it gives a dynamical explanation for the presence of enhanced symmetry. (See also [123,124] for related work on moduli dynamics in string/M theory.) The stringy trapping presented here extends the trapping proposal not

¹⁵ We are grateful to S. Kachru for suggesting this.

just to a new parameter range, but to a regime where the strength of the effect increases dramatically.

The inelasticity of D-brane scattering may be viewed as a calculable example of a more general question: to what extent do particle, string, and brane production affect motion toward or away from a given ‘singular’ configuration? Time-dependent orbifolds [125,126,127,128,129,130,131] (see also [132] and references therein) provide a relatively tractable setting for such a question. Berkooz and Pioline [130] and Berkooz, Pioline and Rozali [131] have emphasized the possibility of resolving a spacelike singularity through the pair production and condensation of winding strings. It would be very interesting to extend these results and repair more general spacelike singularities through the production of branes or strings; see [133] for work in this direction. Our analysis suggests that string production could be surprisingly important in such a setting.

Another interesting open question is whether the inelasticity of quantum-corrected D-brane collisions can be used to place bounds on the elasticity of other sorts of collisions. In the cyclic universe model [134,135], the orbifold boundaries of heterotic M-theory [136] approach each other and collide. An intrinsic assumption of these cyclic models is that the collision is very nearly elastic; this is essential to make possible a large number of collisions and the associated cyclic behavior. Our result makes it plain that D-brane collisions, which appear elastic classically, are highly inelastic when the quantum effects associated to fundamental strings are included.

In the cyclic model, the M2-branes stretched between the boundaries become tensionless at the instant of collision. In the weakly-coupled four-dimensional description these objects are heterotic strings whose tension, in four-dimensional Planck units, goes to zero at the moment of impact. Because the masses vary rapidly during the collision, the nonadiabaticity is large and we expect copious production of these strings. It would be extremely interesting to compute the energy loss through this string/membrane production and to understand the implications for the cyclic models [137].

We should point out that in the most realistic cyclic models, the brane velocities are required, for phenomenological reasons, to be nonrelativistic.¹⁶ The results

¹⁶ We are grateful to P. J. Steinhardt for helpful discussions on this point.

in this chapter appear to give an independent upper bound on the velocity of the branes before collision – this bound is one which is required for the self-consistency of the model, rather than one imposed by observational requirements. However, this argument is qualitative at present; an explicit extension of our results involving stretched fundamental strings to the case of stretched membranes would be nontrivial.

Another interesting application would be to investigate inelasticity in the relativistic dynamics of networks of cosmic strings [138].

4.A Masses of Strings Between Moving Branes

In this appendix we provide a consistency check of our result (4.4.3) for the mass of an open string stretched between moving branes. We motivated this result with several independent arguments for a rescaling of the string tension. We will now show that precisely for this value (4.4.3) of the mass, our WKB estimate of string production (4.2.6) is consistent with the complete string result (4.4.7) in their regime of common validity.

In order to compare these two results, we need to work in a regime where the WKB result is reliable. We therefore require that the occupation numbers of all string states are small, i.e. we work in the nearly-adiabatic limit. By examining the full string result (4.4.7) we see that this can be achieved by requiring that $b^2 \gg \eta$. Moreover, we are interested in the relativistic limit $\eta \gg 1$.

We can use the result of §4.2 to conclude that if the time-dependent χ mass is given by

$$m^2(t) = \frac{C^2(v)}{4\pi^2} (b^2 + v^2 t^2) \quad (4.A.1)$$

then the number of produced χ particles is

$$\nu \propto \exp \left(-\frac{C(v)b^2}{2v} \right). \quad (4.A.2)$$

Requiring consistency with (4.4.7) we see that

$$C(v) = v/\eta, \quad (4.A.3)$$

exactly matching our proposed formula (4.4.3).

This analysis allows us to determine the velocity-dependence of that part of the string energy which comes from stretching, i.e. the second term in (4.4.3). The necessity of working in the nearly-adiabatic limit prevents us from extracting the velocity-dependence of the string oscillator energy, which is the first term in (4.4.3). However, we view the exact agreement between (4.A.3) and the energy resulting from the rescaling of the string tension (4.4.2) as compelling evidence that the rescaled tension correctly encodes the properties of this system. We therefore propose that the oscillator energy is likewise given by the same rescaling of the tension as in (4.4.2). This leads to (4.4.3).

4.B Theta Function Identities

In this section we collect various identities about the elliptic theta functions. Because of the existence of several canonical notations for these functions, we define the functions as used in the chapter.

The theta functions are often expressed in terms of the variables ν and τ , or in terms of the nome $q = \exp(2\pi i\tau)$ and $z = \exp(2\pi i\nu)$. The four theta functions are written down below in both their series and product forms:

$$\begin{aligned}
\theta_{00}(\nu, \tau) &= \theta_3(\nu|\tau) = \sum_{n=-\infty}^{n=\infty} q^{n^2/2} z^n = \prod_{m=1}^{\infty} (1 - q^m)(1 + zq^{m-1/2})(1 + z^{-1}q^{m-1/2}) \\
\theta_{01}(\nu, \tau) &= \theta_4(\nu|\tau) = \sum_{n=-\infty}^{n=\infty} (-1)^n q^{n^2/2} z^n \\
&= \prod_{m=1}^{\infty} (1 - q^m)(1 - zq^{m-1/2})(1 - z^{-1}q^{m-1/2}) \\
\theta_{10}(\nu, \tau) &= \theta_2(\nu|\tau) = \sum_{n=-\infty}^{n=\infty} q^{(n-1/2)^2/2} z^{n-1/2} \\
&= 2e^{\pi i\tau/4} \cos(\pi\nu) \prod_{m=1}^{\infty} (1 - q^m)(1 + zq^m)(1 + z^{-1}q^m) \\
\theta_{11}(\nu, \tau) &= -\theta_1(\nu|\tau) = -i \sum_{n=-\infty}^{n=\infty} (-1)^n q^{(n-1/2)^2/2} z^{n-1/2} \\
&= -2e^{\pi i\tau/4} \sin(\pi\nu) \prod_{m=1}^{\infty} (1 - q^m)(1 - zq^m)(1 - z^{-1}q^m).
\end{aligned} \tag{4.B.1}$$

In addition to the theta functions, we shall also need the Dedekind eta function:

$$\eta(\tau) = q^{1/24} \prod_{m=1}^{\infty} (1 - q^m) = \left[\frac{\partial_{\nu} \theta_{11}(0, \tau)}{-2\pi} \right]^{1/3}. \quad (4.B.2)$$

These functions have the following modular transformation properties:

$$\begin{aligned} \theta_{00}(\nu/\tau, -1/\tau) &= (-i\tau)^{1/2} \exp(\pi i \nu^2/\tau) \theta_{00}(\nu, \tau) \\ \theta_{01}(\nu/\tau, -1/\tau) &= (-i\tau)^{1/2} \exp(\pi i \nu^2/\tau) \theta_{10}(\nu, \tau) \\ \theta_{10}(\nu/\tau, -1/\tau) &= (-i\tau)^{1/2} \exp(\pi i \nu^2/\tau) \theta_{01}(\nu, \tau) \\ \theta_{11}(\nu/\tau, -1/\tau) &= -(-i\tau)^{1/2} \exp(\pi i \nu^2/\tau) \theta_{11}(\nu, \tau) \\ \eta(-1/\tau) &= (-i\tau)^{1/2} \eta(\tau). \end{aligned} \quad (4.B.3)$$

We will often need the asymptotic behavior of the theta and eta functions. When $q \ll 1$ we can immediately find the asymptotics using the above expansions, whereas for $q \rightarrow 1$ we must first perform a modular transformation.

The asymptotic behavior of a particular combination will be especially helpful. Define the fermionic partition function $Z(\tau) \equiv \frac{1}{2} \theta_{10}^4(0|\tau) \eta(\tau)^{-12}$. Then for $-i\tau \equiv s \gg 1$ we have

$$Z(is) = 8 + \mathcal{O}(e^{-2\pi s}) \quad (4.B.4)$$

whereas for $s \ll 1$ we find, using the modular transformations above,

$$Z(is) = \frac{1}{2} s^4 \exp\left(\frac{\pi}{s}\right) \left(1 + \mathcal{O}(e^{-\frac{\pi}{s}})\right) \quad (4.B.5)$$

We will also need a few identities involving the theta functions:

$$\begin{aligned} \theta_{00}^4(0, \tau) - \theta_{01}^4(0, \tau) - \theta_{10}^4(0, \tau) &= 0 \quad \theta_{11}(0, \tau) = 0 \\ \prod_{a=1}^4 Z_0^0(\phi_a, it) - \prod_{a=1}^4 Z_1^0(\phi_a, it) - \prod_{a=1}^4 Z_0^1(\phi_a, it) - \prod_{a=1}^4 Z_1^1(\phi_a, it) &= 2 \prod_{a=1}^4 Z_1^1(\phi'_a, it), \end{aligned} \quad (4.B.6)$$

where

$$\begin{aligned} Z_{\beta}^{\alpha}(\phi, it) &= \frac{\theta_{\alpha\beta}(i\phi t/\pi, it)}{\exp(\phi^2 t/\pi) \eta(it)} \\ \phi'_1 &= \frac{1}{2}(\phi_1 + \phi_2 + \phi_3 + \phi_4) \quad \phi'_2 = \frac{1}{2}(\phi_1 + \phi_2 - \phi_3 - \phi_4) \\ \phi'_3 &= \frac{1}{2}(\phi_1 - \phi_2 + \phi_3 - \phi_4) \quad \phi'_4 = \frac{1}{2}(\phi_1 - \phi_2 - \phi_3 + \phi_4). \end{aligned} \quad (4.B.7)$$

The identity (4.B.6) leads in the case $\phi_2 = \phi_3 = \phi_4 = 0$ to

$$2\theta_{11}^4(\nu/2, \tau) = \theta_{00}(\nu, \tau) \theta_{00}^3(0, \tau) - \theta_{01}(\nu, \tau) \theta_{01}^3(0, \tau) - \theta_{10}(\nu, \tau) \theta_{10}^3(0, \tau). \quad (4.B.8)$$